# A Bacteria-Plant Model System to Study Nitrogen Fixation in Mangrove Ecosystems

by

**Gabriela Alfaro-Espinoza**

A Thesis submitted in partial fulfillment
of the requirements for the degree of

**Doctor of Philosophy**
**in Marine Microbiology**

Approved Dissertation Committee

Prof. Dr. Matthias Ullrich
Jacobs University Bremen

Prof. Dr. Frank Oliver Glöckner
Jacobs University Bremen

Prof. Dr. Jens Harder
Max Planck Institute for Marine Microbiology

PD Dr. Tim Jennerjahn
Leibniz Center for Tropical Marine Ecology

Date of Defense: November 25, 2014

# Abstract

Mangrove ecosystems are highly productive and rich in organic matter. However, they are considered low-nutrient environments, being nitrogen one of the main nutrients limiting mangrove growth. Nitrogen-fixing bacteria are one of the main inputs of nitrogen to these forests. High nitrogen fixation rates have been detected in mangrove sediments and roots. Moreover, studies indicated that the relationship between diazotrophs and mangroves might be mutualistic. Several diazotrophs from mangrove roots and the associated rhizosphere have been isolated or identify by phylogenetic studies of the nitrogenase-coding *nifH* gene. However, our knowledge about the molecular signals and cellular mechanisms that govern diazotroph-mangrove interactions is scarce. Thus, in this thesis a diazotroph-mangrove model system was established to better understand the importance of this interaction for the ecosystem and how environmental changes could impact this organismal interplay. For this, nitrogen-fixing bacteria were isolated from mangrove roots. Moreover, root colonization pattern of the selected nitrogen fixer and the impact of some of the environmental factors that could affect its nitrogen fixation were investigated. The first result showed that the diazotroph *M. mangrovicola* Gal22 was a prominent candidate for the establishment of the model system. This bacterium was shown to possess all features and requirements needed for being a representative model organism. Thus a detail phenotypic and genotypic characterization of strain Gal22 was conducted. A strong mangrove root colonization was observed by *M. mangrovicola* in the absence of carbon and nitrogen sources, suggesting that root exudates were instrumental in establishing the interaction. Nitrogen fixation by this diazotroph was increased in the presence of the roots, supporting the above results. Finally, changes in environmental factors such as temperature and salinity had a rather minor impact on nitrogen fixation by *M. mangrovicola* thereby underlining the environmental robustness of this organism. Only very high temperatures showed a more pronounced effect inhibiting nitrogenase activity. The remarkable wide range of salinity under which Gal22 could conduct nitrogen fixation indicated its environmental versatility and may suggest that this bacterium can outcompete other bacterial organisms in the mangrove rhizosphere undergoing tidal and long-term changes in salinity. Overall, the results presented in this work together with the described model interaction system provide a solid basis for future investigations on the relationship between diazotrophs and mangrove plants as well as on the cycling of nitrogen in coastal environments.

# Acknowledgments

I would like to thank Prof. Dr. Matthias Ullrich for all his advice, for giving me the opportunity to be part of his research team and to work on this exciting topic. I would like to thank my thesis committee members, Prof. Frank Oliver Glöckner, Prof. Jens Harder and PD Dr. Tim Jennerjahn for all their valuable comments during our meetings. Also, I want to express my gratitude to Dr. Christiane Glöckner for all her help.

I am grateful to all former and current members of the Ullrich's Lab, especially to Amna Mehmood, Antje Stahl, Khaled Abdallah, Ahmed Rezk, Neha Kumari, Maria Johansson, Maike Last, Nina Böttcher, Dr. Ingrid Torres, Dr. Shalin Seebah, Dr. Shaunak Khandekar, Dr. Helge Weingart, Dr. Abhishek Srivastava, Dr. Eva Sonnenschein, Dr. Yannic Ramaye Dr. Astrid Gärdes, Dr. Nehaya Al-Karablieh; and to my friends from MarMic, especially to Viola Krukenberg, for their help, advice, for all the good moments, and most importantly for their friendship. Also, I would like to express my gratitude to Dr. Daria Zhurina, for mentoring at early stages of my career therefore, being a great example and motivation during my studies.

My deepest gratitude to my family, Mariela, María Laura, aunt Cecilia, and my parents that always gave me support, good advices and encourage me. My special thanks to my husband for always being there in difficult moments, for all his advice, help, and constant motivation. Finally, to Kartoffelito for making me smile when I most needed.

**This thesis is dedicated to my grandparents, Candelaria Vallejos and Antonio Espinoza**

**Esta tesis está dedicada a mis abuelitos, Candelaria Vallejos y Antonio Espinoza**

# Contents

# 1. Introduction

# 1. Introduction

## 1.1 Mangrove Ecosystems

Mangrove ecosystems are wetlands found along depositional environments of rivers, estuaries, and coastlines in tropical and subtropical climate regions (**Figure 1**) (Alongi et al., 2002; Feller et al., 2010). Mangrove forests cover an area of about $1.8 \times 10^5$ km$^2$ all over the world (Spalding et al., 1997; Valiela et al., 2001). They are characterized by a group of trees and shrubs consisting of 20 plant families belonging to two phyla, Magnoliophyta (angiosperms) and Polypodiophyta (ferns, includes only one family). In total there are 27 genera with 69 described species, from which 50 % belongs to the two orders, Myrtales and Rhizophorales (Duke, 1992).


**Figure 1**. Distribution of mangroves over the world (Giri et al., 2011).
Reproduced with permission of John Wiley and Sons.

Mangroves unique characteristics allow them to adapt to a life in intertidal environments. Many adaptations found in mangroves such as specific root types help to protect the coastal rims by reducing erosion caused by storms or tsunamis (Dahdouh-Guebas et al., 2005; Alongi, 2008). They can also act as a barrier protecting coral reef ecosystems and seagrass beds against the impacts of river-borne siltation (Duke et al., 2007). Another important characteristic is that they are nursery grounds for a diverse array of marine species, and that they host a variety of ecologically and economically important organisms such as crabs, snails, birds, shrimps, fishes, mammals, as well as millions of microorganisms (Ewel et al., 1998; FAO, 2007).

Moreover, mangrove forests are characterized by their high primary productivity, representing about 30 to 40 % of the total primary production on land. Consequently, they act as sink for atmospheric carbon dioxide (Bouillon et al., 2008). A total of $23 \times 10^{12}$ g C per

year (from which 25 % comes from leaf litter) is buried in mangrove sediments (Jennerjahn and Ittekkot, 2002). In addition, mangroves contribute to the export of particulate and dissolved organic carbon (21 ± 22 Tg C $y^{-1}$ POC and 24 ± 21 Tg C $y^{-1}$ DOC) and dissolved inorganic carbon (178 ± 165 Tg C $y^{-1}$ DIC) to adjacent waters (Bouillon et al., 2008; Kristensen et al., 2008). Despite their importance, over the past years these forests have been facing enormous areal losses at a rate of 1 to 2 % per year (Duke et al., 2007). Thus, these ecosystems underwent increasing fragmentation and thereby decreasing the valuable ecosystem services they provide to humans and nature. Those changes are mainly due to anthropogenic influences like urbanization, aquaculture, environmental pollution, wood utilization, and industrial development (Holguin et al., 2001; Alongi, 2002). Additionally, climate change could have an impact on these ecosystems. Changes in temperature, salinity, humidity, nutrient availability, ion concentrations in roots, and light intensity could influence the development of mangrove trees and their associated fauna (Mcleod and Salm, 2006; Feller et al., 2010).

### 1.1.2. Traits of mangrove forest

Mangrove forests are distributed in 124 countries, for which a mixture of marine or terrestrial communities is found (FAO, 2007). Mangrove communities are adapted to rough environmental conditions, growing in areas dominated by tidal fluctuations and the associated changes between high and low salinity, as well as the related desiccation and inundation periods (Duke, 1992). As a consequence, mangrove plants developed properties to tolerate salinity, flooding, and low nutrient availability, and developed specialized reproductive traits, which help them to persist in these environments (Feller et al., 2010). Some of these crucial adaptations of mangroves are summarized below.

- Salinity at high concentrations can have a detrimental effect on the development and the metabolic processes of mangrove plants. Typically, mangrove soils show gradients in salinity related to evaporation and the exposure of fresh water. For example, evaporation leads to an increase in salinity while freshwater inputs dilute salts (Ball, 1998). Consequently, plants that grow in contact with saline water, also known as halophytes, need to respond to changes in osmotic pressure. Some of the mechanisms that mangroves use for osmoregulation are: (a) storage of $Na^+$ and $Cl^-$ ions, and the use of salt glands by some species to excrete salt, (b) isolation of the salt from sensitive organelles, (c) control of the uptake of $Na^+$ and $Cl^-$ ions, and (d) production of organic osmotic solutes (Feller et al., 2010).

- Flooding reduces the oxygen concentration at the mangrove root surface, and as a consequence plant growth is decreased (Lovelock and Ellison, 2007). Mangrove plants are provided with morphological and physiological adaptations that play a key role in flooding tolerance (Feller et al., 2010). Some of these adaptations include aerenchyma and the

typical aerial root systems. Aerial roots are defined as roots, which are temporally - at least at low tide - exposed to the atmosphere (Tomlinson, 1986). Different types of mangrove aerial roots can be distinguished such as: stilt roots, pneumatophores, knee roots, plank roots, and buttress roots (**Figure 2**) (Tomlinson, 1986).

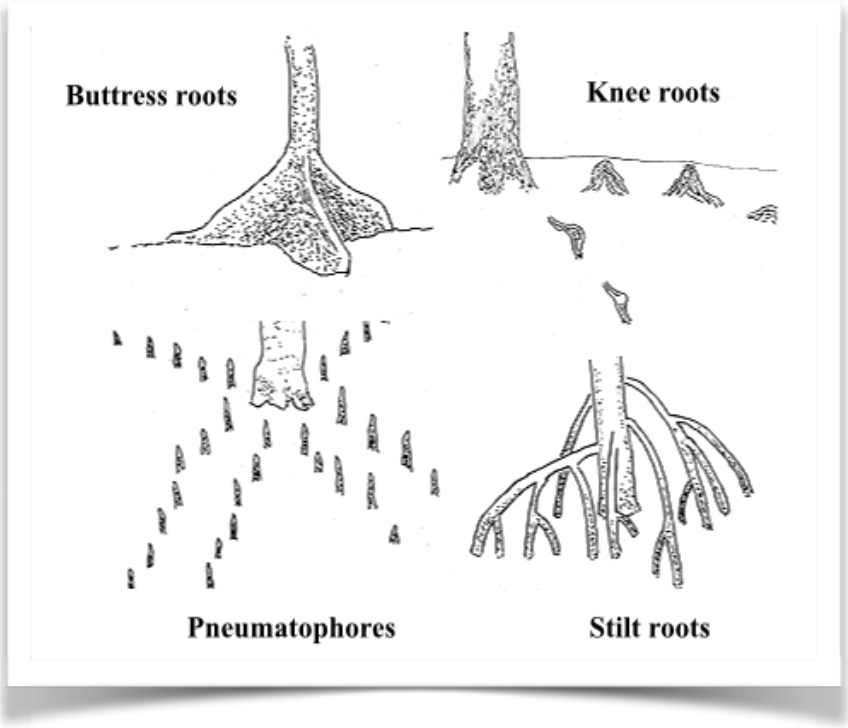


**Figure 2**. Types of mangrove aerial roots.
(Modified from http://www.wettropics.gov.au/mangroves-info).
Reproduced with permission of Wet Tropics.

- Nutrient availability differs within mangrove ecosystems. To maximize nutrient-use efficiency, mangroves develop extensive root systems, extend the leaf life span, increase photosynthetic efficiency, and form sclerophyllous leaves (hard and thick with short internodes to resist dry conditions), among others. Examples of mangrove species that are adapted to low nutrient concentrations are *Rhizophora mangle* and *Laguncularia racemosa* (Feller et al., 2010).

- Specialized reproductive traits are key for mangrove survival and establishment. Seeds are viviparous meaning that they usually lack a dormancy state but rather germinate while they are still attached to the parent plant. Mangrove seedlings are characterized by their buoyancy allowing them to be transported via current tides, which impacts mangrove zonation (Feller et al., 2010).

### 1.1.3 Mangrove Zonation

Mangrove plants are distributed in zones arranged along tidal gradients. Three zones have been identified in relation to tidal position: seaward, mid zone, and landward zone (**Figure 3**) (Duke et al., 1998; Waycott et al., 2011). The seaward zone is usually inundated and exposed to tides, the mid zone is exposed to tidal inundation only during the spring high tides, and the landward zone receives more freshwater inputs and is only inundated during the highest spring tides (Waycott et al., 2011). Additionally to segregation by tidal regimes other factors could constrain the distribution of mangrove plants such as temperature, soil pH, soil texture, soil redox potential, nutrient concentrations, or shade tolerance. Likewise, interspecific interactions such as competition may contribute to drive these vegetation patterns in mangrove forests (Smith, 1992).

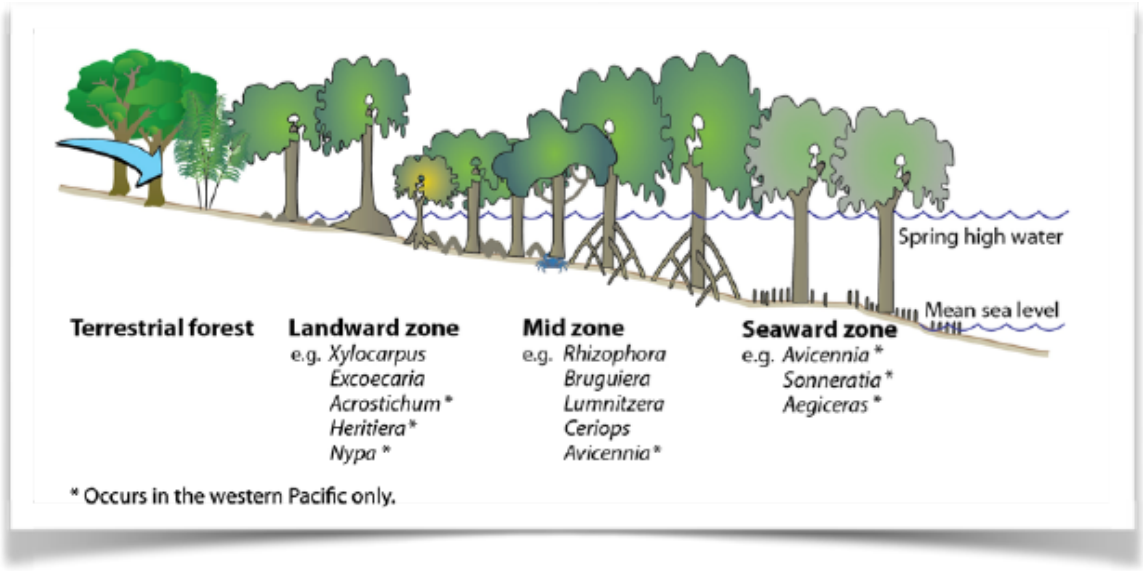


**Figure 3**. Mangrove zonation showing species distribution along the different zones (Waycott et al., 2011).

The observed species distribution pattern within the intertidal zone can vary among different geographic regions. This variation in mangrove distribution will depend on biotic as well as abiotic factors present at each location. For example, the zonation observed in a mangrove ecosystem in Queensland, Australia, is characterized by *Avicennia* spp. and *Sonneratia* spp. associated to the seaward zone, followed by *Rhizophora* spp. in the mid zone (Tomlinson, 1986). In contrast, mangrove forests in Florida and the Caribbean are characterized to have *Rhizophora mangle* in the seaward zone, followed by *Avicennia germinans* and *Laguncularia racemosa* in the landward zone (Feller et al., 2010). In addition to this horizontal distribution (zonation), mangroves exhibit vertical distribution. The vertical stratification is divided in supratidal, intertidal, and subtidal. The supratidal stratum is comprised of the mangrove

canopy, which is dominated by mammals, birds, lizards, snakes, snails, spiders and crabs. In the intertidal stratum a periodic submergence by tides and fluctuating salinity are the typical conditions experienced by organisms inhabiting this zone. It consists of mangrove aerial roots, salt flats, peat banks, and mudflats that are substrate for benthic organisms such as barnacles, crabs, snails, amphipods, oysters, and algae. Last, the subtidal stratum is found below the low water mark and supports organisms adapted to constant submergence, where mangrove roots provide substrate for sponges, tunicates, anemones, algae and epibionts (Feller et al., 2010).

## 1.2 Biological Nitrogen Fixation in Mangrove Ecosystems

Mangrove ecosystems are among the most productive tropical forest (Donato et al., 2011), with a net primary productivity of about 2 to 50 Mg C $ha^{-1}$ $year^{-1}$(Alongi, 2009). Although they are rich in carbon, they are considered low nutrient environments. The low nutrient availability of these forests varies between different mangrove soils and is control by a variety of factors such as soil redox potential, tidal inundation, soil type, plant species, elevation in the tidal frame, litter production, decomposition, and massive microbial activities in the soil (Reef et al., 2010).

Nitrogen and phosphorus have been identified as the main nutrients limiting mangrove growth (Bashan and Holguin, 2002; Feller et al., 2002; Reef et al., 2010). Nitrogen limitation is more pronounce in areas influenced by constant tidal or riverine exchange (Reef et al., 2010). Therefore, tidal export of nitrogen, denitrification, and the soil type are the major factors contributing to nitrogen loss in these areas (Boto and Robertson, 1990; Reef et al., 2010). For example, anaerobic conditions are common in mangrove soils hosting a variety of microorganisms, which are involved in processes such as denitrification and dissimilatory nitrate reduction to ammonium (DNRA) (Oliviera Fernandez et al., 2012). These organisms deplete nitrate from the soils, thus limiting the availably of this resource for mangrove plants (Alongi et al., 1992; Reef et al., 2010).

In contrast, the major nitrogen inputs to the ecosystem are tidal flushing, leaf litter, excrements from macrofauna, as well as microbial activity such as ammonification and nitrogen fixation (**Figure 4**). Microorganisms known as diazotrophs help to overcome the lack of nitrogen in these ecosystems by fixing atmospheric nitrogen into ammonia (Sengupta and Chaudhuri, 1991; Woitchik et al., 1997; Reef et al., 2010). Nitrogenase is the enzyme responsible for the transformation of atmospheric nitrogen into ammonia (**Figure 5**) (Postgate, 1982). Anaerobic conditions in soils of mangrove forests favor nitrogen fixation. This process needs to be carried out under oxygen-free conditions because the enzymatic reaction of nitrogenase is oxygen-sensitive (Gallon, 1981). Diazotrophs use different strategies to avoid inhibition of nitrogenase activity by oxygen, such as a) high metabolic rates of oxygen respiration, b) presence of intracellular structures or modifications that

protect nitrogenase from oxygen, such as heterocysts or thick cell walls, and c) rapid turnover of the enzyme (Karl et al., 2002; Lee and Joye, 2006).

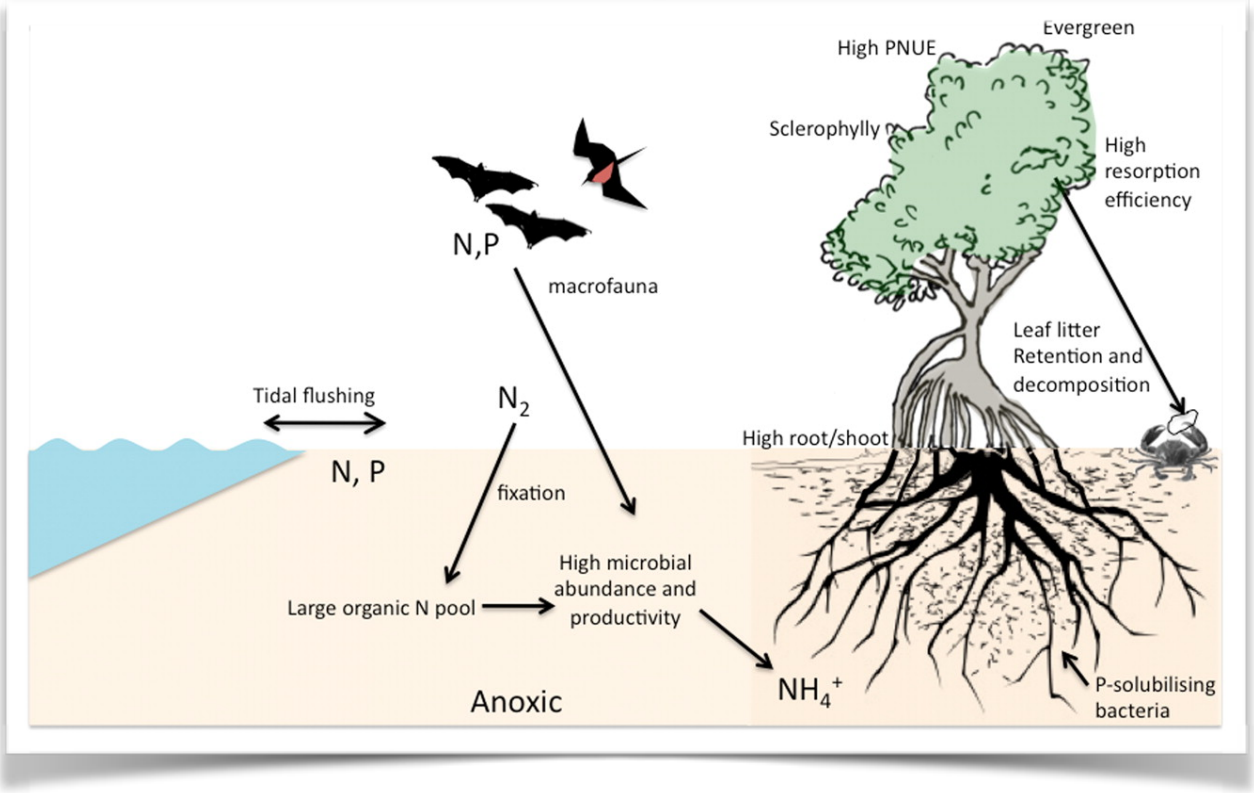


**Figure 4**. Nitrogen inputs to mangrove ecosystems (Reef et al., 2010).
Reproduced with permission of Oxford University Press.

High rates of nitrogen fixation in mangrove forest have been detected in aerial roots, sediments, rhizosphere, tree bark, and decomposing leaves (Gotto and Taylor, 1976; Zuberer and Silver, 1978; Uchino et al., 1984; Hicks and Silvester, 1985; Sengupta & Chaudhuri, 1991; Holguin et al., 1992; Pelegrí et al., 1997). Furthermore, studies showed that nitrogenase activity was higher in mangrove roots than in mangrove rhizosphere (Zuberer and Silver, 1978; Sengupta and Chaudhuri, 1991; Toledo et al., 1995; Lugomela and Bergman, 2002; Ravikumar et al., 2004), indicating a potential beneficial symbiotic interaction, where diazotrophs provide nitrogen to mangrove plants promoting their growth (Bashan et al., 1998; Ravikumar et al., 2004) and potentially utilizing plant root exudates as carbon sources (Flores-Mireles et al., 2007; Zhang et al., 2008).

Examples of diazotrophic bacteria found in association with several mangrove species such as *Rhizophora mangle*, *Avicennia germinans,* and *Laguncularia racemosa*, have been previously identified as *Listonella anguillarum*, *Vibrio campbelli*, *Microcoleus sp*., and *Phyllobacterium sp.* (Holguin et al., 1992; Toledo et al., 1995; Rojas et al., 2001). In addition, members of the genera *Azotobacter* and *Azospirillum* were isolated from mangrove

sediments and identified as nitrogen-fixing microorganisms (Sengupta and Chaudhuri, 1991; Ravikumar et al., 2004). Additional diazotrophs belonging to the genera *Azotobacter*, *Sphingomonas*, *Pseudomonas, Desulfuromonas*, *Derxia*, and *Vibrio* (Flores-Mireles et al., 2007; Zhang et al., 2008) were identified by phylogenetic studies of *nifH,* a gene used as a marker for nitrogen fixation and encoding for the Fe protein subunit of the nitrogenase enzyme (**Figure 5**) (Zehr and McReynolds, 1989; Zehr et al., 2003).

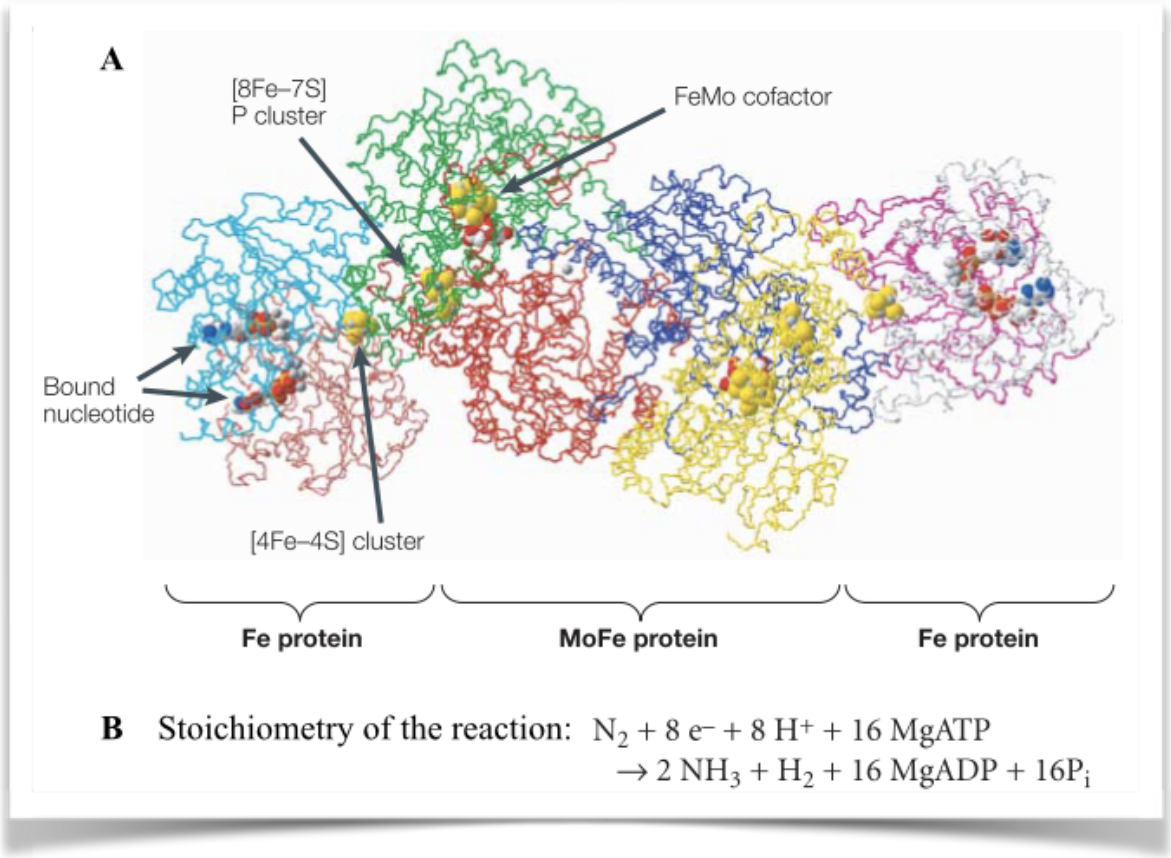


**Figure 5**. **A** | Structure of the nitrogenase enzyme complex. The enzyme is composed of two multisubunit metalloproteins, the Fe protein and the MoFe protein. **B** | Overall stoichiometry of the reaction catalyzed by nitrogenase (modified from Dixon and Kahn, 2004). Reproduced with permission of Nature Publishing Group.

Although several efforts have been made to identify microorganisms responsible of providing nitrogen to mangrove plants, we scarcely know about the molecular signals and cellular mechanisms which govern these interactions. Thus, it is utterly important to investigate the strategies that these nitrogen-fixing bacteria use to colonize mangrove roots and to identify the expressed genes and produced molecules important for this interaction in order to better understand nitrogen pathways in mangrove ecosystems.

## 1.3 Diazotrophic Activities Under a Changing Environment

Mangrove sediments are characterized by variable salinity, low nutrient availability, regular inundations, and a fluctuation between aerobic and anaerobic stages (Reef et al., 2010). It is tempting to speculate that the currently ongoing global climate change will affect mangrove ecosystems in one or the other way. In consequence, diazotrophs living in mangrove sediments or in association with mangrove plants need to cope with frequently changing environmental conditions.

Factors such as temperature, salinity, pH, desiccation, organic matter, or light intensity influence nitrogen fixation in mangrove forest (Lee and Joye, 2006; Flores-Mireles et al., 2007; Vovides et al., 2011). Below it is explained in detail how these different environmental factors could affect the mangrove environment.

- Temperature increases diazotrophic activities (Hicks and Silvester, 1985; Vovides et al., 2011). However, very high temperatures could have negative effects in nitrogen fixation (Zuberer and Silver, 1978).
- Salinity may be one of the factors having a major impact on diazotrophic communities. High salinity concentrations have been associated with a decrease or inhibition of nitrogenase activities (Vovides et al., 2011). Salinity in soils increases with low tides and long desiccation periods (Feller et al, 2010). Some of the mechanisms that bacteria use to adapt to salinity changes are a) the accumulation of organic osmotic solutes such as amino acids, glycine betaine, and tetrahydropyrimidines. b) accumulation of salts c) a combination of both or d) export of ions through ion pumps in the cell membranes (Ventosa et al., 1998).
- High pH in soils may repress nitrogenase. Vovides et al., 2011 reported high rates of nitrogen fixation in mangrove sediments with pH values lower than 6.5. Interestingly, nitrogen fixation could be promoted at high pH when temperature is higher than 28.6 °C (Vovides et al., 2011).
- Experiments have shown that desiccation lowered nitrogen fixation rates. Under long desiccation periods, processes such as denitrification might be enhanced and exceed nitrogen fixation rates in soils (Lee and Joye, 2006).
- Organic matter influences the spatial distribution of diazotrophs and enhances nitrogen fixation (Romero et al., 2011).
- Changes in light intensity have profound effects on photosynthetic communities. Oxygen release is a direct consequence of this (Lee and Joye, 2006). Thus, photosynthetic diazotrophs have to employ different strategies (summarized above) to evade nitrogenase enzyme inhibition by oxygen. For example, many non-heterocyst cyanobacteria employ temporal separation of nitrogen fixation by fixing more nitrogen at night (Lee and Joye, 2006).

The mentioned factors and strategies could also influence the spatial and temporal distribution of bacterial communities in mangrove soils. For example, seasonal variations were observed in an arid mangrove in Mexico due to differences mainly in seawater temperature, where higher bacterial populations were found between January to April with an average temperature of 20 °C, as compared to the very hot months from May to December with temperatures of 30 °C in average (Gonzales-Acosta et al., 2006).

Not all organisms might exhibit the same tolerance towards stress factors. As a consequence, diazotrophs use different strategies to cope with changes in the environmental conditions. However, our knowledge of the different strategies these diazotrophs use to cope with environmental disturbances is scarce. It is important to generate such a knowledge in order to understand the interactions between diazotrophs with mangrove plants, but specifically to answer some of the following questions: Under which conditions are diazotroph-mangrove interactions more prominent? Under which conditions are diazotrophic activities enhanced or inhibited? Which mechanisms do diazotrophs use to cope with environmental stresses? The answers to those questions could shed some light on the complex interactions between diazotrophs, mangrove plants, and their environment.

# 2. Aims of the work

# 2. Aims of the work

Although nitrogen fixation is a very important process in mangrove ecosystems, our knowledge of the role and interactions between nitrogen fixers with its biotic environment is limited. In the current study, an initial experimental framework for a detail molecular study of the interactions between nitrogen-fixing bacteria and mangrove plants was approached. In order to conduct such a study, the isolation and characterization of diazotrophs coming from mangrove plants is an essential initial step, while the influence of environmental factors affecting nitrogen fixation by these organisms should be analyzed in a second step. As colonization of roots by bacterial cells is one of the most important steps in symbiotic interactions, the colonization pattern of the selected diazotroph in mangrove roots had to be assessed and characterized. Thus, the major aims of the present work are:

I. Establishment of a nitrogen-fixing bacterial model system for molecular studies of diazotroph-mangrove interactions;

II. Taxonomic characterization of the nitrogen-fixing model organism, *Marinobacterium mangrovicola* Gal22;

III. Analysis of the effect of changes in temperature and salinity on nitrogen fixation rates of *Marinobacterium mangrovicola* Gal22.

# 3. Results

# 3. Results

The results of this PhD work are presented in the following three manuscripts. Each manuscript tackles one of the specific aims described above.

**A model system to study bacterial $N_2$-fixation in mangrove ecosystems.**
Gabriela Alfaro-Espinoza and Matthias S. Ullrich. (2014). Submitted.

***Marinobacterium mangrovicola* sp. nov., a marine nitrogen-fixing bacterium isolated from mangrove roots of *Rhizophora mangle*.**
Gabriela Alfaro-Espinoza and Matthias S. Ullrich. (2014). *Int. J. Syst. Evol. Microbiol.* 64, 3988-3993. doi:10.1099/ijs.0.067462-0.

**Influence of salinity and temperature on nitrogen fixation rates of the mangrove-associated bacterium, *Marinobacterium mangrovicola*.**
Gabriela Alfaro-Espinoza, Esteban Acevedo-Trejos, Khaled Abdallah and Matthias S. Ullrich. (2014). In preparation.

# 3.1 A model system to study bacterial $N_2$-fixation in mangrove ecosystems

**The following manuscript was submitted**

# A model system to study bacterial $N_2$-fixation in mangrove ecosystems

Gabriela Alfaro-Espinoza* and Matthias S. Ullrich
Jacobs University Bremen, Molecular Life Science Research Center, Campus Ring 1, 28759 Bremen, Germany

*Corresponding author: Gabriela Alfaro-Espinoza; m.alfaroespinoza@jacobs-university.de

Keywords: nitrogen fixation, mangroves, diazotrophs, nitrogen cycle, bacteria-plant interaction, root colonization

Running tittle: Diazotroph-Mangrove Model System

---

## ABSTRACT

Mangrove forests are highly productive ecosystems but represent low nutrient environments. Nitrogen availability is one of the main factors limiting mangrove growth. Diazotroph microbes have been identified as key organisms that provide nitrogen to these environments. $N_2$-fixation by such organisms was found to be higher in the mangrove roots than in surrounding rhizosphere. Moreover, previous studies showed that mangroves grew better in the presence of $N_2$-fixers, indicating a potentially mutualistic relationship. However, the molecular signals and mechanisms that govern these interactions are poorly understood. Here we present a model system consisting of a $N_2$-fixing bacterium and a mangrove species to study the cellular, molecular, and ecophysiological relationships between these two organisms under controlled conditions. Our results showed that the diazotroph *Marinobacterium mangrovicola* Gal22 is a versatile organism capable of competing with other organisms to survive for long periods in mangrove soils. $N_2$-fixation by this bacterium was up-regulated in the presence of mangrove roots, indicating a possible beneficial interaction. The increase in $N_2$-fixation as measured by qRT-PCR of the *nifH* gene, was limited to cells of the exponential growth phase suggesting that $N_2$-fixation differs over the bacterial growth cycle. Bacterial transformants harboring a transcriptional *nifH*::*gusA* fusion showed that *M. mangrovicola* successfully colonized mangrove roots and simultaneously conducted nitrogen fixation. This colonization process was demonstrated to be stimulated by the lack of an external carbon source, suggesting a mutualistic relationship. *M. mangrovicola* might be an interesting genetically accessible diazotroph, which colonize mangrove roots and exhibit higher nitrogen fixation in the presence of the mangrove roots. Consequently, we propose this organism as a model to a) study molecular interactions between $N_2$-fixers and mangrove plants and, b) to understand how changes in the environment could impact these important and relatively unknown interactions.

---

## INTRODUCTION

Mangrove ecosystems are wetlands located along tropical and subtropical coastlines. Mangroves can also refer to a characteristic group of shrubs and woody tress that grow in brackish intertidal environments (Feller et al., 2010). These highly productive environments provide many ecosystem services such as breeding and feeding grounds for diverse marine species, host a variety of organisms such as birds, mammals and invertebrates (Holguin et al., 2001), function as a barrier against tidal currents and tsunamis (Dahdouh-Guebas et al., 2005), and serve as carbon sinks, therefore, playing a key role in the global carbon cycle (Bouillon et al., 2008; Feller et al., 2010; Donato et al., 2011).

Although mangrove ecosystems are highly productive and rich in carbon, they are considered low nutrient environments. Nitrogen and phosphorus have been highlighted as nutrients limiting mangrove growth (Bashan and Holguin, 2002; Feller et al., 2002; Reef et al., 2010). Major factors contributing to nitrogen loss in these ecosystems are tidal export of nitrogen, denitrification and the soil type (Boto and Robertson, 1990; Reef et al., 2010). In contrast, $N_2$-fixation by diazotrophs is a major input of nitrogen to the ecosystem (Sengupta and Chaudhuri, 1991; Woitchik et al., 1997; Reef et al., 2010). $N_2$-fixation in mangrove ecosystems has been detected in sediments, rhizosphere, decomposing leaves, tree bark, pneumatophores, and roots (Gotto and Taylor, 1976; Zuberer and Silver, 1978; Uchino et al., 1984; Hicks and Silvester, 1985; Holguin et al., 1992; Pelegrí et al., 1997). $N_2$-fixation rates are higher in mangrove roots as compared to the rhizosphere soil, suggesting that mangrove plants potentially might obtain nitrogen from diazotrophs (Zuberer and Silver, 1978; Sengupta and Chaudhuri, 1991; Toledo et al., 1995; Ravikumar et al., 2004). Examples of $N_2$-fixing microbes isolated from mangrove roots or sediments are *Marinobacterium mangrovicola*, *Listonella anguillarum*, *Vibrio campbelli*, *Azotobacter*, *Azospirillum*, and *Microcoleus sp*. (Sengupta and Chaudhuri, 1991; Holguin et al., 1992; Toledo et al., 1995; Ravikumar et al., 2004; Alfaro-Espinoza and Ullrich, 2014). In addition, phylogenetic studies of *nifH,* the gene encoding for the Fe protein of the nitrogenase enzyme complex and commonly used as a marker for $N_2$-fixation (Zehr and McReynolds, 1989; Zehr et al., 2003), have shown that members of the genera *Azotobacter*, *Derxia*, *Desulfuromonas*, *Sphingomonas*, *Pseudomonas* and *Vibrio*, among others, could also play a role as $N_2$-fixing organisms in mangrove ecosystems (Flores-Mireles et al., 2007; Zhang et al., 2008).

Although description and isolation of microorganisms responsible for providing nitrogen to these N-poor environments has been done extensively, very little advance has been made on the effects that changing environmental conditions have on the cellular and ecological relationships between these microbes and their mangrove environment. Previous studies indicated that interactions between $N_2$-fixers and mangrove plants might be mutualistic (Bashan et al., 1998; Ravikumar et al., 2004). However, molecular signals and cellular mechanisms that govern these interactions are poorly understood. A model interaction system consisting of a $N_2$-fixing bacterium and a mangrove plant species could strongly facilitate such studies and help us to better understand the importance of this potentially mutualistic interaction for the ecosystem and how future climatic changes could impact this organismal interplay.

Herein, we established a model interaction system consisting of the diazotroph *Marinobacterium mangrovicola* Gal22 and the mangrove species *Rhizophora mangle*, for which we have tested a) the ecological competence and survival of *M. mangrovicola* in the mangrove rhizosphere and roots, b) the influence of nutrient availability on the root

colonization process, and c) the genetic accessibility of the selected diazotroph. The model interaction system thus provides a stepping stone to undertake further research on the symbiosis between diazotrophs and mangroves in these important tropical and subtropical ecosystems.

## MATERIALS AND METHODS

### Bacterial strains, plasmids and primers used

Bacterial strains used in this study are listed in **Table 1**. All plasmids and primers used are listed in **Table 2**. *Marinobacetrium mangrovicola* Gal22 cells were cultivated overnight at 28 ºC on HGB agar plates (supplemented with 0.1 % yeast extract) (Holguin et al., 1992). *Escherichia coli* DH5α cells were grown overnight at 37 ºC on Luria-Bertani (LB) agar plates. *E. coli* ST18 cells were grown on LB agar plates containing 50 µg/ml 5-aminolevulinic acid. *M. mangrovicola* and *E.coli* transformants were maintained in HGB and LB medium supplemented with the appropriate antibiotic, respectively.

**Table 1. Bacterial strains used**

| Bacterial Strains | Characteristic | Source or Reference |
|---|---|---|
| *Escherichia coli* | | |
| DH5α | supE44 D*lac*U169 (F80 *lacZ*DM15) *hsdR*17 *recA*1 *endA*1 *gyrA*96 *thi*-1 *relA*1 | Hanahan, 1985 |
| ST18 | λ*pir* Δ*hemA pro thi hsdR*$^+$ Tpr Smr chromosome::RP4-2 Tc::Mu-Kan::Tn7 | Thoma and Schobert, 2009 |
| *M. mangrovicola* | | |
| Gal22 | wild type | Alfaro and Ullrich, 2014 |
| Gal22.pBBR1MCS.GA.*nifH*::*gusA* | wild type containing *nifH*::*gusA* fusion cloned in pBBR1MCS | This study |
| Gal22ΔnifH | *nifH* deletion mutant, Cm$^R$ | This study |
| Gal22ΔnifH.pBBR1MCS.GA.*gusA* | *nifH* deletion mutant containing *gusA*, Cm$^R$ | This study |
| Gal22ΔnifH.pBBR1MCS-3.GA.*gusA* | *nifH* deletion mutant containing *gusA*, Tc$^R$ | This study |

Cm, Chloramphenicol; Tc, tetracycline; $^R$, resistance.

## Table 2. Plasmids and primers used

| Vectors / Primers | Characteristic | Source or Reference |
|---|---|---|
| **Vectors** | | |
| pUC119 | pMB1 origin, $Ap^R$ | Vieira and Messing, 1991 |
| pSU23 | p15A origin, $Cm^R$ | Bartolomé et al., 1991 |
| pKT210 | IncQ, $Cm^R$, $Sm^R$ | Bagdasarin et al., 1981 |
| pBBR1MCS | Broad-host-range cloning vector, $Cm^R$ | Kovach et al., 1994 |
| pBBR1MCS-3 | Broad-host-range cloning vector, $Tc^R$ | Kovach et al., 1995 |
| pBluescript SK(+) | ColE1 origin, $Ap^R$ | Stratagene |
| pJET1.2 | Replicon from pMBI vector, *eco47IR*, $Ap^R$ | Thermo Fisher Scientific |
| pJETnifHup/down | 450-bp deletion of *nifH*. First and last part of *nifH* (fragment 1 and 2) cloned in pJET1.2 | This study |
| pFCM1 | $Cm^R$ flanked by FRT sequences | Hoang et al., 1998 |
| pEX18TC | *oriT*$^+$ *sacB*$^+$, $Tc^R$, MCS from pUC18 | Hoang et al., 1998 |
| pEX.GA.nifH | Mutagenic construct. 2.7-kb HindIII fragment containing $Cm^R$ flanked by the first and last part of *nifH* gene cloned in pEX18Tc | This study |
| pCAM140 | promoterless *gusA*, $Ap^R$ | Wilson et al., 1995 |
| pJETnif | 1.5-kb fragment containing *nifH* plus upstream regulatory region 1.9-kb fragment containing promoterless *gusA* | This study |
| pJETgus | 3.4-kb fragment containing *nifH::gusA* fusion | This study |
| pJETnif::gus | 3.4-kb HindIII fragment containing a transcriptional fusion of *nifH* | This study |
| pBBR1MCS.GA.*nifH*::*gusA* | gene plus upstream regulatory region with promoterless *gusA*. Cloned in opposite orientation with respect to *lac* promoter, $Cm^R$ | This study |
| pKW117 | 2,2-kb fragment conatining *gusA* plus *tac* promoter and *trpA* transcriptional terminator, $Ap^R$ | Wilson et al., 1995 |
| pBBR1MCS.GA.*gusA* | 2,2-kb fragment conatining *gusA* plus *tac* promoter cloned in pBBR1MCS, $Cm^R$ | This study |
| pBBR1MCS-3.GA.*gusA* | 2.2-kb fragment containing *gusA* plus *tac* promoter cloned in pBBR1MCS-3, $Tc^R$ | This study |
| **Primers** | **Sequence (5'-3')*** | |
| Zf | TGYGAYCCNAARGCNGA | Zerh and McReynolds, 1989 |
| Zr | ADNGCCATCATYTCNCC | Zerh and McReynolds, 1989 |
| RTnifHf | ACCAGACTCGACGCACTTAA | This study |
| RTnifHr | CGAAGCTGGCAAGAAAGTCA | This study |
| RT16Sf | ACCACACACCTTTCCTCACA | This study |
| RT16Sr | CCAAGGCGACGATCTTTAGC | This study |
| nif-M-f | CCACTCGCCGGAGCATACGATGTA | This study |
| nif-M-r | ACACAGAACCTGGTAGCTGCCCTGG | This study |
| Fw.NotI.HindIII.f2 | GCGGCCGCAAGCTTATCGGGCACTCGGACTGGAT | This study |
| Rv.BamHI.f2 | GGATCCTACCGCGCTCTGGCACAGAA | This study |
| Fw.BamHI.f1 | GGATCCCACCAGACTCGACGCACTT | This study |
| Rv.HindIII.f1 | AAGCTTCCAGGATAAGGCTGTCGCT | This study |
| Mut.nifH.Fw | TGCCGACAACTTGCAATACC | This study |
| Mut.nifH.Rv | CCCAGAACACCATCATGGAA | This study |
| F.nifH.reg | AAGCTTCTGTTTTCCATACTCATGGCGG | This study |
| R.nifH.reg | GCATGCCGAATTACTCTTCAGCCGCAGTCT | This study |
| F.gus | GGCATGCTGATTGATTGA**AGGAGC**AACACT*ATG*TTACGTC CTGTAGAAAC** | Egener et al., 1999 |
| R.gus | GTCTAGAAAGCTTAGTTGTTGATTCATTGTTTG | Egener et al., 1999 |

*Underline are the restriction sites incorporated into the primer sequence: GCGGCCGC, NotI; AAGCTT, HindIII; GGATCC, BamHI; GCATGC, PaeI; TCTAGA, XbaI.
**In bold, *nifH* RBS from Gal22; in italics, start codon
Ap, ampicillin; Cm, chloramphenicol; Tc, tetracycline; Sm, streptomycin; $^R$, resistance.

**Isolation and selection of the bacterial model strain**

Nitrogen-fixing bacteria were isolated and identified using the 16S rRNA gene as described in Alfaro-Espinoza and Ullrich (2014). The bacterial model strain was selected according to the following criteria: a) the capability of the strain to fix atmospheric nitrogen, b) its genetic accessibility and, c) its ability to survive in *Rhizophora mangle* rhizosphere in a so-called fitness test when inoculated together with a group of other mangrove root-derived or sediment-borne indigenous bacterial strains.

Nitrogen fixation was tested *in vitro* by the acetylene reduction assay (ARA) and confirmed by PCR amplification of the *nifH* gene with the degenerate primers Zr and Zf (Zehr and McReynolds, 1989) (**Table 2**). Genetic accessibility was tested by transformation of bacterial strains using electroporation (Hamashitna et al., 1995; Wang and Griffiths, 2009) and conjugation, respectively. For this, the following vectors were used: pBBR1MCS (Kovach et al., 1994), pUC119 (Vieira and Messing, 1991), pSU23 (Bartolomé et al., 1991) and pKT210 (Bagdasarian et al., 1981) (**Table 2**). The Fitness test was performed in an open water tank filled with artificial sea water (Tropic Marin (Dr. Biener GmbH, Wartenberg, Germany)). *R. mangle* seedlings were cultured in pots filled with three-fold autoclaved quartz sand (Carl Roth, Karlsruhe, Germany) mixed with 1/10 of sand from mangrove natural ecosystems (mangrove mud special (Marek Mangroven, Vienna, Austria)), and introduced into the sea water tank. After six months, the rhizosphere of the mangrove plants was gentle inoculated with the isolated bacterial strains by mixing the sediment with bacterial inoculum without disturbing the seedling and its root system. The plants were kept at 25 ºC with a photoperiod of 12h. After one month of incubation, bacteria were re-isolated from the rhizosphere and mangrove roots by first a) shaking the rhizosphere soil in liquid HGB medium for 30 min, and b) macerating the mangrove roots. Then, the rhizosphere soil and homogenized roots were subjected to serial dilution and plated on HGB medium. Finally, single colonies were restreaked, and taxonomically identified by sequencing the 16S rRNA gene as described in Alfaro-Espinoza and Ullrich (2014). This experiment was repeated three times with two replicates per sample.

**Colonization of *R. mangle* roots by *M. mangrovicola* Gal22**

**A. Generation of *M. mangrovicola* mutant Gal22ΔnifH**

All restriction enzymes used in this study were obtained from Thermo Fisher Scientific, Schwerte, Germany. A genomic DNA library was constructed to obtain the flanking regions of the *nifH* gene sequence from *M. mangrovicola* Gal22. For this, genomic DNA was treated with the endonuclease XhoI thereby generating DNA fragments of different sizes. The XhoI-treated DNA was randomly cloned in XhoI-treated pBluescript SK(+), and ligation products were introduced to *E.coli* DH5α. The following specific primers were used to pre-screen for the presence of the *nifH* gene of Gal22, nif-M-f and nif-M-r (Table 2). A colony giving a PCR signal of 400-bp corresponding to the Gal22 *nifH* gene was selected. The plasmid of this transformant was isolated and its insert DNA was subsequently sequenced. A total sequence of 2.65-kb was obtained containing the 873-bp *nifH* gene and its flanking regions.

To develop a *nifH* gene deletion mutant, primers Fw.BamHI.f1 and Rv.HindIII.f1 (**Table 2**) were used to PCR amplify a 829-bp fragment (fragment 1) carrying the 5'-end and 558-bp of the upstream sequence of *nifH*. Primers Fw.NotI.HindIII.f2 and Rv.BamHI.f2 (**Table 2**) were

used to amplify a 750-bp fragment (fragment 2) containing the 3'-end and a 597-bp downstream sequence of *nifH*. Next, both fragments were cloned separately in vector pJET1.2 (Thermo Fisher Scientific) resulting in plasmids pJETnifHup and pJETnifHdown, respectively. In a second cloning step, fragment 1 was cloned in pJETnifHdown after BamHI/XhoI treatment, resulting in pJETnifHup/down (**Table 2**). A 1.147-kb chloramphenicol resistance cassette ($Cm^R$) was excised from pFCM1 (Hoang et al., 1998) and cloned in pJETnifHup/down with the help of a BamH1 treatment resulting in an insert fragment of 2.7-kb. Finally, the 2.7-kb fragment was cloned in vector pEX18Tc (Hoang et al., 1998) following a HindIII treatment. The resulting mutagenic construct was designated pEX.GA.nifH (Table 2). To obtain *M. mangrovicola* Gal22 deletion mutants, *E.coli* ST18 was heat shock transformed with pEX.GA.nifH and later used for biparental conjugation with *M. mangrovicola* Gal22.

Biparental conjugation was prepared by growing *M. mangrovicola* Gal22 overnight at 28 ºC on HGB agar plates. *E. coli* ST18 containing the mutagenic construct was grown overnight at 37 ºC on LB agar plates supplemented with 50 µg/ml 5-aminolevulinic acid (LB.AVA) and 25 µg/ml chloramphenicol (Cm). Bacterial cells were scratched from the plates thereby taking double amount of strain Gal22 as compared to strain ST18, resuspended in LB liquid media, and mixed with each other. The mixture was spotted on LB.AVA agar plates and incubated overnight at 28 ºC. After this mating period cells were scratched from plates, resuspended in HGB media and vortexed for 15 minutes. The cell suspension was serially diluted and dilutions plated on HGB agar supplemented with 25 µg/ml Cm. Since strain ST18 cannot grow without the presence of AVA, only *M. mangrovicola* transformants containing the $Cm^R$ from the mutagenic construct transferred by homologous recombination to the bacterial genome will be capable of growing on these agar plates.

Primers Mut.nifH.Fw and Mut.nifH.Rv (**Table 2**) were used to confirm the *nifH* gene knockout in *M. mangrovicola* Gal22. A PCR product of 740 bp was expected for wild type strain Gal22 while a corresponding 1,437-kb band was expected for mutant Gal22ΔnifH.

### B. Transcriptional fusion of *nifH* gene to the β-glucuronidase reporter gene (*nifH*::*gusA*)

A 1.510-kb fragment containing the *nifH* gene and a 632-bp sequence upstream of the transcriptional start site was amplified using primers F.nifH.reg and R.nifH.reg (**Table 2**). The promoterless β-glucuronidase (*gusA*) gene was amplified from plasmid pCAM140 (Wilson et al., 1995) with primers F.gus and R.gus (**Table 2**). Both PCR products were cloned individually in vector pJET1.2. The resulting plasmids were designated pJETnif and pJETgus, respectively. The insert DNA from pJETnif was cloned in pJETgus via PaeI/Xbal treatment, thereby generating a *nifH*::*gusA* fusion in the designated pJETnif::gus (**Table 2**). The *nifH*::*gusA* fusion was excised from pJETnif::gus by HindIII treatment and cloned in vector pBBR1MCS. The orientation of the insert was chosen in such way that expression of the reporter gene by the vector-borne *lac* promoter is avoided. The obtained transcriptional fusion plasmid pBBR1MCS.GA.*nifH*::*gusA*, was introduced to *M. mangrovicola* by conjugation using a corresponding *E. coli* ST18 transformant.

In addition, the *gusA* reporter gene was excised from pKW117 (Wilson et al., 1995) by HindIII restriction and cloned in pBBR1MCS obtaining plasmid pBBR1MCS.GA.*gusA* (**Table 2**), which was introduced to Gal22 by conjugation using *E. coli* ST18. Additionally, *M. mangrovicola* Gal22ΔnifH was marked with another plasmid designated pBBR1MCS-

3.GA.*gusA* (**Table 2**). This plasmid was generated by initially cloning the *gusA* gene from pKW117 via HindIII treatment in pBluescript SK(+), form which *gusA* was excised by XhoI/PstI treatment and cloned in pBBR1MCS-3 (Kovach et al., 1995).

### C. Incubations of *M. mangrovicola* Gal22 and *M. mangrovicola* Gal22ΔnifH with *R. mangle* roots

A basic HGB medium was modified to assess bacterial colonization on mangrove roots in form of a total of four variants (**Table 3**). *M. mangrovicola* carrying pBBR.GA.*nifH.gusA* was used in the two treatments with nitrogen-free HGB medium designated treatment -N / -C and -N / +C. In those cases, the *gusA* reporter gene will only be activated by the *nifH* promoter, consequently a blue color product will be generated when the β-glucuronidase interacts with the substrate 5-bromo-4-chloro-3-indolyl glucuronide (X-Gluc) (Carl Roth, Karlsruhe, Germany). Therefore, cells were only localized in places were strain Gal22 was actually fixing nitrogen.

**Table 3. Description of the four different treatments used to assay colonization of *M. mangrovicola* Gal22 on *R. mangle* roots.**

| Treatment | Description | Strains and vectors | |
|---|---|---|---|
| | | Gal22 | Gal22ΔnifH |
| **-N / -C** | lack of N and C sources | pBBR1MCS.GA.*nifH*::*gusA* | pBBR1MCS-3.GA.*gusA* |
| **-N / +C** | lack of N source | pBBR1MCS.GA.*nifH*::*gusA* | pBBR1MCS-3.GA.*gusA* |
| **+N* / -C** | lack of C source | pBBR1MCS.GA.*gusA* | pBBR1MCS-3.GA.*gusA* |
| **+N* / +C** | supplemented with N and C sources | pBBR1MCS.GA.*gusA* | pBBR1MCS-3.GA.*gusA* |

N: nitrogen ; C: carbon
*$NH_4Cl$ was used as nitrogen source instead of yeast extract.

In treatments were nitrogen (0.1 % $NH_4Cl$) was supplemented to the medium (+N / -C and +N / +C), plasmid pBBR1MCS.GA.*gusA* was employed to localize *M. mangrovicola*. Since under these conditions strain Gal22 does not need to fix atmospheric nitrogen, the constitutively expressed *gusA* allowed to localize the cells. Similarly, pBBR1MCS-3.GA.*gusA* was used to mark *M. mangrovicola* mutant Gal22ΔnifH. Here, the expression of *gus*A reporter gene was driven by a *tac* constitutive promoter, which allowed us to localize the cells under any of the four treatment conditions.

The media used in all treatments was semi-solid with 0.3 % agar content. 3-L glass beakers were filled with 500 ml of medium supplemented with 20 mg of X-Gluc and 12.5 mg of Cm. For treatments with *M. mangrovicola* Gal22ΔnifH 12.5 mg of Tc and 6.25 mg of Cm were added to 500 ml of medium. Subsequently, six-months old *R. mangle* seedlings and bacterial suspensions (adjusted to obtain an initial $OD_{600}$ of 0.07) were added to the beakers. The beakers were covered with aluminum foil to avoid light degradation of the X-Gluc substrate. Incubations were performed at room temperature (~22 °C) for 20 days. The plants were exposed to a photoperiod of 12h. During the incubation period, plants were visually

examined for bacterial colonization and pictures were taken every 5 days. Three independent replicates per treatment were performed.

After the incubation period, *R. mangle* roots were removed, rinsed with phosphate buffered saline (PBS) and fixed overnight in 4 % paraformaldehyde at 4 °C. After fixation, roots were kept in 70 % ethanol for 5 min, then in 0.5 M sucrose in PBS solution for 1 h at 4 °C followed by an overnight incubation in 1 M sucrose in PBS solution at 4 °C. Roots parts showing bacterial colonization were embedded in Jung tissue freezing medium (Leica Microsystems, Nussloch, Germany) and stored at -20 °C. Subsequently, 15 to 20 µm transversal cuts were generated using a CM1900 cryomicrotome (Leica Microsystems). Finally, the roots were analyzed using an Axio light microscope (Carl Zeiss, Jena, Germany) and photographed.

**Quantification of *nifH* gene expression by quantitative reverse transcriptase PCR**

*M. mangrovicola* Gal22 containing the vector pBBR1MCS was incubated in 60 ml of N-free liquid HGB medium (Holguin et al., 1992) supplemented with 25 µg/ml of chloramphenicol (Cm) in a 1-L flask at 28°C and shaking with 150 rpm and an initial optical density at 600 nm ($OD_{600}$) of 0.07. The flask was sealed with a rubber septum and flushed with $N_2$, then the headspace was adjusted to 1% of oxygen. Same conditions were used for the incubation of *M. mangrovicola* Gal22 containing pBBR1MCS with 2 g of roots of *Rhizophora mangle*. After incubation, the cell cultures were harvested at an $OD_{600}$ of 0.3, 0.5, and 0.7, respectively, using a protocol according to Schenk et al. (2008).

For RNA extraction the cell pellet was resuspended in RP buffer [3 mM EDTA,(0.5 M EDTA stock solution, pH 8), 700 mM NaCl and DEPC $H_2O$] with 40 mM DTT from a 1 M DTT stock solution added shortly before use. The cell suspension was added to pre-warmed lysis buffer [3 mM EDTA, (0.5 M EDTA stock solution, pH 8), 700 mM NaCl, 2% (w/v) SDS and DEPC $H_2O$], and shaken at 900 rpm for 3 min at 95 ºC. A phenol/chloroform extraction followed as described by Schenk et al. (2008). After extraction, the RNA was treated with TURBO DNA-free Kit (Life technologies, Darmstadt, Germany) to remove contaminating DNA.

Absorbance at 260 nm ($A_{260}$) was measured in a nanodrop 2000/2000c spectrophotometer (Thermo Fisher Scientific, Schwerte, Germany) to quantify the RNA concentration. The purity of the RNA was checked by determination of $A_{260}/A_{230}$ and $A_{260}/A_{280}$ ratios. Last, 500 ng of RNA were run on 1.5 % agarose gel to determine its integrity. *nifH* gene expression was determined in a Eppendorf mastercycler ep realplex (Eppendorf, Wesseling-Berzdorf, Germany) using the QuantiTect SYBR Green PCR kit (Qiagen, Hilden, Germany). Amplification of the 16S rRNA gene was used as a reference. The following RT primers were used: RTnifHf and RTnifHr for *nifH* gene as well as RT16Sf and RT16Sr for 16S rRNA gene (**Table 2**). Relative quantification (ΔΔCq method) was used to analyze the *nifH* expression data. The complete experiment was performed three times with three independent replicates per sample.

## RESULTS

### Isolation and selection of the bacterial model strain

Seven $N_2$-fixing bacterial strains were isolated from the rhizosphere and roots of *R. mangle*. The isolated strains belong to the classes of Gammaproteobacteria and Alphaproteobacteria. (**Supplementary Figure S1**). Our bacterial selection criteria tests showed the following: There is a tendency that *in vitro* ARA rates of isolate Gal22 are higher than the corresponding rates of the other six isolates (**Supplementary Figure S2**). From the seven isolated bacterial strains used in the Fitness Test only three of the introduced bacterial isolates were recovered (isolate Gal22, isolate Gal12 and isolate Gal4 (**Supplementary Table S1**)). Interestingly, only isolates Gal22 and Gal12 were recovered from all test samples and replicates. Finally, only isolates Gal22 and Gal12 exhibited DNA uptake using the transformation methods applied (**Supplementary Figure S3**). However, isolate Gal12 exhibit very low nitrogenase activity (**Supplementary Figure S2**), therefore, strain Gal22 was selected for further experiments because it best fulfills our three selection criteria.

### Colonization of *M. mangrovicola* Gal22 and its ΔnifH mutant on *R. mangle* roots

Different phenotypes were assessed to determine the bacterial colonization of mangrove roots by strain Gal22 and its ΔnifH mutant. First, the growth phenotypes were visualized in liquid N-free HGB medium (**Figure 1**) showing that in contrast to the wild type the mutant is not capable of growing under nitrogen fixing conditions. **Figure 2** depicts the growth phenotype in semi-solid HGB medium of wild type transformants harboring reporter plasmids. Multiplication of bacterial cells carrying the constitutively expressed *gusA* reporter gene was observed in both, N-containing and N-free medium, respectively (**Figure 2A**). However and as expected, when the *gusA* reporter gene was controlled by the *nifH* promoter, its expression could only be visualized when the cells were cultivated in N-free medium (**Figure 2B**).

Four treatments representing different nitrogen or carbon availabilities were applied to estimate the colonization patterns of *gusA*-carrying transformants of *M. mangrovicola* Gal22 and its ΔnifH mutant on *R. mangle* roots. On lateral roots, colonization of Gal22 transformants was found on the surface and inside the finer lateral roots (**Figure 3A,B,C**). During treatments where nitrogen and carbon were provided, *gusA* activity was observed in the soft-agar medium (Data not shown) but bacterial colonization of roots or lateral roots was not visible (**Figure 3D,E,F**).

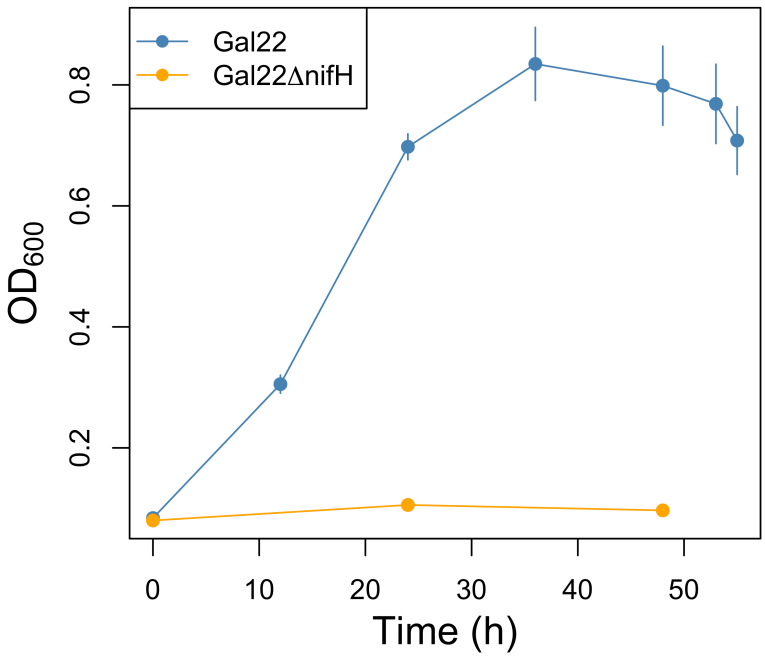


**Figure 1.** Growth curve of Gal22 wild type and mutant Gal22ΔnifH in N-free HGB medium and 1% $O_2$ in headspace flask.

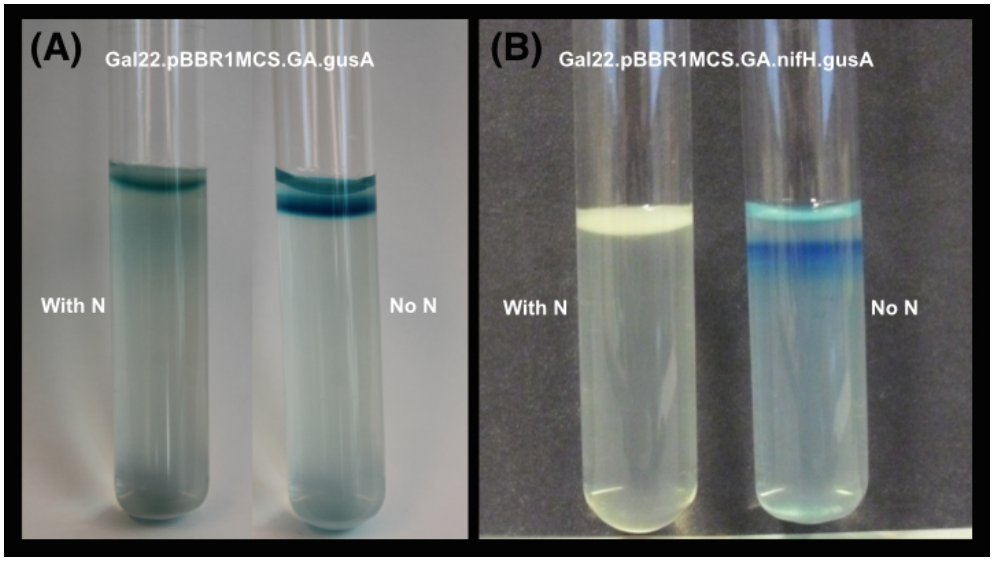


**Figure 2. (A)** *gusA*-carrying transformant of *M. mangrovicola* Gal22. *gusA* expression is under the control of the constitutive promoter *tac*, and can be visualized in N-containing and N-free medium. **(B)** *M. mangrovicola* Gal22 transformant carrying the *nifH::gusA* fusion. *gusA* expression is under the control of the *nifH* promoter, and can only be visualized with a blue color formation under $N_2$-fixing conditions in N-free medium.

*M. mangrovicola* Gal22 transformants carrying the *nifH*::*gusA* fusion exhibited a strong attraction to and a clear colonization of *R. mangle* roots when nitrogen and carbon sources were not provided in the semi-solid medium (**Table 4, Figure 4A**), when only carbon was lacking in the medium, the colonization was moderated (**Figure 4C**). Moreover, transcription of *nifH*::*gusA* revealed that the transformant used atmospheric nitrogen during root colonization under nitrogen and carbon limited conditions (**Figure 4A**). In contrast, when carbon or nitrogen or both were provided in the medium, the colonization efficiency of the Gal22 transformant with constitutively expressed *gusA* declined dramatically (**Figure 4B,D**). Interestingly, root colonization of Gal22ΔnifH transformants constitutively expressing *gusA* was strong in all treatments lacking either a nitrogen source, a carbon source or both suggesting that attraction to the roots was more pronounced when nitrogen fixation was abolished (**Table 4, Figure 5A,B,C**). In support of this, the mutant did not colonize mangrove roots when carbon and nitrogen sources were provided (**Figure 5D**).

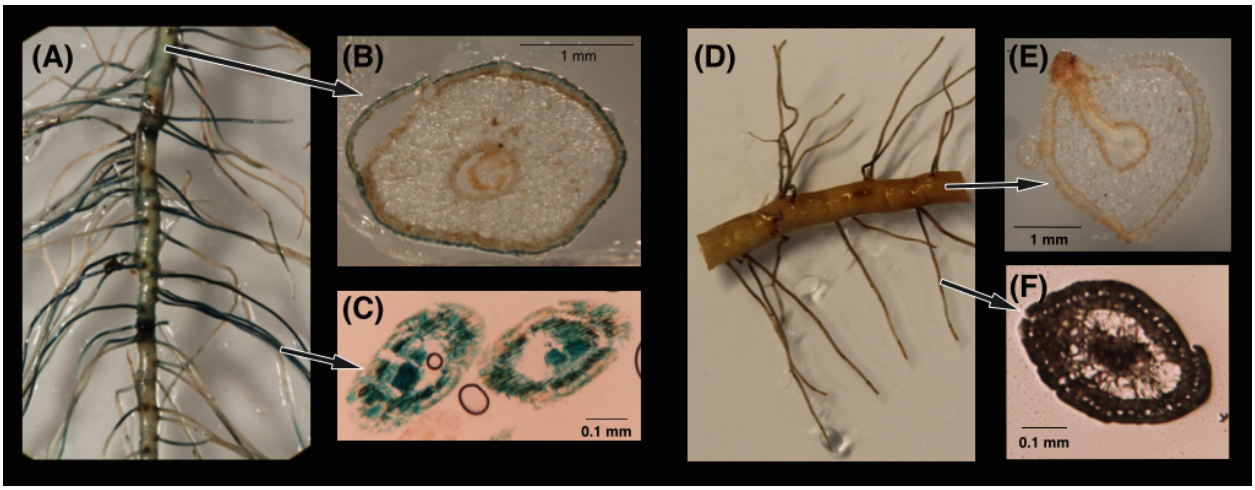


**Figure 3. (A)** Colonization of Gal22 transformant, carrying a *nifH::gusA* fusion, on *R. mangle* roots after the treatment -N / -C. Cells are localized by the blue color formation from *gusA* activity. **(B)** Root surface bacterial colonization. **(C)** Colonization within young-fine lateral roots**. (D), (E),** and **(F)** Root recovered after the treatment +N / +C. No bacterial colonization was observed in treatments were C and N were supplemented in the media.

### Quantification of *nifH* gene expression by quantitative reverse transcriptase PCR

Nitrogen fixation of strain Gal22 was studied by incubating the cells with or without presence of *R. mangle* roots (**Figure 6**). Transcription of *nifH* in Gal22 was significantly increased at low cell density (OD: 0.3; exponential phase) in the presence of the plant roots as compared to bacterial cells incubated without roots (**Figure 6**). However, during late exponential and stationary phases (OD: 0.5 and OD: 0.7) Gal22 did not show any significant mangrove root-mediated differences in *nifH* expression (**Figure 6**). Different growth phases of the wild type of Gal22 are depicted in **Figure 1** were an OD of 0.2 to 0.4 represents the exponential phase while an OD of 0.5 to 0.7 correspond to late exponential and stationary growth phases.

**Table 4. Colonization of *M. mangrovicola* Gal22 on *R. mangle* roots assayed under different treatments**

| | Treatment | | | |
|---|---|---|---|---|
| | **-N / -C** | **-N / +C** | **+N / -C** | **+N / +C** |
| **Gal22** | strong$^{\Psi}$ | weak* | moderate | absent |
| **Gal22ΔnifH** | strong$^{\Psi}$ | strong$^{\Psi}$ | strong$^{\Psi}$ | absent |

*less than 5%, mainly on root surface
$^{\Psi}$more than 40%, mainly on fine lateral roots

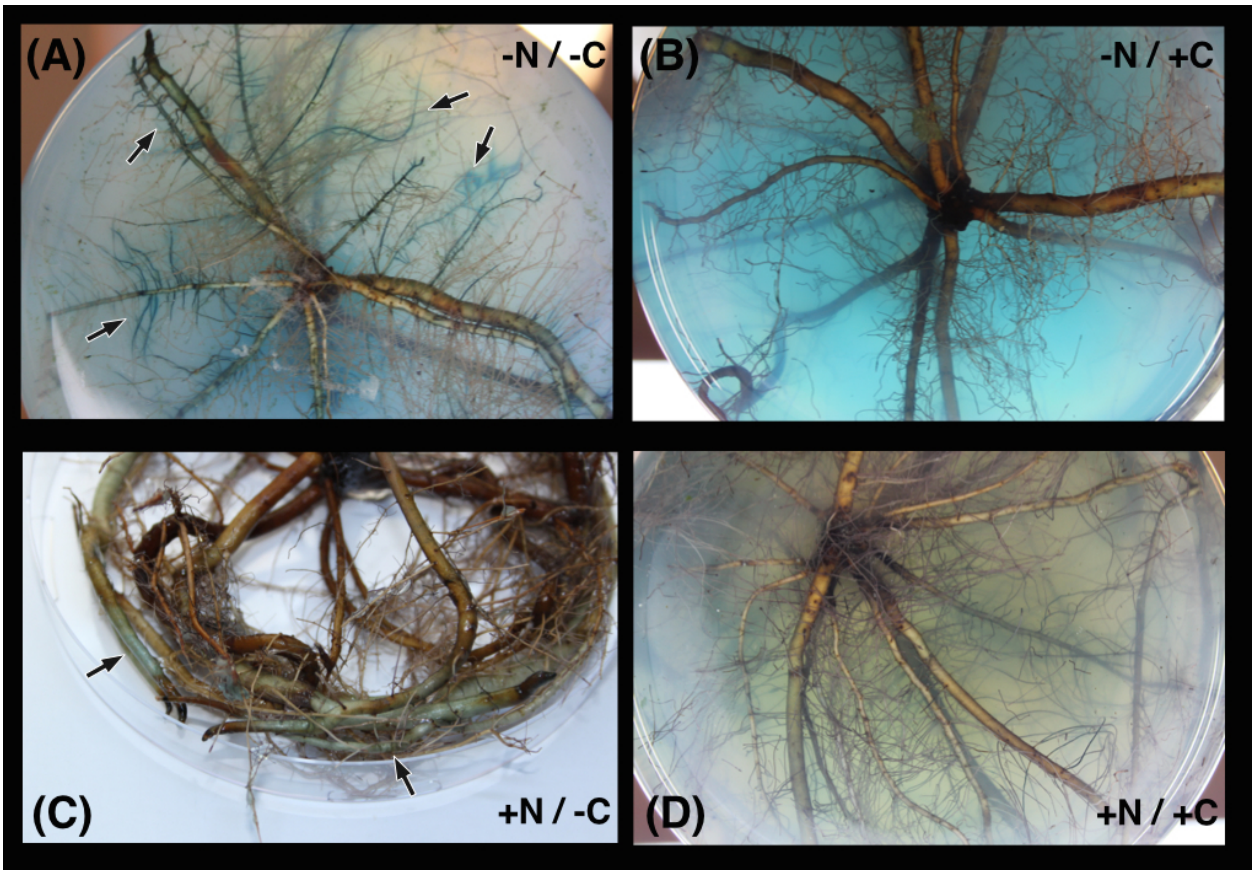


**Figure 4.** Colonization of *M. mangrovicola* Gal22 transformants carrying *gusA* on *R. mangle* roots. **(A)** Strong colonization and nitrogenase activity was visualized by the blue color formation from *gusA* activity in -N / -C treatment. In **(B)** and **(C)** there is a weak and moderate bacterial colonization, respectively. **(D)** Gal22 fail to colonize *R. mangle* roots when the surrounding medium was supplemented with N and C.

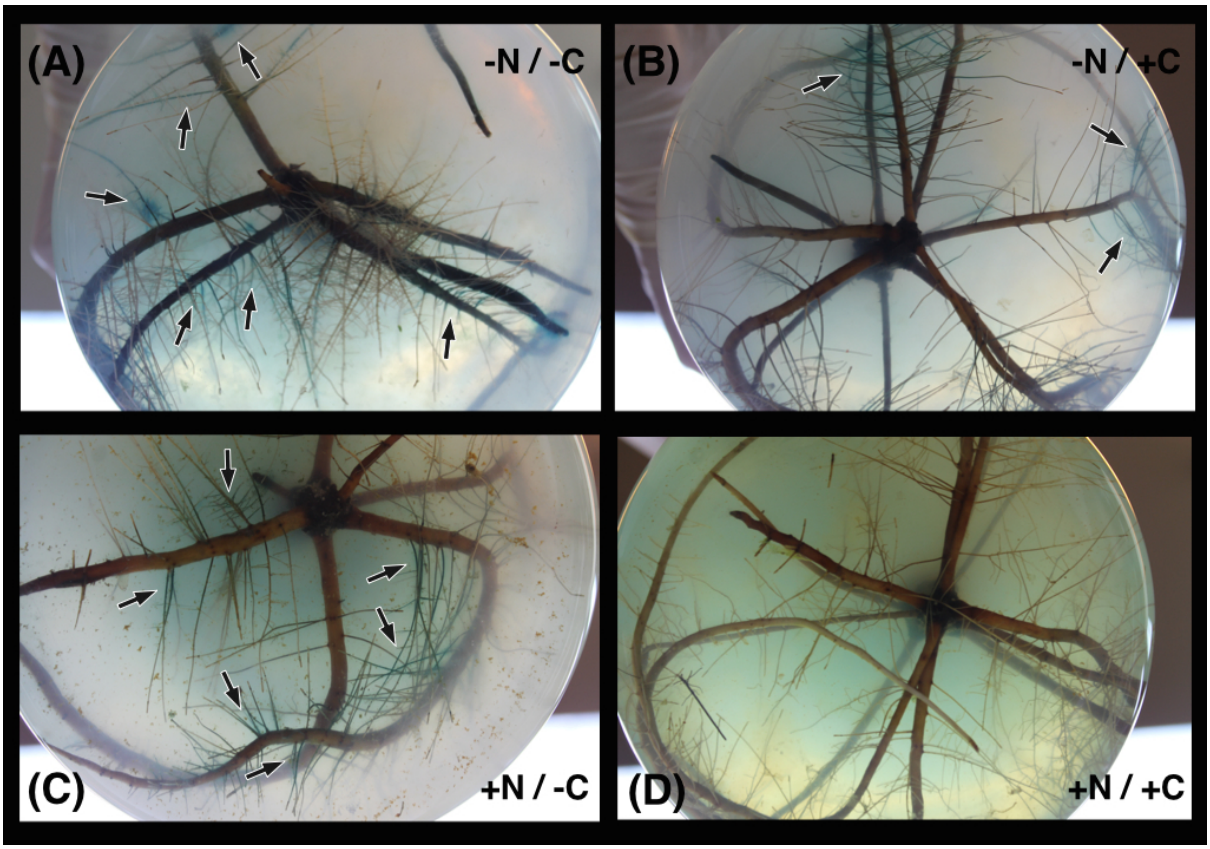


**Figure 5.** Colonization of mutant Gal22ΔnifH on *R. mangle* roots. **(A)**, **(B)**, and **(C)** Strong colonization of Gal22ΔnifH under treatments lacking a source of N or C or both. **(D)** Mutant Gal22ΔnifH root colonization was absent in treatments supplemented with N and C sources.

## DISCUSSION

Nitrogen-fixing bacteria are common in mangrove ecosystems. Although various diazotrophs had been identified in both, the rhizosphere and the root, molecular mechanisms that control the interaction between $N_2$-fixers and mangrove plants are not well understood. Herein we initially propose a genetically accessible bacteria-plant model system to study such interactions in order to foster our understanding of nitrogen fixation processes in mangrove ecosystems.

In previous studies, higher $N_2$-fixation rates had been detected in mangrove roots as compared to the rhizosphere (Zuberer and Silver, 1978; Sengupta and Chaudhuri, 1991; Toledo et al., 1995; Ravikumar et al., 2004) suggesting that plants potentially obtain nitrogen through associated bacterial cells. Herein, it has been investigated if the presence of mangrove roots had an effect on $N_2$-fixation of diazotroph Gal22. For this, we tested cells at different growth stages suggesting that mangrove root-induced expression of *nifH* differed remarkably at different bacterial growth rates (**Figure 6**). Interestingly, bacterial cells in late exponential or stationary phase did not showed significant mangrove root-inducible $N_2$-fixation. Possibly, this might be due to the large amount of dead cells in these two growth phases since cellular content released by decaying cells could have provided sufficient amount of nitrogen to surviving bacteria making fixation of atmospheric nitrogen dispensable. Our results are consistent with those of a previous study conducted by

Mulholland and Capone (2000), which showed higher $N_2$-fixation rates at early exponential phase in *Trichodesmium* spp. and lower rates at stationary phase. Although, in general our bacterial model organism showed comparable $N_2$-fixation patterns to other microbes, this is the first time such a quantification have been made for mangrove associated diazotrophs.

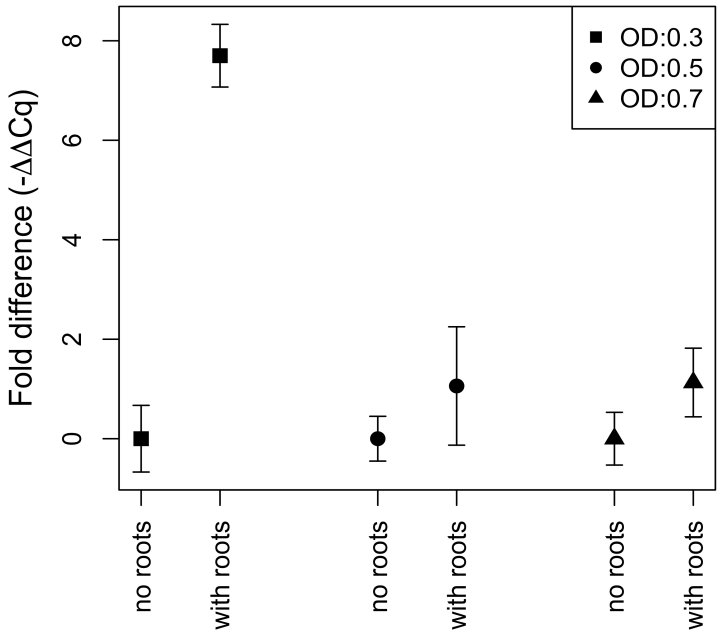


**Figure 6.** Fold difference in expression of *nifH* after cells have been exposed to *R. mangle* roots. The different symbols represent different treatments at optical densities (OD) of 0.3 (square), 0.5 (circle) and 0.7 (triangle). The only significant increase of *nifH* expression is during the exponential phase (OD: 0.3) at the presence of mangrove roots.

One advantage of using an organism such as *M. mangrovicola* Gal22 that can be easily modified genetically was the localization of bacterial cells inside of plant roots and on their surfaces (**Figure 3**), or distributed randomly in the surrounding semi-solid medium (**Figure 2**). The *gusA* reporter gene used in this study to localize bacterial cells on *R. mangle* roots showed that strain Gal22 colonized the surface of all roots and the interior of young lateral roots when no nitrogen or carbon were provided (**Figure 3A,B,C**). Since tissue development of young lateral roots might not be completed yet, bacterial entry might have been facilitated. Similar results had previously been observed for a bacteria-rice interaction where the *gusA* system had been applied (Egener et al., 1999). To our knowledge, this is the first time that a reporter gene has been used to monitor colonization of mangrove roots by diazotrophs.

The colonization of *M. mangrovicola* Gal22 and its *nifH* mutant assayed under four different treatments reveal that mutant Gal22ΔnifH was strongly attracted to the plant root possibly due to the lack of carbon and/or nitrogen in the surrounding medium (**Table 4, Figure 5A,B,C**). The lack of root colonization by Gal22 wild type and its ΔnifH mutant when these nutrients were fully supplied confirmed these results (**Figure 4D and 5D**). Since Gal22ΔnifH was not capable to provide its own nitrogen source by means of $N_2$-fixation its attraction towards the roots was higher in comparison to that of wild type. The attraction of the Gal22 wild type towards the roots occurred mainly when a carbon source was missing (**Table 4,**

**Figure 4A,C**) suggesting that carbon availability on root surfaces might be a major colonization trigger. Malic acid used as a carbon source in this study had previously been shown to be present in root exudates (Jones, 1998; Kamilova et al., 2006; Rudrappa et al., 2008). Since a considerable amount of malic acid was provided in the treatment -N / +C, Gal22 did not need to approach roots to acquire it. Consequently and in support of this, very little attraction towards the roots has been seen when only nitrogen was lacking from the medium (**Figure 4B**). Zuberer and Silver (1978) demonstrated that the addition of a carbon source increased nitrogenase activity in sediments. Similar results were found by Flores-Mireles et al. (2007) and Zhang et al. (2008). In the -N / -C treatment the attraction of Gal22 towards the roots was strong and its *nifH* gene expression was high substantiating the above discussed results (**Figure 4A**).

Since root exudates from *R. mangle* might attract Gal22 cells and foster high $N_2$-fixation, our results may hint at a potentially mutualistic relationship between the diazotroph *M. mangrovicola* Gal22 and *R. mangle*. As shown by Ravikumar et al. (2004) some $N_2$-fixers are beneficial for mangroves plants increasing root and shoot biomass and leaf area. *M. mangrovicola* Gal22 has proven to be a versatile organism being successful in competing and surviving for long periods in mangrove soil (**Supplementary Table S1**) making it a good candidate for *in vitro* studies and potentially for field studies. Its nitrogen fixation is high when colonizing mangrove roots and the organism can be genetically manipulated. Due to the above mentioned qualities, we proposed *M. mangrovicola* Gal22 as a model organism to study molecular interactions between $N_2$-fixers and mangrove plants. Further studies aiming to address the type of symbiotic relationship should focus on the transfer of the fixated nitrogen from Gal22 to the plant and on the molecular and cellular signaling between both interaction partners. With the described model interaction system a basis for future investigations has been established.

## REFERENCES

Alfaro-Espinoza, G., and Ullrich, M. S. (2014). *Marinobacterium mangrovicola* sp. nov., a marine nitrogen-fixing bacterium isolated from mangrove roots of *Rhizophora mangle*. *Int. J. Syst. Evol. Microbiol.* 64, 3988–3993. doi:10.1099/ijs.0.067462-0.

Bagdasarian, M., Lurz, R., Rückert, B., Franklin, F. C. H., Bagdasarian, M. M., Frey, J., and Timmis, K. N. (1981). Specific-purpose plasmid cloning vectors II. Broad host range, high copy number, RSFlOlO-derived vectors, and a host-vector system for gene cloning in Pseudomonas. *Gene* 16, 237–247.

Bartolomé, B., Jubete, Y., Martínez, E., and de la Cruz, F. (1991). Construction and properties of a family of pACYC184-derived cloning vectors compatible with pBR322 and its derivatives. *Gene* 102, 75–78.

Bashan, Y., and Holguin, G. (2002). Plant growth-promoting bacteria: a potential tool for arid mangrove reforestation. *Trees* 16, 159–166. doi:10.1007/s00468-001-0152-4.

Bashan, Y., Puente, M. E., Myrold, D. D., and Toledo, G. (1998). In vitro transfer of fixed nitrogen from diazotrophic filamentous cyanobacteria to black mangrove seedlings. *FEMS Microbiol. Ecol.* 26, 165–170.

Boto, K., and Robertson, I. (1990). The relationship between nitrogen fixation and tidal exports of nitrogen in a tropical mangrove system. *Estuar. Coast. Shelf Sci.* 31, 531–540.

Bouillon, S., Borges, A. V., Castañeda-Moya, E., Diele, K., Dittmar, T., Duke, N. C., Kristensen, E., Lee, S. Y., Marchand, C., Middelburg, J. J., et al. (2008). Mangrove production and carbon sinks: A revision of global budget estimates. *Global Biogeochem. Cycles* 22, 1–12. doi:10.1029/2007GB003052.

Dahdouh-Guebas, F., Jayatissa, L. P., Di Nitto, D., Bosire, J. O., Lo Seen, D., and Koedam, N. (2005). How effective were mangroves as a defence against the recent tsunami? *Curr. Biol.* 15, R443–R447. doi:10.1016/j.cub.2005.06.008.

Donato, D. C., Kauffman, J. B., Murdiyarso, D., Kurnianto, S., Stidham, M., and Kanninen, M. (2011). Mangroves among the most carbon-rich forests in the tropics. *Nat. Geosci.* 4, 293–297. doi:10.1038/ngeo1123.

Egener, T., Hurek, T., and Reinhold-hurek, B. (1999). Endophytic expression of *nif* Genes of *Azoarcus sp*. strain BH72 in rice roots. *Mol. Plant. Microbe. Interact.* 12, 813–819.

Feller, I. C., Lovelock, C. E., Berger, U., Mckee, K. L., Joye, S. B., and Ball, M. C. (2010). Biocomplexity in mangrove ecosystems. *Ann. Rev. Mar. Sci.* 2, 395–417. doi:10.1146/annurev.marine.010908.163809.

Feller, I. C., Mckee, K. L., Whigham, D. F., and Neill, J. P. O. (2002). Nitrogen vs. phosphorus limitation across an ecotonal gradient in a mangrove forest. *Biogeochemistry* 62, 145–175.

Flores-Mireles, A. L., Winans, S. C., and Holguin, G. (2007). Molecular characterization of diazotrophic and denitrifying bacteria associated with mangrove roots. *Appl. Environ. Microbiol.* 73, 7308–7321. doi:10.1128/AEM.01892-06.

Gotto, J. W., and Taylor, B. F. (1976). $N_2$ fixation associated with decaying leaves of the red mangrove (*Rhizophora mangle*). *Appl. Environ. Microbiol.* 31, 781–783.

Hamashitna, H., Iwasaki, M., and Taketoshi, A. (1995). "A simple and rapid method for transformation of Vibrio species by electroporation," in *Methods in Molecular Biology, Vol.47: Electroporation protocols for microorganisms*, ed. J. A. Nickoloff (Totowa, NJ: Humana Press Inc), 155–160.

Hanahan, D. (1985). "Techniques for transformation of *E. coli*," in *DNA cloning: a practical approach. Vol. 1.*, ed. D. M. Glover (Oxford, United Kindgdom: IRL Press), 109–135.

Hicks, B. J., and Silvester, W. B. (1985). Nitrogen fixation associated with the New Zealand mangrove (*Avicennia marina* (Forsk.) Vierh. var. *resinifera* (Forst. f.) Bakh.). *Appl. Environ. Microbiol.* 49, 955–959.

Hoang, T. T., Karkhoff-Schweizer, R. R., Kutchma, a J., and Schweizer, H. P. (1998). A broad-host-range Flp-FRT recombination system for site-specific excision of chromosomally-located DNA sequences: application for isolation of unmarked *Pseudomonas aeruginosa* mutants. *Gene* 212, 77–86.

Holguin, G., Guzman, M. A., and Bashan, Y. (1992). Two new nitrogen-fixing bacteria from the rhizosphere of mangrove trees: Their isolation, identification and in vitro interaction with rhizosphere *Staphylococcus sp. FEMS Microbiol. Ecol.* 101, 207–216. doi:10.1016/0168-6496(92)90037-T.

Holguin, G., Vazquez, P., and Bashan, Y. (2001). The role of sediment microorganisms in the productivity, conservation, and rehabilitation of mangrove ecosystems: an overview. *Biol. Fertil. Soils* 33, 265–278. doi:10.1007/s003740000319.

Jones, D. L. (1998). Organic acids in the rhizosphere – a critical review. *Plant Soil* 205, 25–44.

Kamilova, F., Kravchenko, L. V, Shaposhnikov, A. I., Azarova, T., Makarova, N., and Lugtenberg, B. (2006). Organic acids, sugars, and L-tryptophane in exudates of vegetables growing on stonewool and their effects on activities of rhizosphere bacteria. *Mol. Plant. Microbe. Interact.* 19, 250–256. doi:10.1094/MPMI-19-0250.

Kovach, M. E., Elzer, P. H., Hill, D. S., Robertson, G. T., Farris, M. a, Roop, R. M., and Peterson, K. M. (1995). Four new derivatives of the broad-host-range cloning vector pBBR1MCS, carrying different antibiotic-resistance cassettes. *Gene* 166, 175–176.

Kovach, M. E., Phillips, R., Elzer, P. H., Roop, R. M., and Peterson, K. M. (1994). pBBR1MCS: a broad-host-range cloning vector. *Biotechniques* 16, 800–802.

Mulholland, M. R., and Capone, D. G. (2000). The nitrogen physiology of the marine $N_2$-fixing cyanobacteria *Trichodesmium spp*. *Trends Plant Sci.* 5, 148–53.

Pelegrí, S., Rivera-monroy, V., and Twilley, R. (1997). A comparison of nitrogen fixation (acetylene reduction) among three species of mangrove litter, sediments, and pneumatophores in south Florida, USA. *Hidrobiología* 356, 73–79.

Ravikumar, S., Kathiresan, K., Ignatiammal, S. T. M., Babu Selvam, M., and Shanthy, S. (2004). Nitrogen-fixing azotobacters from mangrove habitat and their utility as marine biofertilizers. *J. Exp. Mar. Bio. Ecol.* 312, 5–17. doi:10.1016/j.jembe.2004.05.020.

Reef, R., Feller, I. C., and Lovelock, C. E. (2010). Nutrition of mangroves. *Tree Physiol.* 30, 1148–1160. doi:10.1093/treephys/tpq048.

Rudrappa, T., Czymmek, K. J., Paré, P. W., and Bais, H. P. (2008). Root-secreted malic acid recruits beneficial soil bacteria. *Plant Physiol.* 148, 1547–1556. doi:10.1104/pp.108.127613.

Schenk, A., Weingart, H., and Ullrich, M. S. (2008). Extraction of high-quality bacterial RNA from infected leaf tissue for bacterial *in planta* gene expression analysis by multiplexed fluorescent Northern hybridization. *Mol. Plant Pathol.* 9, 227–235. doi:10.1111/J.1364-3703.2007.00452.X.

Sengupta, A., and Chaudhuri, S. (1991). Ecology of heterotrophic dinitrogen fixation in the rhizosphere of mangrove plant community at the Ganges river estuary in India. *Oecologia* 87, 560–564.

Thoma, S., and Schobert, M. (2009). An improved *Escherichia coli* donor strain for diparental mating. *FEMS Microbiol. Lett.* 294, 127–132. doi:10.1111/j.1574-6968.2009.01556.x.

Toledo, G., Bashan, Y., and Soeldner, A. (1995). *In vitro* colonization and increase in nitrogen fixation of seedling roots of black mangrove inoculated by a filamentous cyanobacteria. *Can. J. Microbiol.* 41, 1012–1020. doi:10.1139/m95-140.

Uchino, F., Hambali, G. G., and Yatazawa, M. (1984). Nitrogen-fixing bacteria from warty lenticellate bark of a mangrove tree, *Bruguiera gymnorrhiza* (L.) Lamk. *Appl. Environ. Microbiol.* 47, 44–48.

Vieira, J., and Messing, J. (1991). New pUC-derived cloning vectors with different selectable markers and DNA replication origins. *Gene* 100, 189–194.

Wang, H., and Griffiths, M. W. (2009). $Mg^{2+}$-free buffer elevates transformation efficiency of *Vibrio parahaemolyticus* by electroporation. *Lett. Appl. Microbiol.* 48, 349–354. doi:10.1111/j.1472-765X.2008.02531.x.

Wilson, K. J., Sessitsch, A., Corbo, J. C., Giller, K. E., Akkermans, a D., and Jefferson, R. a (1995). β-Glucuronidase (GUS) transposons for ecological and genetic studies of rhizobia and other Gram-negative bacteria. *Microbiology* 141, 1691–1705.

Woitchik, A. F., Ohowa, B., Kazungu, J. M., Rao, R. G., Goeyens, L., and Dehairs, F. (1997). Nitrogen enrichment during decomposition of mangrove leaf litter in an east African coastal lagoon (Kenya): Relative importance of biological nitrogen fixation. *Biogeochemistry* 39, 15–35.

Zehr, J. P., Jenkins, B. D., Short, S. M., and Steward, G. F. (2003). Nitrogenase gene diversity and microbial community structure: a cross-system comparison. *Environ. Microbiol.* 5, 539–554.

Zehr, J. P., and McReynolds, L. a (1989). Use of degenerate oligonucleotides for amplification of the *nifH* gene from the marine cyanobacterium *Trichodesmium thiebautii*. *Appl. Environ. Microbiol.* 55, 2522–2526.

Zhang, Y., Dong, J., Yang, Z., Zhang, S., and Wang, Y. (2008). Phylogenetic diversity of nitrogen-fixing bacteria in mangrove sediments assessed by PCR-denaturing gradient gel electrophoresis. *Arch. Microbiol.* 190, 19–28. doi:10.1007/s00203-008-0359-5.

Zuberer, D. A., and Silver, W. S. (1978). Biological dinitrogen fixation (acetylene reduction) associated with Florida mangroves. *Appl. Environ. Microbiol.* 35, 567–575.

## SUPPLEMENTARY MATERIAL

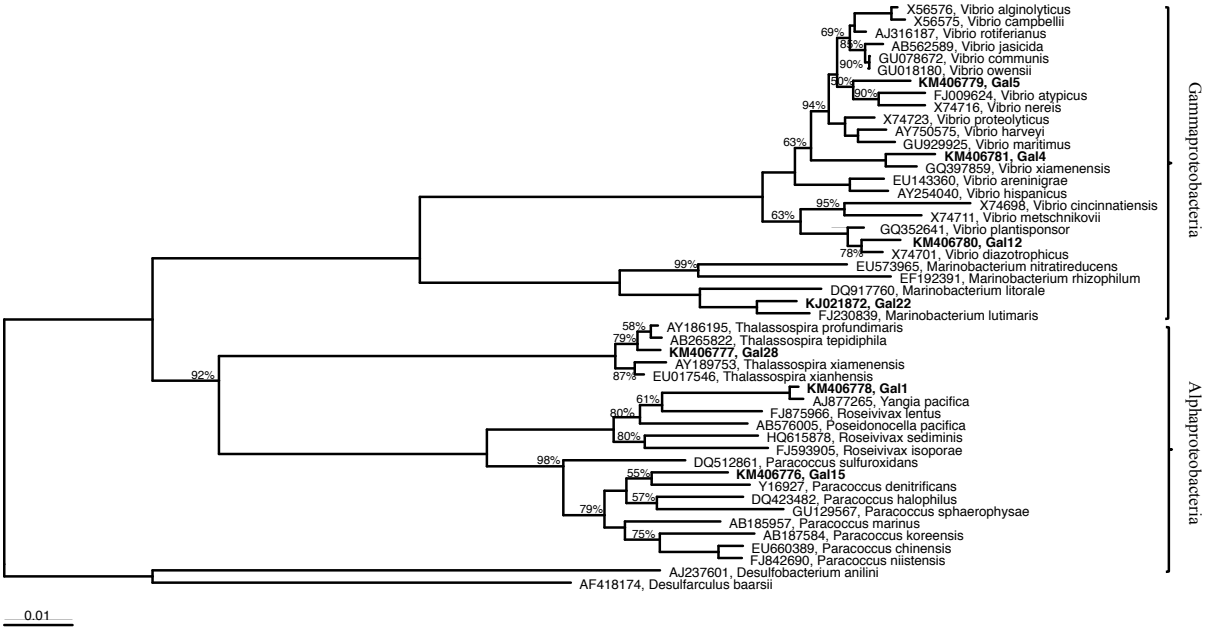


**Supplementary Figure S1**. Phylogenetic tree based on neighbor-joining method using 16S rRNA gene sequences. Bootstrap values of >50 % after 1.000 simulations are shown at the respective nodes. Bar, 0.01 substitutions per nucleotide position. Deltaproteobacteria sequences were used as outgroup.

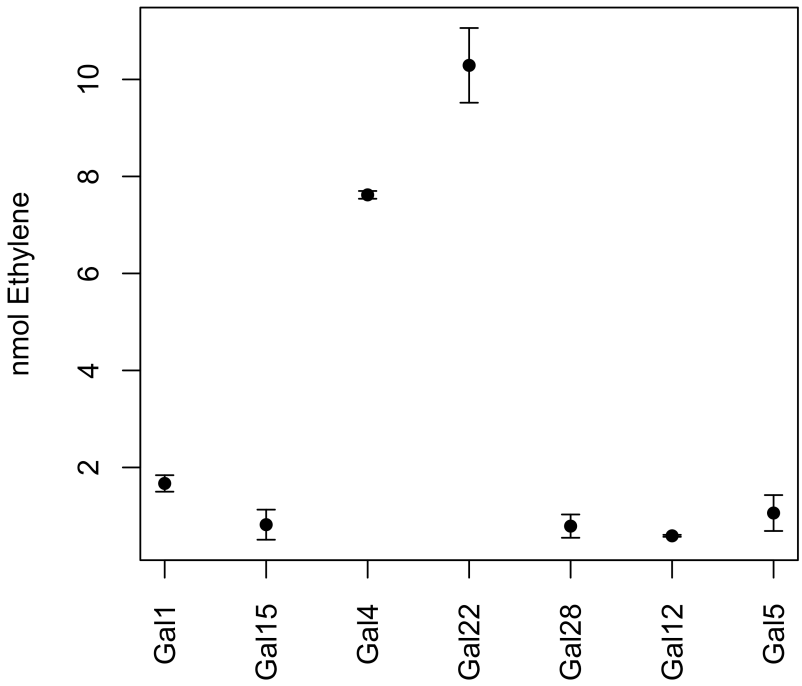


**Supplementary Figure S2**. Acetylene reduction assay of seven bacterial strains isolated from *Rhizophora mangle* roots.

**Supplementary Table S1**. Fitness Test: Organisms, isolates and sediment-born bacteria, recovered from mangrove roots and rhizosphere after one month of incubation.

| **Recovered Organisms*** | **Sample 1** | **Sample 2** | **Sample 3** | **Control** (No bacterial isolates added) |
|---|---|---|---|---|
| Isolate Gal12 | + | + | + | – |
| Isolate Gal22 | + | + | + | – |
| Isolate Gal4 | – | + | – | – |
| *Pseudoalteromonas sp.* | – | – | – | + |
| *Vibrio alginolyticus* | + | + | – | + |
| *Vibrio sp.* | + | + | + | + |
| *Bacillus sp.* | – | – | – | + |
| *Mangroveibacter sp.* | – | + | + | + |
| *Vibrio diazotrophicus* | + | + | + | + |
| *Zobellella denitrificans* | – | – | – | + |
| *Vibrio rhizosphaerae* | – | – | + | – |

+, organism found in the sample; **–**, organism absent in the sample
*16S rRNA sequences of recovered organisms were BLAST in NCBI database.

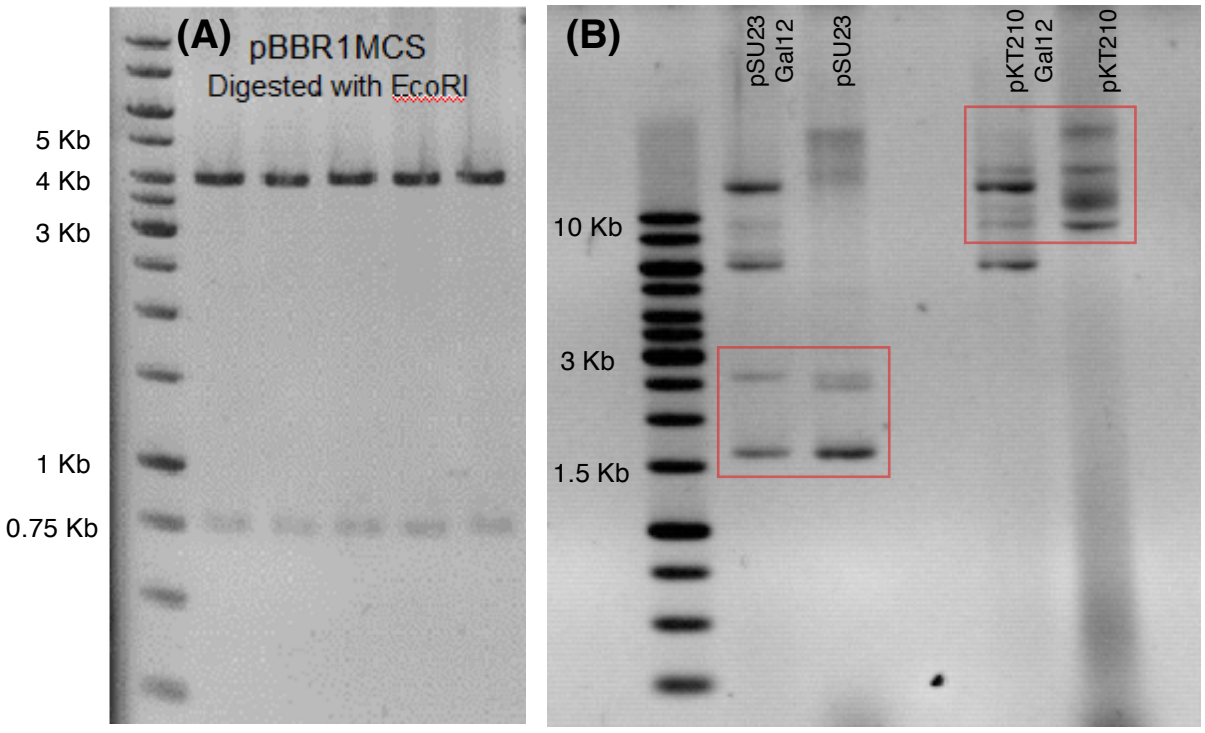


**Supplementary Figure S3**. **(A)** Electrophoresis gel showing plasmid pBBR1MCS after EcoRI treatment. pBBR1MCS was introduced in isolate Gal22 by conjugation. **(B)** Electrophoresis gel of isolate Gal12 transformed by electroporation with pSU23 and pKT210 plasmids. An undigested empty vector was run next to the undigested vector isolated from isolate Gal12. Bands within the red box correspond to the recombinant plasmid, while bands outside the red box correspond to the native plasmids.

# 3.2 *Marinobacterium mangrovicola* sp. nov., a marine nitrogen-fixing bacterium isolated from mangrove roots of *Rhizophora mangle*

**The following manuscript was published in International Journal of Systematic and Evolutionary Microbiology (2014) 64, 3988–3993. doi:10.1099/ijs.0.067462-0**

# *Marinobacterium mangrovicola* sp. nov., a marine nitrogen-fixing bacterium isolated from mangrove roots of *Rhizophora mangle*

Gabriela Alfaro-Espinoza* and Matthias S. Ullrich
Jacobs University Bremen, Molecular Life Science Research Center, Campus Ring 1, 28759 Bremen, Germany

*Corresponding author: Gabriela Alfaro-Espinoza; m.alfaroespinoza@jacobs-university.de

Running title: Description of the novel species *Marinobacterium mangrovicola*

Abbreviations: PSU, practical salinity unit; PBS, phosphate buffered saline; ARA, acetylene reduction assay; PHB, poly-β-hydroxybutyrate.

The GenBank accession number for the 16S rRNA and *nifH* gene sequences of strain Gal22$^T$ are KJ021872 and KJ021871 respectively, and for *nifH* gene sequence of strain DSM 22012$^T$ is KJ021873.

---

**ABSTRACT**

A nitrogen-fixing marine bacterium, designated strain Gal22$^T$, was isolated from mangrove roots of *Rhizophora mangle*. Cells were Gram-negative rods, motile with a single polar flagellum. Growth was observed at 4–42 ºC, pH 5.5 to 10 and 0–18 % (w/v) NaCl. Strain Gal22$^T$ was positive for catalase and oxidase. Q-8 was the predominant lipoquinone. The DNA G+C content was 57.0 mol%. Based on phylogenetic analysis of 16S rRNA gene, strain Gal22$^T$ belongs to the genus *Marinobacterium*. The closely related strains were *Marinobacterium lutimaris* DSM 22012$^T$ and *Marinobacterium litorale* IMCC1877$^T$ with 99 % and 96 % sequence similarity, respectively. DNA-DNA relatedness analysis indicated that strain Gal22$^T$ was different from *M. lutimaris* DSM 22012$^T$. On the basis of genotypic, morphological and biochemical characteristics, a novel type species *Marinobacterium mangrovicola* sp. nov. (type strain, Gal22$^T$ =DSM 27697$^T$ =CIP 110653$^T$) is proposed.

---

The word mangrove refers to a characteristic group of trees and shrubs usually found in coastal and depositional environments of rivers and estuaries (Tomlinson, 1986). Mangrove ecosystems are widely recognized for a) being highly productive systems, playing an important role in the sequestration of atmospheric $CO_2$ (Donato *et al.*, 2011), b) acting as a barrier for sediments, providing coastal protection to erosion and natural disasters, and c) sustaining a high biodiversity and acting as a nursery ground for many economical important species (Aburto-Oropeza *et al.*, 2008; Duke *et al.*, 2007). Not so broadly recognized are the

very important remineralization processes that occur in mangrove ecosystems. A variety of microorganisms that lay on mangrove sediments and rhizosphere, such as denitrifiers and nitrogen fixers, are involve in these remineralization processes controlling the chemical environment of such ecosystems (Reef *et al.*, 2010).

Nitrogen fixing bacteria inhabiting mangroves play an important role in nutrient transformation. High rates of nitrogen fixation have been found in these ecosystems (Holguin *et al.*, 2001; Lee & Joye, 2006); in addition, some nitrogen fixers are able to interact with mangrove roots making nitrogen available for plants (Bashan *et al.*, 1998). Although, nitrogen fixation is a very important process in mangrove ecosystems, very little is known about these microorganisms and their colonization strategies or their physiological impacts on mangrove plants. In the course of investigations into the role of diazotrophs that inhabit mangrove sediments and roots, a novel nitrogen-fixing bacterium, strain Gal22$^T$, was isolated from roots of a mangrove plant.

Nitrogen fixation rates have not been reported within the genus *Marinobacterium*. This genus belongs to the *Gammaproteobacteria* and currently comprises 12 species isolated from different marine environments such as a salt marsh on the coast of Georgia (González *et al.*, 1997), sea water of Hawaii (Baumann *et al.*, 1983; Bowditch *et al.*, 1984; Satomi *et al.*, 2002), tidal flats of Korea (Chang *et al.*, 2007; Kim *et al.*, 2010), surface water of the Yellow Sea (Kim *et al.*, 2007; Kim *et al.*, 2009a), rhizosphere of a coastal plant (*Suaeda japonica*) in Korea (Kim *et al.*, 2008), marine sediment of East China Sea (Huo *et al.*, 2009), Artic marine sediment (Kim *et al.*, 2009b) and mucus of a reef builder coral from Brazil (Chimetto *et al.*, 2011).

Strain Gal22$^T$ was isolated from mangrove roots of *Rhizophora mangle*, cultivated in an aquarium (*in vitro* mangrove ecosystem). The *in vitro* ecosystem consisted of mangrove seedlings grown in pots containing autoclaved sand (Carl Roth) mixed with 1/10 volume of sand coming from a natural mangrove ecosystem (mangrove mud special. Marek mangroven, Austria). The pots were kept in an aquarium filled with marine water (marine salt mixture. Tropic Marine, Dr Biener GmbH, Aquarientechnik, Germany). The salinity and temperature of the marine water were 30 PSU (practical salinity unit) and 25-28 ºC. The mangroves were exposed to 12 h light: 12 h dark photoperiod. Root material from seedlings of *Rhizophora mangle* was cut into 3 cm segments and serially rinsed in sterile marine water. Root tissues were homogenized with a mortar and pestle in 50 ml nitrogen-free HGB medium [g $l^{-1}$: 20 NaCl, 3 $MgSO_4.7H_2O$, 0.02 CaCl, 5 DL-malic acid, 3 NaOH, 10 ml trace elements solution (for 500 ml: 0.5 g $FeCl_3$, 0.1 g $NaMoO_4.2H_2O$, 0.105 g $MnSO_4$, 0.14 g $H_3BO_4$, 1.4 mg $CuCl.2H_2O$, 12 mg $ZnSO_4$), 100 ml of 0.39 M phosphate buffered saline (PBS, added separately to the medium after autoclaving), pH 7.2] (Holguin *et al.*, 1992). The homogenized tissues were subjected to dilution series. 1 ml of the most diluted samples was used for inoculation of 9 ml nitrogen-free HGB medium supplemented with 0.3 % agar (semi-solid). Samples were incubated under microaerophilic conditions at 28 °C for 5 days. After incubation, colonies were picked using a sterile Pasteur pipette and streaked on HGB plates supplemented with 0.1 % yeast extract. The strain Gal22$^T$ was further purified and stored at -80 ºC in HGB media with 15 % (v/v) glycerol.

Colony morphology analysis of Gal22$^T$ and the closely related strains *M. lutimaris* DSM 22012$^T$ and *M. litorale* DSM 23545$^T$ (obtained from Leibniz-Institute DSMZ - Deutsche Sammlung von Mikroorganismen und Zellkulturen GmbH, Braunschweig, Germany) were carried out on marine agar after 24 h. Gram staining, cell motility and morphology were examined by phase-contrast microscopy (Axiostar plus, Zeiss) and transmission electron microscopy (EM900, Zeiss). Liquid HGB medium supplemented with 0.1 % yeast extract was used for growth determination at different temperatures (5–45 ºC) and pH. The different pH range was adjusted by adding NaOH or HCl to the media. Different buffers were used to keep the pH constant, 50 mM $l^{-1}$ of MES (pH 5–6.5), HEPES (pH 7–8), Tris (pH 8.5–9) or CAPS (pH 9.5–11). Liquid HGB medium and modified artificial seawater [$l^{-1}$: 0.15 g $CaCl_2$, 0.2 g KB, 0.75 g KCl, 1 g $MgCl_2.6H_2O$, 4.93 g $MgSO_4.7H_2O$, pH 7.2] (Seymour *et al.*, 2008) supplemented with 2.5 g peptone and 1 g yeast extract were used to determine NaCl tolerance. The range of NaCl tolerance or requirement was determined by adding 0–20 % (w/v) NaCl, at 0.5 % intervals, to the media. The salinity in both media was 10 PSU, without the addition of NaCl.

Nitrogen fixation was confirmed by the acetylene reduction assay (ARA). Cells were incubated at 30 ºC, 200 rpm in 1-liter Erlenmeyer flasks with 60 ml N-free HGB medium. The flasks were sealed with rubber septa, and the headspace was adjusted to 1 % $O_2$ and 5 % acetylene. Ethylene production was measured in a gas chromatograph equipped with a Porapak N 80/100 mesh size column and a hydrogen flame-ionization detector. Likewise, the *nifH* gene sequence encoding for nitrogenase reductase was amplified by PCR. The primers nif-F1 and nif-R1 used to amplify the *nifH* gene of strains Gal22$^T$ and DSM 22012$^T$ were designed using the *nifH* gene sequence from a genomic library of strain Gal22$^T$. The PCR reaction was carried out in a final volume of 50 µl containing 1 pmol of primers nif-F1 (AATCTACGGAAAAGGCGGCA) and nif-R1 (GCGTCTTCCTCGTCCATGAT), 1X ThermoPol reaction buffer (New England BioLabs), 0.2 mM dNTP's (Thermo scientific), 1.25 U Vent DNA polymerase (New England BioLabs) and DNA template (obtained via colony PCR). The thermal program consisted of 2 min at 94 °C for initial denaturation, 30 cycles of 15 s at 94 °C for denaturation, 30 s at 59 °C for annealing and 40 s at 72 °C for extension. 7 min at 72 °C was used for a final extension. The PCR product was further sequenced.

Biochemical characteristics such as carbon utilization and enzyme activity were determined with the GN2 microplate system (Biolog), API 20 NE (bioMérieux) and API ZYM strips (bioMérieux) with artificial seawater (Kim*, et al.*, 2007) and according to the manufacturer's instructions. The reference strains *M. lutimaris* DSM 22012$^T$ and *M. litorale* DSM 23545$^T$ were included in the analysis.

The susceptibility to the following antibiotics was tested by the agar diffusion assay (Jorgensen & Turnidge, 2007): ampicillin (10 µg), tetracycline (30 µg), gentamicin (30 µg), chloramphenicol (25 µg), streptomycin (10 µg), erythromycin (15 µg) and kanamycin (30 µg). Catalase activity was tested in fresh cells by the addition of 3% hydrogen peroxide. 1 % (w/v) N,N,N′,N′-tetramethyl-ρ-phenylenediamine dihydrochloride (Sigma-Aldrich) was used to determine Oxidase activity (Kovacs, 1956). Poly-β-hydroxybutyrate (PHB) granules were verified using Nile blue A staining (Ostle & Holt, 1982). Stained cells were visualized in an Axioplan 2 fluorescence microscope (Carl Zeiss).

The G+C content of the genomic DNA, quinones and fatty acids analysis of strain Gal22$^T$ were carried out by Leibniz-Institute DSMZ. Analysis of G+C content of genomic DNA was conducted as described by Cashion *et al.* (1977), Mesbah *et al.* (1989) and Tamaoka & Komagata (1984). Respiratory lipoquinones were extracted and analyzed using the method described by Tindall (1990a, b). Fatty acids were obtained from 30 mg freeze dried cells by saponification, methylation and extraction according to Kuykendall *et al.* (1988) and Miller (1982), using minor modifications of the method. The separation and analysis were performed by using the Sherlock Microbial Identification System (MIS) (MIDI, Microbial ID, Newark, DE 19711 U.S.A.).

For phylogenetic analysis, genomic DNA was prepared by boiling 1 colony at 95 ºC for 10 min in 15 µl nuclease free water. The lysates cells were centrifuged, 1 µl of the supernatant containing the genomic DNA was used to PCR amplify the 16S rRNA gene. PCR of this gene was carried out using the 16S rRNA universal primers (5'-AGAGTTTGATCCTGGCTCAG-3' and 5'-TACGGYTACCTTGTTACGACTT-3'). The amplification product was sequenced on an ABI377 sequencer instrument and according to the manufacturer's recommendation (Applied Biosystems, USA). The 16S rRNA sequence was analyzed with the ARB software (Ludwig *et al.*, 2004) and the Living Tree Project database provided the reference alignment (Yarza *et al.*, 2008). The following methods, neighbor-joining, maximum-likelihood and maximum-parsimony were used to construct the phylogenetic trees.

DNA-DNA hybridization was performed in duplicate by Leibniz-Institute DSMZ. The hybridization test was carried out with the strains that share >97 % 16S rRNA gene sequence similarity (Stackebrandt & Goebel, 1994; Tindall *et al.*, 2010), in this case only with *M. lutimaris* DSM 22012$^T$. The DNA was purified as described by Cashion*, et al.* (1977) and the hybridization was conducted as described by De Ley *et al.* (1970) and Huss *et al.* (1983).

Cells of isolate Gal22$^T$ were Gram-negative rods (approximately 1.5–2 µm long and 0.7–0.85 µm wide) with a single polar flagellum (**Fig. 1**). Colonies were convex, circular, cream-colored and bigger in size (1 mm) than that of *M. lutimaris* DSM 22012$^T$ (0.8 mm) and *M. litorale* DSM 23545$^T$ (0.3 mm). Growth of isolate Gal22$^T$ was observed from 4 ºC to 42 ºC, but not at temperatures above 42 ºC. The optimal growth temperatures were 28–37 ºC. It grew at a pH range of 5.5 to 10, (optimum from pH 6.5–8) and in the presence of 0–18 % (w/v) NaCl (optimum from 1–4 %). Growth in 18 % (w/v) NaCl was observed after 7 days of incubation. The high salinity tolerance showed by this bacterium could be an adaptation to the inhabiting environment. In mangrove ecosystems, salinity concentrations can increase on the sediments due to changes in the tides and evaporation (Feller *et al.*, 2010). Strain Gal22$^T$ grows at higher salinity than *M. lutimaris* DSM 22012$^T$ and *M. litorale* DSM 23545$^T$, 15 % and 14 % (w/v) NaCl respectively. However, Kim*, et al.* (2010) and Kim*, et al.* (2007) reported lower salinity tolerance for *M. lutimaris* DSM 22012$^T$ and *M. litorale* DSM 23545$^T$, respectively. This contradiction might be due to time of incubation.

The presence of the *nifH* gene together with the ARA test (**Supplementary Fig. S1**), confirmed the ability of strain Gal22$^T$ to fix atmospheric nitrogen. The *nifH* sequence was compared with sequences from the two closely related strains. Therefore, the strain Gal22$^T$ had 93 % and 90 % *nifH* gene sequence similarity with *M. lutimaris* DSM 22012$^T$ (GenBank accession number KJ021873) and *M. litorale* DSM 23545$^T$ (GenBank accession number AUAZ01000022, G403DRAFT_scaffold00021.21_C), respectively. The phenotypic characteristics that differentiate Gal22$^T$ from other *Marinobacterium* species are listed in

Table 1. Gal22$^T$ is susceptible to tetracycline, gentamicin, chloramphenicol, streptomycin, erythromycin and kanamycin, but resistant to ampicillin. The production of PHB was positive (**Supplementary Fig. S2**). Oxidase- and catalase-positive. The G+C content of genomic DNA was 57.0 mol%. The major quinone was Q-8, which is in accordance with that of other *Marinobacterium* species. The predominant fatty acids were $C_{18:1}\omega7c$, $C_{16:0}$, summed feature 3, and $C_{17:0}$ cyclo. Where the last fatty acid was not present in the closely related strain *M. litorale* DSM 23545$^T$ (**Supplementary Table S1**). Since unsaturated fatty acids help to keep membrane fluidity under NaCl stress (Zhou *et al*., 2013), the high percentage of $C_{18:1}\omega7c$ found in strains Gal22$^T$, DSM 22012$^T$ and DSM 23545$^T$ (Supplementary Table S1) could be playing a role in NaCl tolerance.

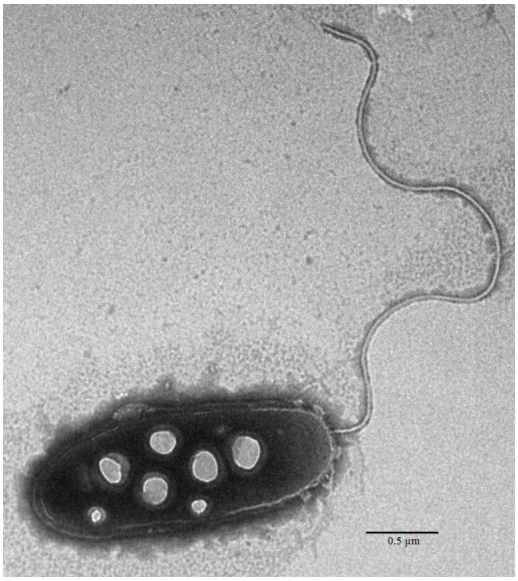


**Fig. 1.** Transmission electron micrograph of the negatively stained Gal22$^T$ cells, showing the PHB granules.

Phylogenetic analysis based on 16S rRNA gene indicates that the strain Gal22$^T$ was affiliated to the genus *Marinobacterium*. Strain Gal22$^T$ shows a coherent cluster with the closest related strains *M. lutimaris* AN9$^T$ (99 % sequence similarity) and *M. litorale* IMCC1877$^T$ (96 % sequence similarity). Gal22$^T$ shows <97 % sequence similarity to other described species within the genus *Marinobacterium*. Neighbor-joining and maximum-likelihood trees showed a similar overall topology as that of the maximum-parsimony tree (**Fig. 2**).

Values of DNA-DNA hybridization between Gal22$^T$ and *M. lutimaris* DSM 22012$^T$ were 51.1 % and 59.7 % (duplicate). Based on morphological and biochemical characteristics (**Table 1**), DNA-DNA relatedness and the 16S rRNA gene sequence similarity, the strain Gal22$^T$ represents a novel species within the genus *Marinobacterium*.

**Table 1.** Phenotypic characteristics that differentiate Gal22$^T$ from other related *Marinobacterium* species.

Strains: 1, Gal22$^T$; 2, *M. lutimaris* DSM 22012$^T$; 3, *M. litorale* DSM 23545$^T$; 4, *M. marisflavi* IMCC4074$^T$ (data from Kim *et al*., 2009); 5, *M. nitratireducens* CN44$^T$ (data from Huo *et al*., 2009). All strains are motile, Q-8 is the predominant quinone, oxidase and esterase lipase (C8) positive. +, Positive; –, negative; w, weakly positive; ND, no data available.

| **Characteristic** | **1** | **2** | **3** | **4** | **5** |
|---|---|---|---|---|---|
| PHB accumulation | + | w | – | – | + |
| Growth at/in: | | | | | |
| 4°C | + | –† | –¶ | – | – |
| 42°C | + | –† | +¶ | + | – |
| 18% NaCl | + | – | – | – | – |
| pH 10 | + | –† | +¶ | + | – |
| Susceptible to: | | | | | |
| Ampicillin (10 µg) | – | + | + | + | + |
| Kanamycin (30 µg) | + | + | + | – | + |
| Enzyme activity: | | | | | |
| Catalase | + | + | + | – | + |
| α-glucosidase | – | – | – | – | + |
| Naphthol-AS-BI-phosphohydrolase | w | + | – | – | – |
| Urease | + | +* | + | + | – |
| Assimilation of: | | | | | |
| Malate | + | +* | +* | – | + |
| D-Glucose | – | – | – | – | + |
| ρ-Hydroxyphenylacetic acid | – | + | + | – | ND |
| L-Aspartic acid | w | –§ | – | + | + |
| Sucrose | – | – | – | – | + |
| DNA G+C content (mol%) | 57.0 | 58.0† | 60.7¶ | 56.0 | 62.5 |

*Negative according to Kim *et al.*, 2010 and Kim *et al*, 2007.
§Positive according to Kim *et al.*, 2010.
†Data from Kim *et al*., 2010 ; ¶ Data from Kim *et al*., 2007

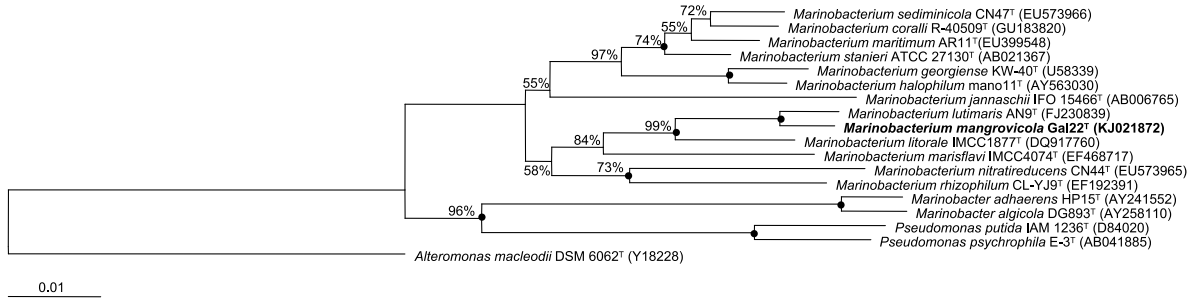


**Fig. 2.** Neighbor-joining 16S rRNA gene tree showing the phylogenetic relationship of *Marinobacterium mangrovicola* Gal22$^T$ and related taxa. Bootstrap values (>55 %) performed with 1000 repetitions are shown. Bootstrap values of >60 % recovered with maximum-likelihood and maximum-parsimony trees are shown with black circles. Bar, 0.01 substitutions per nucleotide position.

## Description of *Marinobacterium mangrovicola* sp. nov.

*Marinobacterium mangrovicola* (man.gro.vi´co.la. N.L. n. *mangrovum*, mangrove; L. suff. *cola* inhabitant, dweller; N.L. n. *mangrovicola* mangrove inhabitant).

The cells are Gram-negative, rods (1.5–2 μm long) and motile. Colonies on MB are of 1 mm size, cream-colored, convex and with a smooth edge. Growth occurs at pH range of 5.5 to 10, (optimum at pH 6.5–8). Temperature ranges and NaCl concentrations for growth are 4–42 ºC and 0–18 % (w/v), with optimum at 28–37 ºC and 1–4 % NaCl. Capable of nitrogen-fixation under microaerophilic conditions. Positive for the following substrates of the Biolog GN2 microplates: glycogen, methyl pyruvate, mono-methyl-succinate, acetic acid, *cis*-aconitic acid, citric acid, formic acid, β-hydroxy butyric acid, α-keto glutaric acid, D,L-lactic acid, malonic acid, propionic acid, quinic acid, succinic acid, bromosuccinic acid, succinamic acid, L-alaninamide, D- and L-alanine, L-asparagine, L-glutamic acid, L-proline, L-serine and putrescine. Tween 40, L-aspartic acid, L-pyroglutamic acid, and γ-amino butyric acid are utilized weakly. The following enzymatic activities are present: alkaline phosphatase, esterase (C 4), esterase lipase (C 8), leucine arylamidase and acid phosphatase. Weak enzyme activity for valine arylamidase, naphthol-AS-BI-phosphohydrolase and the reduction of nitrates to nitrites. Positive for urease activity, malate and trisodium citrate assimilation. Indole production, glucose fermentation, β-glucoronidase, β-galactosidase, arginine dihydrolase, esculin and gelatin hydrolysis are negative. Oxidase- and catalase-positive. The DNA G+C content is 57.0 mol%. Q-8 is the mayor lipoquinone. The fatty acids profile comprising >5 % of the total are composed of $C_{18:1}\omega 7c$, $C_{16:0}$, $C_{17:0}$ cyclo and summed feature 3 ($C_{16:1}\omega 7c$ and/or iso-$C_{15:0}$ 2-OH).

The type strain Gal22$^T$ (=DSM 27697$^T$ =CIP 110653$^T$) was isolated from mangrove roots of *Rhizophora mangle*.

**ACKNOWLEDGMENTS**

We thank Prof. Jens Harder and Prof. Barbara Reinhold-Hurek for their support with sequencing and ARA test respectively.

**REFERENCES**

Aburto-Oropeza, O., Ezcurra, E., Danemann, G., Valdez, V., Murray, J. & Sala, E. (2008). Mangroves in the Gulf of California increase fishery yields. *Proc Natl Acad Sci USA* 105, 10456-10459.

Bashan, Y., Puente, M. E., Myrold, D. D. & Toledo, G. (1998). In vitro transfer of fixed nitrogen from diazotrophic filamentous cyanobacteria to black mangrove seedlings. *FEMS Microbiol Ecol* 26, 165-170.

Baumann, P., Bowditch, R. D., Baumann, L. & Beaman, B. (1983). Taxonomy of Marine *Pseudomonas* Species: *P. stanieri* sp. nov.; *P. perfectomarina* sp. nov., nom. rev.; *P. nautica*; and *P. doudorofii*. *Int J Syst Bacteriol* 33, 857-865.

Bowditch, R. D., Baumann, L. & Baumann, P. (1984). Description of *Oceanospirillum kriegii* sp. nov. and *O. jannaschii* sp. nov. and assignment of two species of *Alteromonas* to this genus as *O. commune* comb. nov. and *O. vagum* comb. nov. *Curr Microbiol* 10, 221-230.

Cashion, P., Holderfranklin, M. A., McCully, J. & Franklin, M. (1977). Rapid method for base ratio determination of bacterial DNA. *Anal Biochem* 81, 461-466.

Chang, H.-W., Nam, Y.-D., Kwon, H.-Y., Park, J. R., Lee, J.-S., Yoon, J.-H., An, K.-G. & Bae, J.-W. (2007). *Marinobacterium halophilum* sp. nov., a marine bacterium isolated from the Yellow Sea *Int J Syst Evol Microbiol* 57, 77-80.

Chimetto, L. A., Cleenwerck, I., Brocchi, M., Willems, A., De Vos, P. & Thompson, F. L. (2011). *Marinobacterium coralli* sp. nov., isolated from mucus of coral (*Mussismilia hispida*). *Int J Syst Evol Microbiol* 61, 60-64.

De Ley, J., Cattoir, H. & Reynaerts, A. (1970). The quantitative measurement of DNA hybridization from renaturation rates. *Eur J Biochem* 12, 133-142.

Donato, D. C., Kauffman, J. B., Murdiyarso, D., Kurnianto, S., Stidham, M. & Kanninen, M. (2011). Mangroves among the most carbon-rich forests in the tropics. *Nature Geosci* 4, 293-297.

Duke, N. C., Meynecke, J.-O., Dittmann, S., Ellison, A. M., Anger, K., Berger, U., Cannicci, S., Diele, K., Ewel, K. C. & other authors (2007). A World Without Mangroves? *Science* 317, 41-42.

Feller, I. C., Lovelock, C. E., Berger, U., McKee, K. L., Joye, S. B. & Ball, M. C. (2010). Biocomplexity in Mangrove Ecosystems. *Annu Rev Mar Sci* 2, 395-417.

González, J. M., Mayer, F., Moran, M. A., Hodson, R. E. & Whitman, W. B. (1997). *Microbulbifer hydrolyticus* gen. nov., sp. nov., and *Marinobacterium georgiense* gen. nov., sp. nov., two marine bacteria from a lignin-rich pulp mill waste enrichment community. *Int J Syst Bacteriol* 47, 369-376.

Holguin, G., Guzman, M. A. & Bashan, Y. (1992). Two new nitrogen-fixing bacteria from the rhizosphere of mangrove trees: Their isolation, identification and in vitro interaction with rhizosphere *Staphylococcus sp*. *FEMS Microbiol Ecol* 101, 207-216.

Holguin, G., Vazquez, P. & Bashan, Y. (2001). The role of sediment microorganisms in the productivity, conservation, and rehabilitation of mangrove ecosystems: an overview. *Biol Fertility Soils* 33, 265-278.

Huo, Y.-Y., Xu, X.-W., Cao, Y., Wang, C.-S., Zhu, X.-F., Oren, A. & Wu, M. (2009). *Marinobacterium nitratireducens* sp. nov. and *Marinobacterium sediminicola* sp. nov., isolated from marine sediment. *Int J Syst Evol Microbiol* 59, 1173-1178.

Huss, V. A. R., Festl, H. & Schleifer, K. H. (1983). Studies on the spectrophotometric determination of DNA hybridization from renaturation rates. *Syst Appl Microbiol* 4, 184-192.

Jorgensen, J. & Turnidge, J. (2007). Antibacterial susceptibility tests: dilution and disk diffusion methods. In *Manual of Clinical Microbiology*, pp. 1152-1172. Edited by P. Murray, E. Baron, J. Jorgensen, M. Landry and M. Pfaller. Washington, DC: ASM Press.

Kim, H., Choo, Y.-J., Song, J., Lee, J.-S., Lee, K. C. & Cho, J.-C. (2007). *Marinobacterium litorale* sp. nov. in the order Oceanospirillales. *Int J Syst Evol Microbiol* 57, 1659-1662.

Kim, H., Oh, H.-M., Yang, S.-J., Lee, J.-S., Hong, J.-S. & Cho, J.-C. (2009a). *Marinobacterium marisflavi* sp. nov., Isolated from a Costal Seawater. *Curr Microbiol* 58, 511-515.

Kim, J. M., Lee, S. H., Jung, J. Y. & Jeon, C. O. (2010). *Marinobacterium lutimaris* sp. nov., isolated from a tidal flat. *Int J Syst Evol Microbiol* 60, 1828-1831.

Kim, S.-J., Park, S.-J., Yoon, D.-N., Park, B.-J., Choi, B.-R., Lee, D.-H., Roh, Y. & Rhee, S.-K. (2009b). *Marinobacterium maritimum* sp. nov., a marine bacterium isolated from Arctic sediment. *Int J Syst Evol Microbiol* 59, 3030-3034.

Kim, Y.-G., Jin, Y.-A., Hwang, C. Y. & Cho, B. C. (2008). *Marinobacterium rhizophilum* sp. nov., isolated from the rhizosphere of the coastal tidal-flat plant *Suaeda japonica*. *Int J Syst Evol Microbiol* 58, 164-167.

Kovacs, N. (1956). Identification of *Pseudomonas pyocyanea* by the Oxidase Reaction. *Nature* 178, 703.

Kuykendall, L. D., Roy, M. A., O'Neill, J. J. & Devine, T. E. (1988). Fatty acids, antibiotic resistance, and deoxyribonucleic acid homology groups of *Bradorhizobium japonicum*. *Int J Syst Bacteriol* 38, 358-361.

Lee, R. Y. & Joye, S. B. (2006). Seasonal patterns of nitrogen fixation and denitrification in oceanic mangrove habitats. *Mar Ecol Prog Ser* 307, 127-141.

Ludwig, W., Strunk, O., Westram, R., Richter, L., Meier, H., Yadhukumar, Buchner, A., Lai, T., Steppi, S. & other authors (2004). ARB: a software environment for sequence data. *Nucleic Acids Res* 32, 1363-1371.

Mesbah, M., Premachandran, U. & Whitman, W. B. (1989). Precise measurement of the G+C content of deoxyribonucleic acid by high-performance liquid chromatography. *Int J Syst Bacteriol* 39, 159-167.

Miller, L. T. (1982). A single derivatization method for bacterial fatty acid methyl esters including hydroxy acids. *J Clin Microbiol* 16, 584-586.

Ostle, A. G. & Holt, J. G. (1982). Nile blue A as a fluorescent stain for poly-beta-hydroxybutyrate. *Appl Environ Microbiol* 44, 238-241.

Reef, R., Feller, I. C. & Lovelock, C. E. (2010). Nutrition of mangroves. *Tree Physiol* 30, 1148-1160.

Satomi, M., Kimura, B., Hamada, T., Harayama, S. & Fujii, T. (2002). Phylogenetic study of the genus *Oceanospirillum* based on 16S rRNA and *gyrB* genes: emended description of the genus *Oceanospirillum*, description of *Pseudospirillum* gen. nov., *Oceanobacter* gen. nov. and *Terasakielia* gen. nov. and transfer of *Oceanospirillum jannaschii* and *Pseudomonas stanieri* to *Marinobacterium* as *Marinobacterium jannaschii* comb. nov. and *Marinobacterium stanieri* comb. nov. *Int J Syst Evol Microbiol* 52, 739-747.

Seymour, J. R., Ahmed, T., Marcos & Stocker, R. (2008). A microfluidic chemotaxis assay to study microbial behavior in diffusing nutrient patches. *Limnol Oceanogr:Methods* 6, 477-488.

Stackebrandt, E. & Goebel, B. M. (1994). Taxonomic Note: A place for DNA-DNA reassociation and 16S rRNA sequence analysis in the present species definition in bacteriology. *Int J Syst Bacteriol* 44, 846-849.

Tamaoka, J. & Komagata, K. (1984). Determination of DNA base composition by reversed-phase high-performance liquid chromatography. *FEMS Microbiol Lett* 25, 125-128.

Tindall, B. J. (1990a). A comparative study of the lipid composition of *Halobacterium saccharovorum* from various sources. *Syst Appl Microbiol* 13, 128-130.

Tindall, B. J. (1990b). Lipid composition of *Halobacterium lacusprofundi*. *FEMS Microbiol Lett* 66, 199-202.

Tindall, B. J., Rossello-Mora, R., Busse, H. J., Ludwig, W. & Kaempfer, P. (2010). Notes on the characterization of prokaryote strains for taxonomic purposes. *Int J Syst Evol Microbiol* 60, 249-266.

Tomlinson, P. B. (1986). *The botany of mangroves*. Cambridge: Cambridge University Press.

Yarza, P., Richter, M., Peplies, J., Euzeby, J., Amann, R., Schleifer, K.-H., Ludwig, W., Glöckner, F. O. & Rosselló-Móra, R. (2008). The All-Species Living Tree project: A 16S rRNA-based phylogenetic tree of all sequenced type strains. *Syst Appl Microbiol* 31, 241-250.

Zhou, A., Baidoo, E., He, Z., Mukhopadhyay, A., Baumohl, J. K., Benke, P., Joachimiak, M. P., Xie, M., Song, R. & other authors (2013). Characterization of NaCl tolerance in *Desulfovibrio vulgaris* Hildenborough through experimental evolution. *ISME J* 7, 1790-1802.

## SUPPLEMENTARY MATERIAL

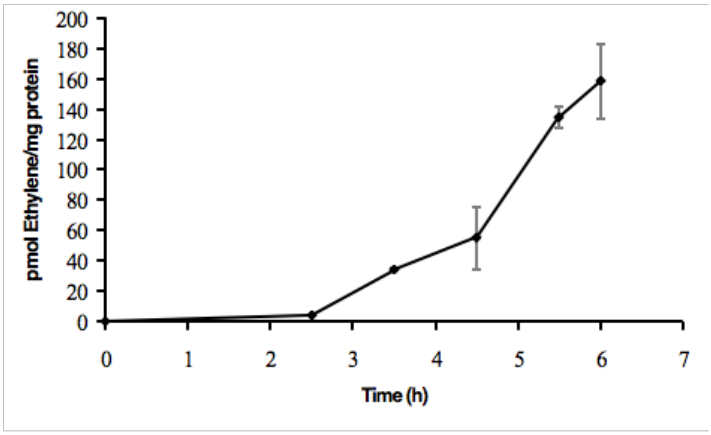


**Fig. S1.** ARA of strain Gal22$^T$. Cells grown on N-free HGB medium and 1% $O_2$ in flask headspace.

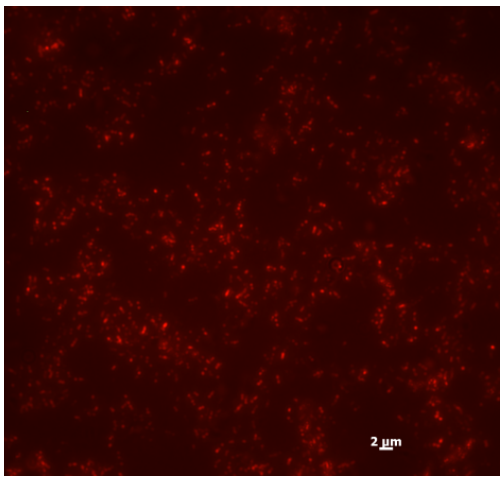


**Fig. S2.** PHB granules of strain Gal22$^T$.Cells were stained with Nile blue A and visualized at 460 nm.

**Table S1.** Fatty acids composition of strain Gal22$^T$ and the closely related strains.

Strains: 1, Gal22$^T$; 2, *M. lutimaris* DSM 22012$^T$ and 3, *M. litorale* DSM 23545$^T$. Data generated in this study. ECL, equivalent chain length.

| Fatty acids (%) | 1 | 2 | 3 |
|---|---|---|---|
| $C_{10:0}$ | 0.56 | 0.47 | 0.55 |
| $C_{12:0}$ | 4.13 | 2.65 | 3.68 |
| $C_{14:0}$ | – | 0.12 | 0.24 |
| $C_{16:0}$ | 26.06 | 27.62 | 25.78 |
| $C_{18:0}$ | 0.89 | 1.61 | 0.5 |
| $C_{16:1}\omega5c$ | – | – | 0.12 |
| $C_{18:1}\omega7c$ | 47.3 | 46.91 | 40.54 |
| $C_{19:0}\omega8c$ cyclo | – | 0.2 | – |
| $C_{20:1}\omega7c$ | – | 0.23 | – |
| $C_{17:0}$ cyclo | 6.3 | 3.82 | – |
| $C_{10:0}$ 3-OH | 4.19 | 4.49 | 4.16 |
| $C_{12:0}$ 2-OH | 0.9 | 1.36 | – |
| Summed feature 3* | 9.68 | 10.27 | 23.58 |
| Unknown (ELC 11.799) | – | 0.26 | 0.85 |

*Summed feature 3 ($C_{16:1}\omega7c$ and/or iso-$C_{15:0}$ 2-OH)

# 3.3 Influence of salinity and temperature on nitrogen fixation rates of the mangrove-associated bacterium, *Marinobacterium mangrovicola*

**The following manuscript is in preparation**

# Influence of salinity and temperature on nitrogen fixation rates of the mangrove-associated bacterium, *Marinobacterium mangrovicola*

Gabriela Alfaro-Espinoza[1]*, Esteban Acevedo-Trejos[2], Khaled Abdallah[1], and Matthias S. Ullrich[1]
[1]Jacobs University Bremen, Molecular Life Science Research Center, Campus Ring 1, 28759 Bremen, Germany.
[2] Leibniz Center for Tropical Marine Ecology, Fahrenheitstrae 6, 28359 Bremen, Germany

*Corresponding author: Gabriela Alfaro-Espinoza; m.alfaroespinoza@jacobs-university.de

---

## ABSTRACT

Nitrogen is a limiting resource in mangrove ecosystems. Nitrogen fixation by microorganisms known as diazotrophs represents one of the main sources of nitrogen to these ecosystems. However, environmental factors such as fluctuating salinity and temperature might have a major influence on nitrogen fixation processes. Due to climate change, individual mangrove ecosystems might experience changes in temperature and salinity. However, is still poorly known if these changes might have a positive or negative effect on diazotrophic communities. We used the mangrove-associated diazotroph *Marinobacterium mangrovicola* Gal22 to study *in vitro* how future temperature and salinity changes could affect nitrogen fixation in mangrove ecosystems. Our results revealed high bacterial nitrogenase activities at both, 18 °C with low salinity (15-30 ‰), and 36 °C with a salinity of 50 ‰. A high temperature of 40 °C inhibited nitrogen fixation. The wide range of temperature and salinity tolerance showed by this bacterium could offer an advantage to survive to future environmental changes, and during mangrove root colonization. The results of this study contribute to our general understanding on how nitrogen fixation by diazotrophs might affect bacteria-mangrove interactions under a changing environment.

---

## INTRODUCTION

Mangrove ecosystems are wetlands located in the tropics and subtropics. They are mainly characterized by oligotrophic soils, woody plants, warm temperatures, salinity gradients and constant tidal influences (Feller et al, 2010). Mangrove soils are nutrient-poor environments with nitrogen being one of the limiting resources (Bashan and Holguin, 2002; Feller et al., 2002; Reef et al., 2010). Several authors have suggested that nitrogen fixation mediated by bacteria is a dominant process from which mangrove plants obtain this scarce nutrient (Holguin et al., 1992; Pelegrí et al., 1997; Bashan et al., 1998; Ravikumar et al., 2004; Reef et al., 2010). Nitrogen fixation by heterotrophic bacteria might be influenced by many

environmental factors such as oxygen, nitrogen, temperature, salinity, and pH. An increase in oxygen and nitrogen concentrations may inhibit the nitrogenase enzyme (Zehr and Paerl, 2008). The particular effects of temperature, salinity, or pH on nitrogen fixation are likely to depend on differences in mangrove zonations or soil biogeochemical properties (Lee and Joye, 2006; Vovides et al., 2011). Interestingly, diazotrophs are not evenly distributed in mangrove ecosystems. They are rather associated with different mangrove intertidal zones, where each of these zones has specific biogeochemical profiles (Flores-Mireles et al., 2007). In addition, Lee and Joye (2006) found that bacterial nitrogenase activity was associated with seasonal patterns in mangroves, for which temperature, salinity, desiccation, and light intensity play a major role. However, it is still not known how future changes of environmental conditions could affect diazotrophs distribution and nitrogen fixation activity in mangrove ecosystems.

In this context, salinity has been highlighted as a factor having a major influence on diazotrophic communities in mangrove ecosystems (Vovides et al., 2011). High salinity concentrations had negative effects on overall nitrogen fixation rates (Vovides et al., 2011). However, salinity may increase in soils due to evaporation or very warm low tides, or decrease by freshwater input (Feller et al, 2010). In future scenarios, climate change-associated sea-level rises as well as temperature and precipitation changes might impact salinity concentrations in mangrove soils (Field, 1995; Mcleod and Salm, 2006; Solomon et al., 2007; Alongi 2008; Gilman et al., 2008). For example, mangroves in Florida are expanding poleward (Cavanaugh et al., 2014) due to a reduction in extreme cold events. A similar pattern was observed in a region where mangroves influenced by sea-level rise have migrated onto salt and brackish marsh habitats (Krauss et al., 2011). These shiftings of the distribution ranges of mangroves and associated changes in salinity might affect mangrove-associated bacterial communities.

In addition, temperature changes have also been suggested as one of the most influential environmental factors possibly affecting bacterial communities (Zuberer and Silver, 1978; Gonzales-Acosta et al., 2006) and their nitrogen fixation rates (Hicks & Silvester, 1985). Woitchik et al. (1997) showed that nitrogen fixation increase over the rainy season in wet mangroves. However, those data were later contrasted by Vovides et al. (2011) who found higher nitrogen fixation rates in arid mangroves during summer. Generally, it had been shown that temperature increases lead to higher bacterial activities in mangrove ecosystems (Hicks and Silvester, 1985; Vovides et al., 2011) although very high temperatures could inhibit or decrease nitrogen fixation (Zuberer and Silver, 1978). It has been predicted that the global mean surface air temperature may increase up to 1.1-6.4 °C by the year 2100 (Meehl et al., 2007), which could have profound effects on diazotrophic activity associated with mangrove roots. Consequently, it is of paramount importance to study salinity and temperature tolerance in diazotrophs and their capacity to adapt to new environmental conditions in order to better understand how future changes in these environmental variables could influence mangrove ecosystems.

*Marinobacterium mangrovicola* is a diazotroph model organism for studying bacteria-mangrove interactions (Alfaro-Espinoza and Ullrich, 2014b). This bacterium can cope with a wide range of temperatures (4 to 42 °C) and exhibited high NaCl tolerance (up to 180 ‰) under aerobic and non-$N_2$-fixing conditions (Alfaro-Espinoza and Ullrich, 2014a). Herein, this mangrove-associated bacterium is used to investigate how future changes in temperature and salinity could affect nitrogenase activity of diazotrophs.

## MATERIALS AND METHODS

### Experimental design

The diazotroph *Marinobacterium mangrovicola* Gal22, which colonize mangrove roots (Alfaro-Espinoza and Ullrich, 2014b), was grown on modified HGB medium [g $l^{-1}$: 20 NaCl, 3 $MgSO_4.7H_2O$, 0.02 CaCl, 5 DL-malic acid, 3 NaOH; 100 ml of 0.39 M phosphate buffered saline (PBS), 0.1 % yeast extract, and 10 ml trace elements solution (for 500 ml: 0.5 g $FeCl_3$, 0.1 g $NaMoO_4.2H_2O$, 0.105 g $MnSO_4$, 0.14 g $H_3BO_4$, 1.4 mg $CuCl.2H_2O$, 12 mg $ZnSO_4$); final pH 7.2] (Holguin et al., 1992), and shaken at 250 rpm overnight at 28 °C. After incubation, cells were harvested, washed two times with PBS, and cultured under nitrogen fixing conditions (see below) at different temperatures [18, 24, 30, 36, and 40 °C] and salinities [15, 30, 50, and 70 ‰]. For the latter treatment, NaCl in the medium was adjusted to obtain the desired salinity concentrations. To culture strain Gal22 under nitrogen fixing conditions, 60 ml of nitrogen-free HGB medium (without yeast extract) in 1-L erlenmeyer flask was used. The flask was sealed with a rubber septum, flushed with $N_2$, and the oxygen concentration in the headspace was adjusted to 1 %. The above mention cultures were used to measure nitrogen fixation rates. All experiments were conducted with three replicates per sample.

### Determination of nitrogen fixation rates

The acetylene reduction assay (ARA) (Dilworth, 1966; Hardy et al., 1986) was used to determined nitrogen fixation rates during early exponential growth phase of strain Gal22 grown in nitrogen-free HGB medium. When cell cultures had reached an $OD_{600}$ of about 0.2, the headspace of the culture flasks was adjusted to 7 % acetylene. A flask containing nitrogen-free HGB medium was treated in the same way and used as a negative control. Each two hours, 1 ml of gas from the headspace of the flasks was taken for analysis. Additionally, at each time point 1 ml cell culture samples were removed to measure bacterial growth via $OD_{600}$ determination. Ethylene production in the gas samples was analyzed using a GC-14B gas chromatograph (Shimadzu, Duisburg, Germany). The instrument was equipped with a 6 Ft x 1/8" Porapak 80/100 column, a hydrogen flame ionization detector (FID), and $N_2$ as carrier gas. The temperatures of column, injector and detector were 70, 120, and 200 °C, respectively.

### Statistical analysis

Initially, a linear regression was adjusted to the results obtained for each treatment, i.e. for each salinity and temperature, with nitrogenase activity (acetylene reduction in µmol ethylene / mg protein) as the response variable and time (hours) as the explanatory variable. Next, an Analysis of Variance (ANOVA) was performed to compare acetylene reduction rates (i.e. slope of the linear trend in units of µmol ethylene / mg protein / hour) at different environmental conditions with the acetylene reduction rates as response variables and temperature and salinity as explanatory variables. All analyses were carried out using R version 3.1.1 (The R Foundation for Statistical Computing, Vienna, Austria).

## RESULTS

The acetylene reduction assay (ARA) was performed to determine how changes in temperature and salinity affect nitrogenase activity of *M. mangrovicola*. The slopes of the acetylene reduction rates (**Table 1**) were used in the analysis shown in **Figure 1**. Our results showed higher nitrogenase activity at temperatures of 18 and 36 °C as opposed to 24 and 30 °C. Moreover, a high salinity of 50 ‰ impacted nitrogen fixation at 18 °C while it promoted nitrogen fixation at 36 °C. The highest applied salinity of 70 ‰ negatively affected nitrogenase activity at 36 °C. Growth of *M. mangrovicola* at 40 °C is possible in a medium supplemented with a nitrogen source. However, under nitrogen fixing conditions nitrogenase activity was inhibited at this temperature.

**Table 1.** Summary statistics of the linear regression fits for the relationships between nitrogenase activity and time. All fits are statistically significant with $R^2$ values over 29%, with the exception of all treatments for 40 °C.

| | Temperature | Salinity | Intercept | Intercept Standard Error | Intercept P-value | Slope | Slope Standard Error | Slope P-value | $R^2$ |
|---|---|---|---|---|---|---|---|---|---|
| 1 | 18 °C | 15 ‰ | 1.105 | 4.866 | 0.828 | 2.865 | 0.888 | 0.018 | 0.573 |
| 2 | 18 °C | 30 ‰ | 3.883 | 2.575 | 0.162 | 2.408 | 0.470 | 0.000 | 0.697 |
| 3 | 18 °C | 50 ‰ | 1.483 | 1.559 | 0.378 | 1.462 | 0.285 | 0.002 | 0.784 |
| 4 | 18 °C | 70 ‰ | -1.488 | 1.063 | 0.192 | 1.587 | 0.194 | 9.712e-06 | 0.857 |
| 5 | 24 °C | 15 ‰ | 1.788 | 0.984 | 0.119 | 0.357 | 0.180 | 0.094 | 0.297 |
| 6 | 24 °C | 30 ‰ | -1.875 | 0.563 | 0.008 | 1.097 | 0.103 | 8.681e-07 | 0.911 |
| 7 | 24 °C | 50 ‰ | 0.404 | 0.596 | 0.514 | 1.679 | 0.115 | 1.410e-07 | 0.955 |
| 8 | 24 °C | 70 ‰ | 0.483 | 1.648 | 0.776 | 0.884 | 0.318 | 0.021 | 0.403 |
| 9 | 30 °C | 15 ‰ | 2.317 | 1.136 | 0.069 | 1.171 | 0.207 | 0.000 | 0.737 |
| 10 | 30 °C | 30 ‰ | 1.955 | 1.038 | 0.089 | 1.114 | 0.190 | 0.000 | 0.753 |
| 11 | 30 °C | 50 ‰ | 0.175 | 1.211 | 0.890 | 0.942 | 0.221 | 0.005 | 0.710 |
| 12 | 30 °C | 70 ‰ | 0.700 | 1.751 | 0.703 | 1.746 | 0.320 | 0.002 | 0.804 |
| 13 | 36 °C | 15 ‰ | 3.778 | 1.406 | 0.043 | 2.191 | 0.280 | 0.001 | 0.909 |
| 14 | 36 °C | 30 ‰ | 2.763 | 2.392 | 0.292 | 1.123 | 0.437 | 0.042 | 0.445 |
| 15 | 36 °C | 50 ‰ | 4.173 | 2.366 | 0.128 | 2.730 | 0.432 | 0.001 | 0.848 |
| 16 | 36 °C | 70 ‰ | 0.860 | 0.240 | 0.005 | 0.155 | 0.044 | 0.006 | 0.509 |
| 17 | 40 °C | 15 ‰ | 0.587 | 0.237 | 0.033 | -0.041 | 0.043 | 0.363 | -0.009 |
| 18 | 40 °C | 30 ‰ | 0.208 | 0.154 | 0.206 | -0.002 | 0.028 | 0.954 | -0.100 |
| 19 | 40 °C | 50 ‰ | 0.708 | 0.243 | 0.016 | -0.024 | 0.044 | 0.606 | -0.070 |
| 20 | 40 °C | 70 ‰ | 0.110 | 0.116 | 0.367 | 0.002 | 0.021 | 0.939 | -0.099 |

The ANOVA analysis did not suggest any statistical difference between acetylene reduction rates at different temperatures and salinities (**Supplementary Table S1**). Treatments at 40 °C were excluded from analysis, where no bacterial growth could be detected, therefore revealing negative slopes (**Table 1**). Overall salinity did not show a clear pattern. However, nitrogenase activity was detected at all ranges of salinities tested, but in different amounts and for most of the temperatures the slopes were increasing with respect to an increase in time (**Table 1**). Slopes of **Table 1** reveal that the highest nitrogenase activity found were in the treatment at 18 °C with a salinity of 15 ‰, followed by 36 °C with a salinity of 50 ‰. The results of specific acetylene reduction assays for *M. mangrovicola* at combination of each temperature and salinity are summarized in **Supplementary Figures S1 to S5.**

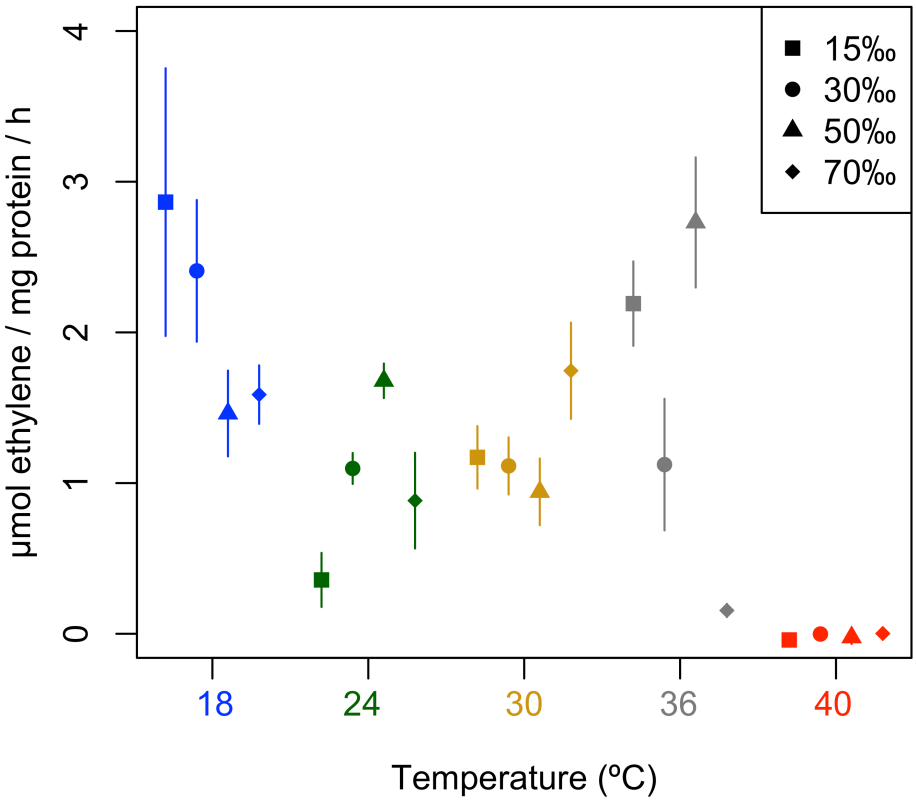


**Figure 1.** Influence of temperature and salinity on nitrogenase activity of *M. mangrovicola* Gal22. The acetylene reduction assay was used to elucidate $N_2$-fixation rates. The dots represent the value of the slope of the rates. 15 to 70 ‰ represent the salinity of HGB medium.

## DISCUSSION

Diazotrophs living in mangrove ecosystems need to cope with environmental changes such as variations in salinity and temperature. These changes might be intensified under current and future climate change conditions. Herein, we addressed the effects of varying salinity and temperature on nitrogenase activity of the mangrove-associated diazotroph *Marinobacterium mangrovicola* Gal22 and how these changes could affect biological nitrogen fixation under future environmental conditions.

*M. mangrovicola* exhibited higher nitrogen fixation rates at 36 °C than at 24-30 °C (**Figure 1**). Similar results were found for some diazotrophs were nitrogen fixation was promoted under conditions that foster growth (Hicks and Silvester, 1985; Lehtimaki et al, 1997; Vovides et al, 2011; Brauer et al., 2013). Moreover, the highest nitrogenase activity was observed at a salinity of 50 ‰, which suggests that this organism might be able to cope with increasing sediment salinity while fixing atmospheric nitrogen. Vovides et al. (2011) reported that nitrogen fixation in an arid mangrove was low at salinities higher than 48 ‰. For *M. mangrovicola*, salinity had no influence on nitrogenase activity at 24 and 30 °C. This could represent a selective advantage over other organisms with a more restricted tolerance to high salinity. However, a very high salinity concentration, i.e. 70 ‰, did affect nitrogen fixation at higher temperatures as seen at 36 °C. Changes in precipitation, high temperatures and sea

level rise could modify salinity in mangrove ecosystems (Gilman et al., 2008) or could shift the distribution range of specific mangrove species leading to habitats with altered sediment salinities (Krauss et al., 2011). Precipitation in the tropics and subtropics, for example, was predicted to decrease by the year 2050 (Solomon et al., 2007; Gilman et al., 2008). In consequence, this might lead to an increase in salinity due to the decreased freshwater input.

Nitrogen fixation was inhibited at 40 °C, this result is in accordance with other studies were nitrogenase decline towards 37 °C (Zuberer and Silver, 1978). Interestingly, higher nitrogen fixation rates were found for *M. mangrovicola* at 18 °C. Since the maximum rates for this temperature were found at lower salinities, there might be a yet-to-be-understood interesting synergistic effect of temperature and salinity on nitrogen fixation. Nitrogen fixation in marine bacteria has been observed at low temperatures, such as for *Aphanizomenon flos-aquae*, where highest nitrogen fixation rates were found at 16 °C (Lehtimaki et al, 1997). In subtropic mangrove ecosystems, however, low nitrogen fixation had previously been associated with low temperatures (Hicks and Silvester, 1985; Vovides et al, 2011). In the case of sea-level rise, one potential scenario might include mangroves migrating landward or towards higher latitudes (Snedaker, 1995; Gilman et al., 2008). In arid mangroves nitrogen fixation at 18 °C by *M. mangrovicola* might represent an advantage for faster colonization of mangrove plants. Nevertheless, how fast *M. mangrovicola* can adapt to diurnal variations in temperature and salinity to fix $N_2$ remains to be determined in future experiments.

In this study high nitrogenase activity was observed at 18 °C and 36 °C. The wide range of temperature and salinity tolerance could potentially offer an advantage to *M. mangrovicola* to colonize mangrove plants. The observed effects of temperature and salinity provided an indication of how climate change might impact diazotroph-mangrove interaction in these fragile ecosystems.

## ACKNOWLEDGEMENTS

We thank Prof. Dr. Michael W. Friedrich for his support with the gas chromatograph (GC).

## REFERENCES

Alfaro-Espinoza, G., and Ullrich, M. S. (2014a). *Marinobacterium mangrovicola* sp. nov., a marine nitrogen-fixing bacterium isolated from mangrove roots of *Rhizophora mangle*. *Int. J. Syst. Evol. Microbiol.* 64, 3988–3993. doi:10.1099/ijs.0.067462-0.

Alfaro-Espinoza, G., and Ullrich, M. S. (2014b). A model system to study bacterial $N_2$-fixation in mangrove ecosystems. Submitted.

Alongi, D. M. (2008). Mangrove forests: Resilience, protection from tsunamis, and responses to global climate change. *Estuar. Coast. Shelf Sci.* 76, 1–13. doi:10.1016/j.ecss.2007.08.024.

Bashan, Y., and Holguin, G. (2002). Plant growth-promoting bacteria: a potential tool for arid mangrove reforestation. *Trees* 16, 159–166. doi:10.1007/s00468-001-0152-4.

Bashan, Y., Puente, M. E., Myrold, D. D., and Toledo, G. (1998). *In vitro* transfer of fixed nitrogen from diazotrophic filamentous cyanobacteria to black mangrove seedlings. *FEMS Microbiol. Ecol.* 26, 165–170.

Brauer, V. S., Stomp, M., Rosso, C., van Beusekom, S. a M., Emmerich, B., Stal, L. J., and Huisman, J. (2013). Low temperature delays timing and enhances the cost of nitrogen fixation in the unicellular cyanobacterium *Cyanothece*. *ISME J.* 7, 2105–2115. doi:10.1038/ismej.2013.103.

Cavanaugh, K. C., Kellner, J. R., Forde, A. J., Gruner, D. S., Parker, J. D., Rodriguez, W., and Feller, I. C. (2014). Poleward expansion of mangroves is a threshold response to decreased frequency of extreme cold events. *Proc. Natl. Acad. Sci. U. S. A.* 111, 723–727. doi:10.1073/pnas.1315800111.

Dilworth, M. J. (1966). Acethylene reduction by nitrogen-fixing preparations from *Clostridium pasteurianum*. *Biochem. Biophys. Acta* 127, 285–294. doi:10.1016/0304-4165(66)90383-7.

Feller, I. C., Lovelock, C. E., Berger, U., McKee, K. L., Joye, S. B., and Ball, M. C. (2010). Biocomplexity in mangrove ecosystems. *Ann. Rev. Mar. Sci.* 2, 395–417. doi:10.1146/annurev.marine.010908.163809.

Feller, I. C., Mckee, K. L., Whigham, D. F., and Neill, J. P. O. (2002). Nitrogen vs. phosphorus limitation across an ecotonal gradient in a mangrove forest. *Biogeochemistry* 62, 145–175.

Field, C. D. (1995). Impact of expected climate change on mangroves. *Hydrobiologia* 295, 75–81. doi:10.1007/BF00029113.

Flores-Mireles, A. L., Winans, S. C., and Holguin, G. (2007). Molecular characterization of diazotrophic and denitrifying bacteria associated with mangrove roots. *Appl. Environ. Microbiol.* 73, 7308–7321. doi:10.1128/AEM.01892-06.

Gilman, E. L., Ellison, J., Duke, N. C., and Field, C. (2008). Threats to mangroves from climate change and adaptation options: A review. *Aquat. Bot.* 89, 237–250. doi:10.1016/j.aquabot.2007.12.009.

Gonzalez-Acosta, B., Bashan, Y., Hernandez-Saavedra, N. Y., Ascencio, F., and Cruz-Agüero, G. (2006). Seasonal seawater temperature as the major determinant for populations of culturable bacteria in the sediments of an intact mangrove in an arid region. *FEMS Microbiol. Ecol.* 55, 311–321. doi:10.1111/j.1574-6941.2005.00019.x.

Hardy, R. W. F., Holsten, R. D., Jackson, E. K., and Burns, R. C. (1986). The acetylene - ethylene assay for $N_2$ fixation: laboratory and field evaluation. *Plant Physiol.* 43, 1185–1207.

Hicks, B. J., and Silvester, W. B. (1985). Nitrogen fixation associated with the New Zealand mangrove (*Avicennia marina* (Forsk.) Vierh. var. *resinifera* (Forst. f.) Bakh.). *Appl. Environ. Microbiol.* 49, 955–959.

Holguin, G., Guzman, M. A., and Bashan, Y. (1992). Two new nitrogen-fixing bacteria from the rhizosphere of mangrove trees: Their isolation, identification and in vitro interaction with rhizosphere *Staphylococcus sp*. *FEMS Microbiol. Ecol.* 101, 207–216. doi:10.1016/0168-6496(92)90037-T.

Krauss, K. W., From, A. S., Doyle, T. W., Doyle, T. J., and Barry, M. J. (2011). Sea-level rise and landscape change influence mangrove encroachment onto marsh in the Ten Thousand Islands region of Florida, USA. *J. Coast. Conserv.* 15, 629–638. doi:10.1007/s11852-011-0153-4.

Lee, R., and Joye, S. (2006). Seasonal patterns of nitrogen fixation and denitrification in oceanic mangrove habitats. *Mar. Ecol. Prog. Ser.* 307, 127–141. doi:10.3354/meps307127.

Lehtimaki, J., Moisander, P., Sivonen, K., and Kononen, K. (1997). Growth, nitrogen fixation, and nodularin production by two Baltic Sea cyanobacteria. *Appl. Environ. Microbiol.* 63, 1647–1656.

Mcleod, E., and Salm, R. V (2006). Managing mangroves for resilience to climate change. IUCN. Gland, Switzerland.

Meehl, G., Stocher, T., Collins, W., Friedlingstein, P., Gaye, A., Gregory, J., Kitoh, A., Knutti, R., Murphy, J., Noda, A., et al. (2007). "Global climate projections," in *Climate change 2007: The physical science basis. Contribution of working group I to the fourth assessment report of the intergovernmental panel on climate change* (Cambridge, United Kingdom and New York, NY, USA.: Cambridge University Press).

Pelegrí, S., Rivera-monroy, V., and Twilley, R. (1997). A comparison of nitrogen fixation (acetylene reduction) among three species of mangrove litter, sediments, and pneumatophores in south Florida, USA. *Hidrobiología* 356, 73–79.

Ravikumar, S., Kathiresan, K., Ignatiammal, S. T. M., Babu Selvam, M., and Shanthy, S. (2004). Nitrogen-fixing azotobacters from mangrove habitat and their utility as marine biofertilizers. *J. Exp. Mar. Bio. Ecol.* 312, 5–17. doi:10.1016/j.jembe.2004.05.020.

Reef, R., Feller, I. C., and Lovelock, C. E. (2010). Nutrition of mangroves. *Tree Physiol.* 30, 1148–1160. doi:10.1093/treephys/tpq048.

Snedaker, S. C. (1995). Mangroves and climate change in the Florida and Caribbean region: scenarios and hypotheses. *Hydrobiologia* 295, 43–49.

Solomon, S., Qin, D., Manning, M., Chen, Z., Marquis, M., Averyt, K., Tignor, M., and Miller, H. (2007). *Climate Change 2007. The physical science basis. Contribution of working group I to the fourth assessment report of the intergovernmental panel on climate change*. Cambridge, United Kingdom and New York, NY, USA.: Cambridge University Press.

Vovides, A. G., Bashan, Y., López-Portillo, J. a., and Guevara, R. (2011). Nitrogen fixation in preserved, reforested, naturally regenerated and impaired mangroves as an indicator of functional restoration in mangroves in an arid region of Mexico. *Restor. Ecol.* 19, 236–244. doi:10.1111/j.1526-100X.2010.00713.x.

Woitchik, A. F., Ohowa, B., Kazungu, J. M., Rao, R. G., Goeyens, L., and Dehairs, F. (1997). Nitrogen enrichment during decomposition of mangrove leaf litter in an east African coastal lagoon (Kenya): Relative importance of biological nitrogen fixation. *Biogeochemistry* 39, 15–35.

Zehr, J. P., and Paerl, H. W. (2008). "Molecular ecological aspects of nitrogen fixation in the marine environment," in *Microbial ecology of the oceans*, ed. D. L. Kirchman (John Wiley & Sons, Inc.), 481–525.

Zuberer, D. A., and Silver, W. S. (1978). Biological dinitrogen fixation (acetylene reduction) associated with Florida mangroves. *Appl. Environ. Microbiol.* 35, 567–575.

## SUPPLEMENTARY MATERIAL

**Supplementary Table S1.** ANOVA summary statistics with acetylene reduction rates (i.e. slope of the linear trend) as the response variables and temperature and salinity as the explanatory variables. Since $N_2$-fixation was inhibited at 40 °C, this temperature was excluded from the analysis.

| | Degrees of freedom | Sum of squares | Mean sum of square | F-value | P-value |
|---|---|---|---|---|---|
| Temperature | 3 | 2.590 | 0.8634 | 1.381 | 0.310 |
| Salinity | 3 | 0.915 | 0.3050 | 0.488 | 0.699 |
| Residuals | 9 | 5.628 | 0.6253 | | |

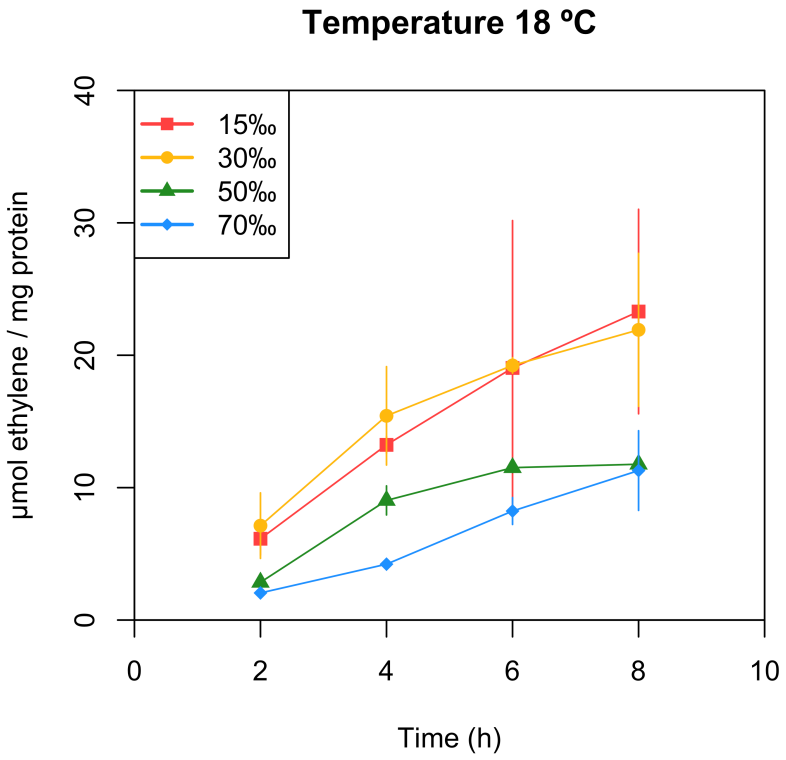


**Supplementary Figure S1.** Acetylene reduction assay of *M. mangrovicola* cultivated in N-free media, under different salinities (15 to 70 ‰) and at 18 °C.

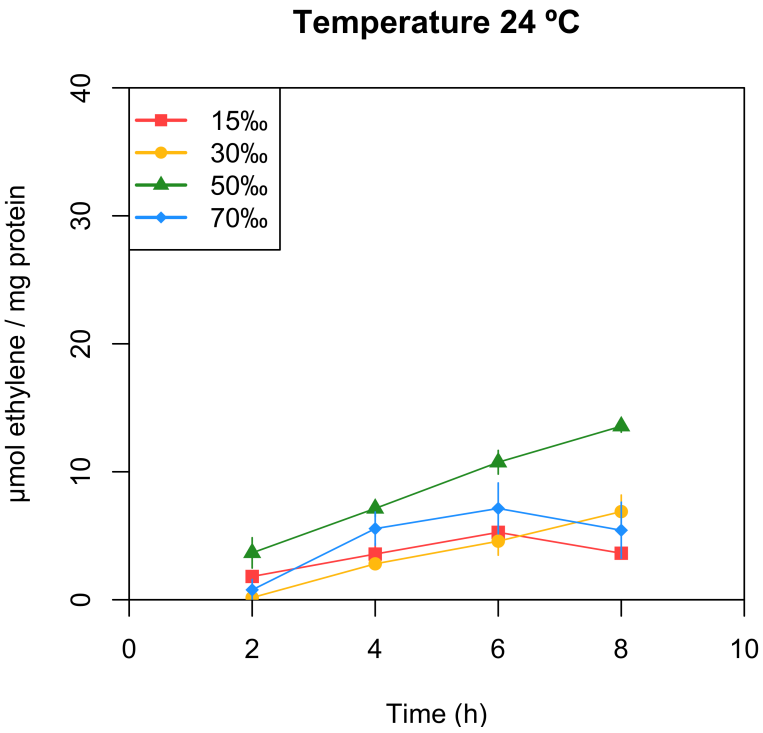


**Supplementary Figure S2.** Acetylene reduction assay of *M. mangrovicola* cultivated in N-free media, under different salinities (15 to 70 ‰) and at 24 °C.

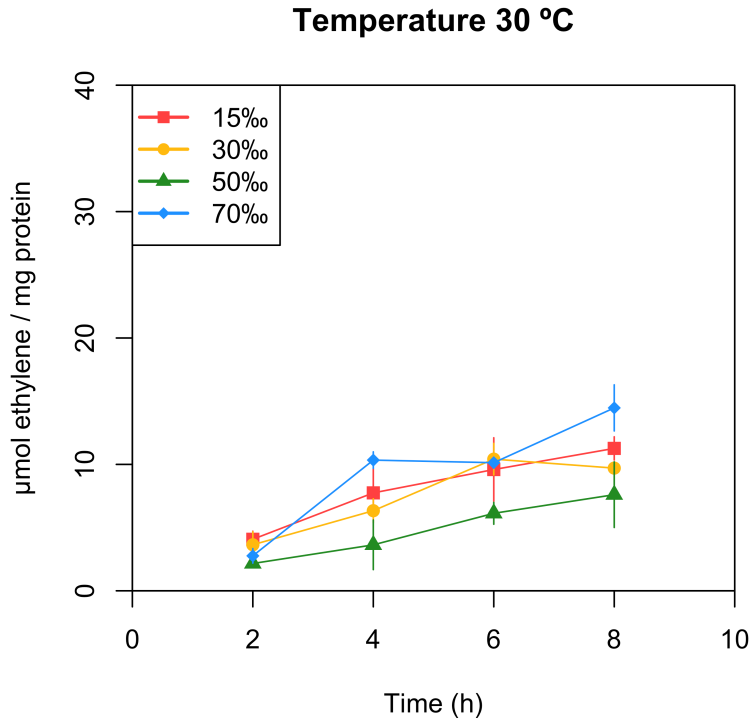


**Supplementary Figure S3.** Acetylene reduction assay of *M. mangrovicola* cultivated in N-free media, under different salinities (15 to 70 ‰) and at 30 °C.

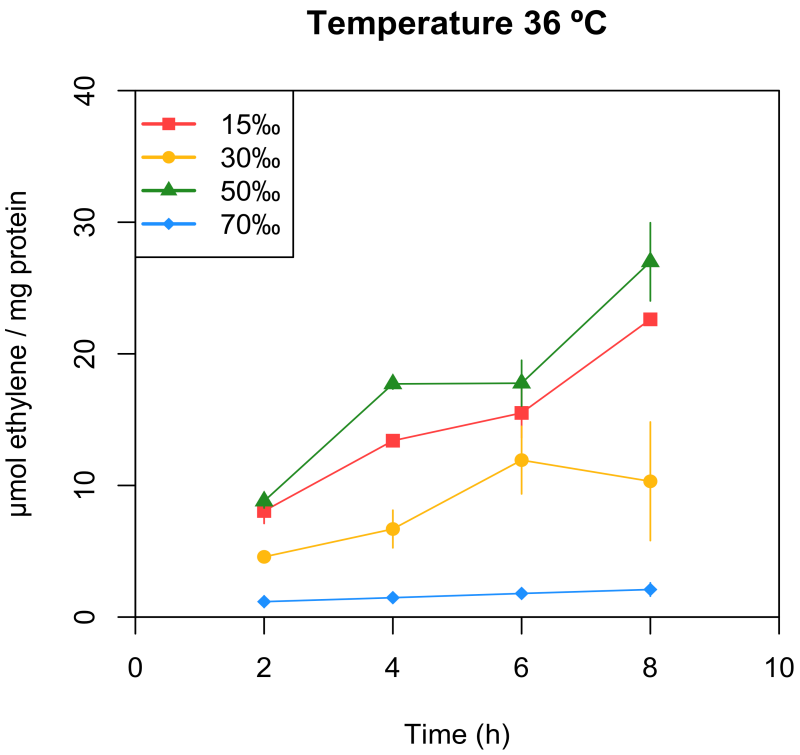


**Supplementary Figure S4.** Acetylene reduction assay of *M. mangrovicola* cultivated in N-free media, under different salinities (15 to 70 ‰) and at 36 °C.

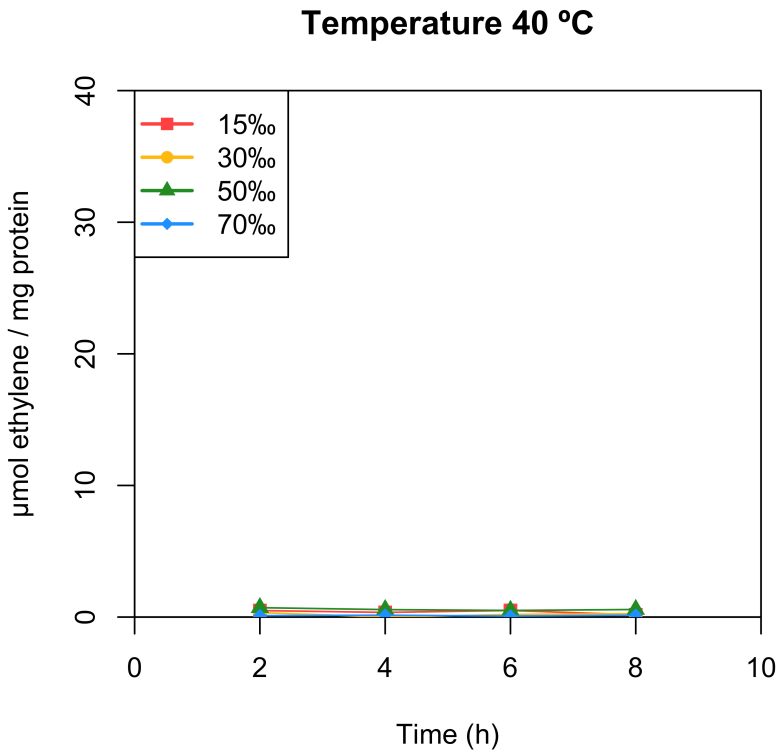


**Supplementary Figure S5.** Acetylene reduction assay of *M. mangrovicola* cultivated in N-free media, under different salinities (15 to 70 ‰) and at 40 °C.

# 4. Concluding Remarks

# 4. Concluding Remarks

## 4.1 Selection and characterization of the bacterial model organism

Identifying a nitrogen-fixing organism that colonize mangrove roots and is genetically accessible was essential to establish a bacteria-mangrove interaction model system. Moreover, for a bacterium to be considered as a model organism, several characteristics needed to be fulfill such as easy handling, short life cycle, feasibility of genetic manipulation, and suitability for the study of specific traits or phenomena of interest (Hedges, 2002).

In this study, we carried out several tests to select and characterize the identified bacterial model organism taking into account the characteristics mentioned above. Several microorganisms were isolated and tested for nitrogen fixation by using the acetylene reduction assay. In addition, an evaluation of the presence of genes encoding for nitrogen fixation (i.e. *nifH*) was performed. Among seven bacterial isolates, strain Gal22, later taxonomically identified as *M. mangrovicola*, showed high nitrogen fixation rates and the presence of the *nifH* gene in its genome was confirmed by PCR.

Furthermore, a detailed phenotypic characterization based on morphological, physiological and biogeochemical properties of *M. mangrovicola* was conducted. *M. mangrovicola* is an aerobic, fast growing, and motile Gram-negative bacterium. Growth was observed in a wide range of temperatures (4 to 42 °C), pH (5.5 to 10) and salinity (up to 180 ‰). It can utilize several substrates; for example malic acid and succinic acid were suitable substrates for this organism. In addition a full analysis of its enzymatic activity was performed. Phylogenetic analysis of the 16S rRNA gene allowed to conclude that this bacterium belongs to the genus *Marinobacterium*. Based on genotypic, morphological and biogeochemical characteristics *M. mangrovicola* was described as a new candidate species.

The capacity of *M. mangrovicola* to colonize mangrove roots and survive within the rhizosphere was tested. This bacterium was capable of colonizing the roots of the mangrove species *Rhizophora mangle*, and it could successfully compete with other organisms and survive for long periods in non-sterile mangrove rhizosphere. Additionally, plasmid DNA uptake by this bacterium, expression of the reporter gene coding for ß-glucuronidase, and site-directed mutagenesis of the *nifH* gene were proven genetically and phenotypically, therefore providing convincing evidence that this bacterium is genetically accessible. Based on the characteristics mention above, *M. mangrovicola* fulfilled all prerequisites of a model organism and has proven to be the most suitable candidate for the establishment of a bacteria-plant model system to study the pathways of nitrogen in mangrove ecosystems.

## 4.2 Relevance of *M. mangrovicola - R. mangle* model system

Nitrogen fixation is one of the most important processes in mangrove ecosystems. Since anoxic sediments in mangrove ecosystem are common, most of the nitrogen is lost by denitrification processes. Nitrogen-fixing bacteria have been identified as key organisms that provide nitrogen to these nitrogen-poor sediments and mangrove plants (Holguin et al., 1992; Holguin et al., 2001; Flores-Mireles et al., 2007). However, the interactions between nitrogen fixers and mangroves are poorly understood. Thus, we proposed a model system consisting of the nitrogen-fixing bacterium *M. mangrovicola*, and the mangrove plant *R. mangle* to facilitate the study of the molecular signals and cellular mechanisms that govern this interaction, and to better understand the role of nitrogen fixers in mangrove ecosystems.

In this study, we showed that nitrogen fixation by *M. mangrovicola* was increased in the presence of mangrove roots. The bacterium was capable of efficiently colonizing *R. mangle* roots. Root colonization was found in the surface and inside the finer lateral roots. Moreover, absence of carbon and nitrogen sources led to a stronger bacterial colonization. *M. mangrovicola* transformants carrying a *nifH*::*gusA* fusion revealed that atmospheric nitrogen was fixed during root colonization under nitrogen- and carbon-limiting conditions. Furthermore, root colonization of the *M. mangrovicola* mutant ΔnifH was strong in the absence of a nitrogen or carbon source indicating that root exudates from *R. mangle* attract the bacterium and foster bacterial growth irrespective of nitrogen fixation. The above findings are the first step to further study enzymatic pathways, gene expression, and molecular signaling taking place during the interaction, as well as bacterial ecological relationships within the mangrove environment.

To understand the role of nitrogen-fixers in mangrove ecosystems we have to comprehend how these bacteria coexist and interact with mangrove plants and thus indirectly are of benefit to the entire ecosystem. With the proposed model system we can – in the future – not only study bacteria-plant interactions, but also the interaction of these diazotrophs with other organisms. In addition, environmental factors and future environmental changes that might affect nitrogen fixation or the mutualistic interaction can now be studied *in vitro*. Thus, by setting up a model interaction system the basis for further investigations has been established.

## 4.3 Biological nitrogen fixation influenced by temperature and salinity

Mangrove ecosystems are exposed to different environmental conditions such as tidal inundation, desiccation, changes in temperature, salinity, pH, and high input of organic matter (Duke, 1992; Feller et al., 2010). These factors not only affect mangrove plants development, but also nitrogen fixation by diazotrophic bacteria (Lee and Joye, 2006; Flores-Mireles et al., 2007; Vovides et al., 2011). Temperature and salinity have been highlighted as factors having a major impact on the composition of bacterial communities in mangrove ecosystems, therefore the effects of temperature and salinity on nitrogen fixation rates of the proposed model organism *M. mangrovicola* was studied in detail.

Nitrogen fixation by *M. mangrovicola* Gal22 was inhibited at high temperatures such as 40 °C. The highest nitrogen fixation rates were observed at 36 and 18 °C. Moreover, salinity ranges between 15-70 ‰ had no negative effect on nitrogen fixation at 24 and 30 °C. However, lower salinity increased nitrogen fixation efficiency at lower temperatures such as 18 °C. The wide range of salinity tolerance observed by the nitrogenase of *M. mangrovicola* gives an indication that this organism is well adapted to cope with changes in environmental conditions found in mangrove ecosystems. Moreover, this feature could represent an advantage for *M. mangrovicola* during mangrove root colonization over other organisms with more restricted temperature and salinity tolerances. Nevertheless, if abrupt changes are combined such as very high temperature and salinity concentration, then nitrogen fixation might be compromised.

Since our newly established model organism can grow in a wide range of temperature and salinity, these characteristics allowed us to study how future changes in the environment, due to climate change, could affect nitrogen fixation, diazotroph-mangrove interactions, and bacterial distribution within the mangrove forest.

# 5. Future Scope

# 5. Future Scope

Salinity fluctuations in mangrove ecosystems are common. Desiccation and evaporation increase salinity in mangrove sediments whereas freshwater coming from rivers dilute salts. Thus, organisms that live in mangrove soils need to adapt to such fluctuating conditions. One interesting characteristic of the proposed model organism *M. mangrovicola* is its ability to tolerate up to 180 ‰ NaCl. However the mechanism used to achieve intracellular osmotic balance is unknown. A proteomics analysis of *M. mangrovicola* were cells are exposed to different concentrations of salts could help us to unravel this enigma. In the Appendix I, two-dimensional (2D) protein gels were standardized for the visualization of total *M. mangrovicola* protein extracts obtained after the cells had been exposed to osmotic stress. Preliminary results showed some differences in the protein profiles exposed to different salinity concentrations (15, 40 and 70 ‰), were the biggest changes were found between protein samples obtained from cells treated with osmotic stress imposed by 15 and 70 ‰ salts. The protein spots from the gels were subjected to MALDI-TOF MS analysis. However, the lack of a genome sequence and the absence of detection of similar protein masses from genomes available from species of the genus *Marinobacterium* made the analysis inconclusive. Consequently, in order to identify and analyze the proteins induced during an osmotic stress, a complete genome sequence of *M. mangrovicola* is needed.

Another interesting new insight would be to investigate the transfer of nitrogen fixed by *M. mangrovicola* during mangrove root colonization to the plant. In this thesis, it was shown that the presence of mangrove roots increased nitrogen fixation by *M. mangrovicola* indicating a possible mutualistic interaction. However to determine the type of symbiotic relationship, it is necessary to evaluate the transfer of the fixated nitrogen from the bacterium to the plant. For this, *M. mangrovicola* and the mangrove plant need to be incubated after the addition of $^{15}N$. After incubation, the plant tissue is examined for $^{15}N$ incorporation. Another alternative would be the use NanoSIMS (Foster et al., 2011) to determine the fate of the fixated nitrogen.

Moreover, studies focusing on particular genes that are expressed or up-regulated during the bacteria-plant interaction are essential to understand the process of bacterial colonization and nitrogen fixation within the plant tissue. *In vitro* studies where molecular techniques such as transcriptomics are used in the diazotroph-mangrove model system could help us to unravel which genes are expressed during the interaction.

Since *M. mangrovicola* Gal22 was isolated from mangrove roots from an *in vitro* cultivation system, the distribution of this organism in the different mangrove ecosystems is unknown. The biogeography of this organism and its distribution within the different zones in the mangrove forest could help us to unravel its ecological significance in the ecosystem, as well as the study of abiotic factors that are more specific for its habitat and could influence

nitrogen fixation. The above mentioned subjects are still open questions that could be the next step for future investigations on this very interesting topic.

# 6. Appendix

# 6. Appendix I:

## 6.1 Protocol for proteomic analysis of *Marinobacterium mangrovicola* under different NaCl stress

Gabriela Alfaro-Espinoza, Khaled Abdallah and Matthias S. Ullrich
Jacobs University Bremen, Molecular Life Science Research Center, Campus Ring 1, 28759 Bremen, Germany.

### INTRODUCTION

Salinity has been identified as one of the main factors impacting nitrogen-fixing bacteria (Vovides et al., 2011). In mangrove ecosystems salinity varies along tidal gradients. Diazotrophs living in mangrove sediments cope with regular changes in salinity generated by desiccation, tidal action, evaporation or inputs of freshwater (Feller et al, 2010). Bacteria may adapt to changes in salinity by accumulating osmotic organic solutes, accumulating salts, a combination of both, or by the export of ions through ion pumps located in the cell membranes (Ventosa et al., 1998). However, these mechanisms have never been studied in diazotrophic bacteria inhabiting mangrove forests.

The model organism *Marinobacterium mangrovicola* Gal22 is capable of growing and fixing atmospheric nitrogen under high salinity concentrations (Alfaro and Ullrich, 2014). However, the mechanism used by this bacterium to withstand high concentrations of salts is unknown. A proteomics analysis were cells are exposed to different osmotic stress could help us to reveal the pathway used to achieve osmotic balance. Here a protocol was developed for the visualization and further study of *M. mangrovicola* proteins that are induced during an osmotic stress.

### MATERIALS AND METHODS

#### A. Protein extraction and quantification.

*M. mangrovicola* Gal22 was grown in liquid HGB medium at 28 °C. The salinity of the medium was adjusted by the addition of NaCl to 15, 40, and 70 ‰, respectively. Bacterial cells were harvested at $OD_{600}$ of 0.37, resuspended in sonication buffer [100 mM Tris-HCl, 1% SDS, 1% DTT, pH 8.1 (1 tablet of proteinase inhibitor was added / 10 ml buffer)] and disrupted by sonication (3 times for 10 sec). To remove the cell debris, the samples were centrifuged at 3.000 x g at 4 °C for 1h. Then, the proteins were precipitated by adding acetone [sample to acetone ratio 1:4 (v/v)] and resuspended in 50 mM Tris-HCl pH 7.5. Total

protein content was determined by using the Pierce BCA protein assay kit (Thermo Fisher Scientific, Schwerte, Germany.).

**B. Two dimensional polyacrylamide gel electrophoresis (2D-PAGE) and MALDI-TOF MS analysis.**

Proteins (60 µg) were mixed with 100 µl of rehydration buffer (ReadyPrep rehydration/sample buffer, (Bio-Rad, München, Germany)) and 2 µl of Bio-Lyte ampholytes (Bio-Rad), and then added to a ReadyStrip IPG strip (pH range 4-7, 7 cm length, BioRad). The IPG strips were incubated at room temperature for 16 h and latter subjected to the first dimension, Isoelectric focusing (IEF) in a Protean i12 IEF system (BioRad). The following parameters were used to focused the samples: 1.10 h at 50 volts (V), 20 min at 150 V, 15 min at 300 V, 10 min at 600 V, 15 min at 600 V, 10 min at 1500 V, 30 min at 1500 V, 20 min at 3000 V, and 3,3 h at 3000 V. After the IEF, the strips were equilibrated first for 15 min in 10 ml equilibration buffer [6 M Urea, 30% glycerol, 2% SDS, 50 mM Tris-HCl (pH 8.8)] plus 0.1 g DTT and second, for 15 min in 10 ml equilibration buffer plus 0.4 g iodoacetamide. Then the strips were subjected to a 12.5% SDS-PAGE (second dimension) using a Mini-PROTEAN Tetra Cell System (Bio-Rad). Finally, the gels were stained with silver staining and compared visually. The protein spots from the gels marked in Figure 1A, B and C undergo a tryptic in-gel treatment, according to Speicher et al., (2000); Shevchenko et al. (2006); and Granvogl et al., (2007); then analyzed by MALDI-TOF MS using an Autoflex II TOF/TOF mass spectrometer (Bruker Daltonik, Bremen, Germany).

**Preliminary Results and Future Work**

*M. mangrovicola* 2D protein gels reveal that the cells exposed to different osmotic stress showed differences in their protein profile. These differences were more pronounced between cells grown in medium with the lowest salinity concentration (15 ‰) and the highest (70 ‰) (**Figure 1**). The identification of the proteins by MALDI-TOF MS was not possible due to the lack of a genome sequence of our model organism, and the absence of detection of similar protein masses from genomes available from species of the genus *Marinobacterium.* For future studies and to better identify the proteins induced during an osmotic stress, the genome of *M. mangrovicola* needs to be sequenced. Overall, these results suggested that this protocol is suitable for the extraction and visualization of *M. mangrovicola* proteins.

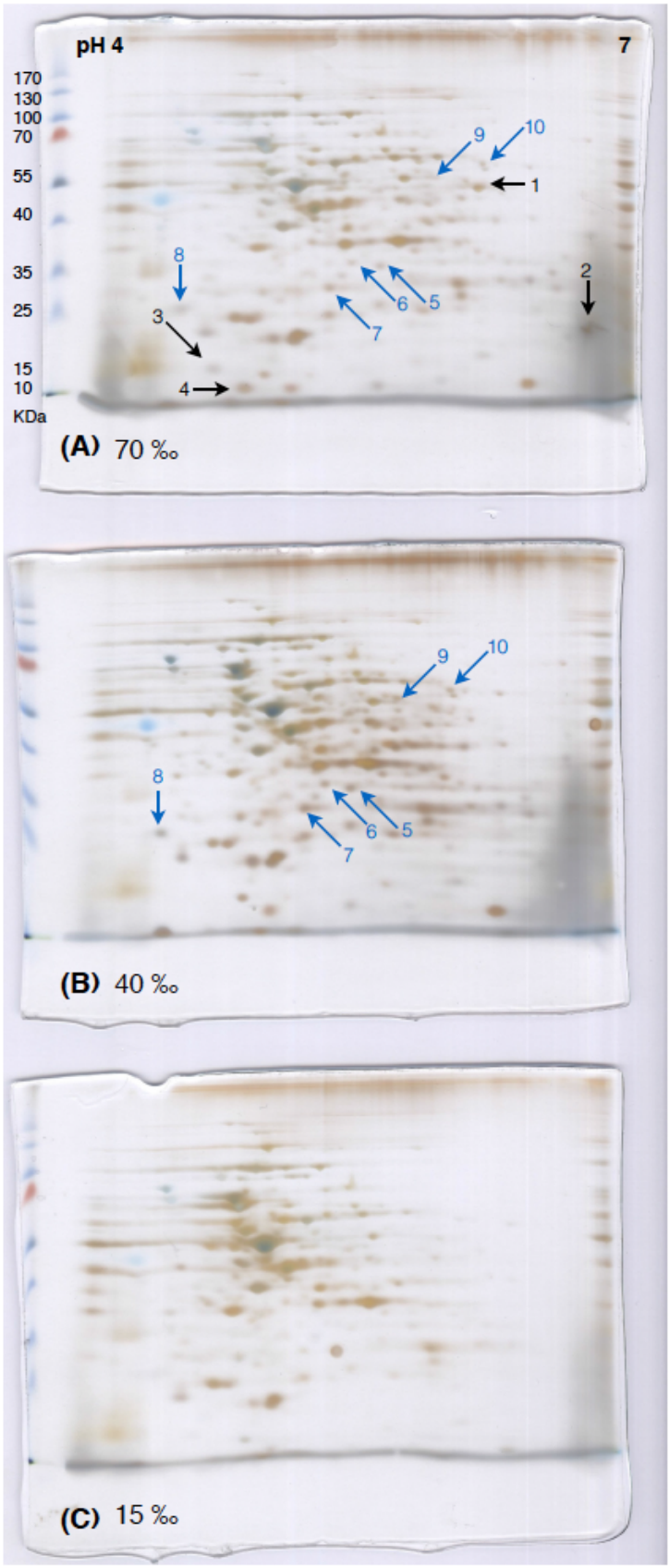


**Figure 1.** 2D-PAGE of proteins from *M. mangrovicola* Gal22. Bacterial cells grown in HGB medium with a salinity of (A) 70, (B) 40, and (C) 15 ‰. Back arrows indicated protein spots only found in the gel corresponding to the highest salinity, 70 ‰. Blue arrows indicated protein spots missing in the gel corresponding to the lower salinity, 15 ‰.

**REFERENCES**

Alfaro-Espinoza, G., Acevedo-Trejos, E., Abdallah, K., and Ullrich M.S. (2014). Influence of salinity and temperature on nitrogen fixation rates of the mangrove-associated bacterium, *Marinobacterium mangrovicola*. In preparation.

Feller, I. C., Lovelock, C. E., Berger, U., Mckee, K. L., Joye, S. B., and Ball, M. C. (2010). Biocomplexity in mangrove ecosystems. *Ann. Rev. Mar. Sci.* 2, 395–417. doi:10.1146/annurev.marine.010908.163809.

Granvogl, B., Plöscher, M., and Eichacker, L. A. (2007). Sample preparation by in-gel digestion for mass spectrometry-based proteomics. *Anal. Bioanal. Chem.* 389, 991–1002. doi:10.1007/s00216-007-1451-4.

Shevchenko, A., Tomas, H., Havlis, J., Olsen, J. V, and Mann, M. (2006). In-gel digestion for mass spectrometric characterization of proteins and proteomes. *Nat. Protoc.* 1, 2856–2860. doi:10.1038/nprot.2006.468.

Speicher, K. D., Kolbas, O., Harper, S., and Speicher, D. W. (2000). Systematic analysis of peptide recoveries from in-gel digestions for protein identifications in proteome studies. *J. Biomol. Tech.* 11, 74–86.

Ventosa, A., Nieto, J. J., and Oren, A. (1998). Biology of moderately halophilic aerobic bacteria. *Microbiol. Mol. Biol. Rev.* 62, 504–544.

Vovides, A. G., Bashan, Y., López-Portillo, J. a., and Guevara, R. (2011). Nitrogen fixation in preserved, reforested, naturally regenerated and impaired mangroves as an indicator of functional restoration in mangroves in an arid region of Mexico. *Restor. Ecol.* 19, 236–244. doi:10.1111/j.1526-100X.2010.00713.x.

# 6. Appendix II:

## Additional contributions

The following manuscripts are not related to the main research topic "A bacteria-plant model system to study $N_2$-fixation in mangrove ecosystems" but were also originated in the course of my PhD thesis. My contribution to both manuscripts was to test the responses of several microorganisms towards different chemical compounds. In Barsukova-Stuckart et al. (2012), three polyoxotungstates were synthesized to be used as antibacterials in wound covering devises. Their antimicrobial capacity was tested in several microorganisms by the minimum inhibitory concentration assay. In Bartok et al. (2014), the toxicity of benzalkonium chloride (a preservative in ophthalmic solutions) towards human corneal epithelial cells was reduced in the presence of Brilliant Blue G. However, to ensure that the bacteriostatic effect was not compromised different Gram-positive and Gram-negative bacteria were tested.

**Synthesis and biological activity of organoantimony(III)-containing heteropolytungstates.**
Maria Barsukova-Stuckart, Luis F. Piedra-Garza, Bimersha Gautam, Gabriela Alfaro-Espinoza, Natalya V. Izarova, Abhishek Banerjee, Bassem S. Bassil, Matthias S. Ullrich, Hans J. Breunig, Cristian Silvestru, and Ulrich Kortz (2012). *Inorg Chem.* 51, 12015-12022.

**Reduction of cytotoxicity of benzalkonium chloride and octenidine by Brilliant Blue G.**
Melinda Bartok, Rashmi Tandon, Gabriela Alfaro-Espinoza, Matthias S. Ullrich and Detlef Gabel (2015). EXCLI Journal. 14, 123-132. doi:10.17179/excli2014-556

## 6.2 Synthesis and Characterization of Organoantimony(III)-containing Heteropolytungstates

Maria Barsukova-Stuckart,[†] Luis F. Piedra-Garza,[†] Bimersha Gautam,[†] Gabriela Alfaro-Espinoza,[†] Natalya V. Izarova,[†, ‡] Abhishek Banerjee,[†] Bassem Bassil,[†] Matthias Ullrich,[†] Hans Joachim Breunig,[§] Cristian Silvestru,[¥] Ulrich Kortz*[,†]

[†] Jacobs University, School of Engineering and Science, P.O. Box 750 561, 28725 Bremen, Germany

[‡] Permanent address: Nikolaev Institute of Inorganic Chemistry SB RAS, Prospekt Lavrentyeva 3, 630090 Novosibirsk, Russia

[§] Institut für Anorganische and Physikalische Chemie, Universität Bremen, Leobener Strasse, 28334 Bremen, Germany

[¥] Faculty of Chemistry and Chemical Engineering, Babes-Bolyai University, Arany Janos Str. No. 11, RO-400028 Cluj-Napoca, Romania

*E-mail: u.kortz@jacobs-university.de

Keywords: Polyoxometalate; Organoantimony; Single crystal XRD; Multinuclear NMR; Biological activity

**Reprinted with permission from:** Barsukova-Stuckart, M., Piedra-Garza, L., Gautam, B., Alfaro-Espinoza, G., Izarova, N., Banerjee, A., Bassil, B., Ullrich, M., Breunig, H., Silvestru, C., and Kortz, U. (2012). Synthesis and biological activity of organoantimony(III)-containing heteropolytungstates. *Inorg Chem.* 51, 12015–12022. Copyright (2012) American Chemical Society.

---

**ABSTRACT**

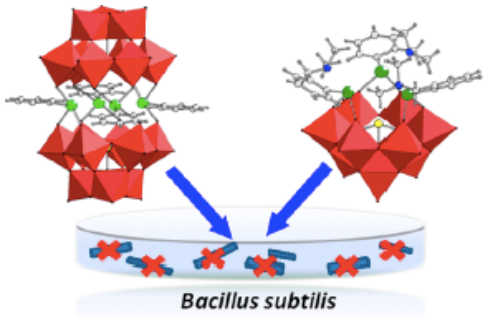


Three discrete organoantimony(III)-containing heteropolytungstates $[(PhSb^{III})_4(A\text{–}\alpha\text{–}Ge^{IV}W_9O_{34})_2]^{12-}$ (1), $[(PhSb^{III})_4(A\text{–}\alpha\text{–}P^{V}W_9O_{34})_2]^{10-}$ (2) and $[\{2\text{-}(Me_2NCH_2C_6H_4)Sb^{III}\}_3(B\text{–}\alpha\text{–}As^{III}W_9O_{33})]^{3-}$ (3) have been synthesized through one-pot reactions in aqueous medium using the appropriate lacunary heteropolyanion precursor and organoantimony(III) source. They were isolated as hydrated salts $(NH_4)_{12}[(PhSb^{III})_4(A\text{–}\alpha\text{–}Ge^{IV}W_9O_{34})_2]\cdot 20H_2O$ (**1a**), $Rb_9Na[(PhSb^{III})_4(A\text{–}\alpha\text{–}P^{V}W_9O_{34})_2]\cdot 20H_2O$ (**2a**), and $Rb_3[\{2\text{–}(Me_2NCH_2C_6H_4)Sb^{III}\}_3(B\text{–}\alpha\text{–}As^{III}W_9O_{33})]\cdot 7H_2O$ (**3a**). The compounds were fully characterized in the solid state by IR spectroscopy, single-crystal XRD, thermogravimetric and elemental analyses. The stability of the polyanions 1-3 in aqueous solution was confirmed by multinuclear NMR ($^{1}H$, $^{13}C$, $^{31}P$, and $^{183}W$) spectroscopy. Preliminary studies on the biological activity of the compounds showed that all three compounds might act as potent antimicrobial agents.

---

## INTRODUCTION

Polyoxometalates (POMs) represent a large class of discrete polynuclear metal-oxo anions usually formed by early transition elements (e.g. $W^{VI}$, $Mo^{VI}$, $V^{V}$) in high oxidation states.[1] Organic derivatives of polyoxometalates (POMs) are of particular interest nowadays, since it allows the features of both POMs and incorporated organic units to combine together in one molecular assembly. The functionalization of POMs with organometallic moieties allows for the tuning of their size, shape, solubility, as well as redox and acid–base properties. Furthermore, it can lead to improved stability in various solvents and pH ranges, especially of biological nature, resulting in variations and modifications in toxicity and biological activity of these functionalized POMs.[2] Hybrid organic-inorganic POMs may also combine several interesting features, e.g. chirality,[3] magnetic, electrical[4] and catalytic properties.[5]

Several successful attempts were made in order to prepare organometallic-containing POMs and study their biological and pharmacological activity.[6] In particular, organotin species have been of wide use due to the stability of the Sn–C bond and also the fact that $Sn^{IV}$ can substitute the addenda metals in POM skeletons.[6c, 7-9] Our group has already reported a variety of such organotin-containing polyoxoanions, namely $[\{Me_2Sn^{IV}(H_2O)_2\}_3(\beta\text{–}X^{III}W_9O_{33})]^{3-}$ (X = As, Sb),[9a] $[(PhSn^{IV})_2As^{III}{}_2W_{19}O_{67}(H_2O)]^{8-}$,[9b] $[\{Me_2Sn^{IV}(H_2O)\}_{24}(Me_2Sn^{IV})_{12}(A\text{–}\alpha\text{–}X^{V}W_9O_{34})_{12}]^{36-}$ (X = P, As),[9d] $[\{PhSn^{IV}(OH)\}_3(A\text{–}\alpha\text{–}X^{IV}W_9O_{34})]^{4-}$ (X = Ge, Si),[9j] $[\{PhSn^{IV}(OH)\}_3(A\text{–}\beta\text{–}X^{IV}W_9O_{34})]^{4-}$ (X = Ge, Si), as well as $[\{PhSn^{IV}(A\text{–}\beta\text{–}H_3SiW_9Sn^{IV}{}_2O_{37})\}_2O_2]^{8-}$ [9n]. By contrast, POMs functionalized by organoantimony fragments are rather few in literature. In 1989, the group of Liu reported the solid-state structure of $[(Ph_2Sb^{V})_2(\mu\text{–}O)_2(\mu\text{–}MoO_4)_2]^{2-}$, in which two separated $\{MoO_4\}$ tetrahedra bridge two octahedrally coordinated antimony ions.[10] The isostructural tungsten analogue was also reported.[1d] Recently, a reverse Keggin ion was prepared in the Winpenny's group; it comprises twelve $\{PhSb^{V}\}$ units in the addenda positions and a central $\{M^{II}O_4\}$ (M = Mn, Zn) group.[11] The reactivity of organostibonic acids towards formation of polyoxostibonates is also intensively studied these days, and several representatives of the novel class of POMs built exclusively by organoantimony units are already obtained.[12]

To our knowledge, only the organoantimony(V)-containing polyoxotungstate $[\{PhSb^{V}(OH)\}_3(A\text{–}\alpha\text{–}P^{V}W_9O_{34})_2]^{9-}$ has been reported to date. It was synthesized by our group in 2007 *via* hydrothermal reaction of $Ph_2Sb^{V}Cl_3$ and $Na_9[A\text{–}\alpha\text{–}P^{V}W_9O_{34}]\cdot 13H_2O$ in aqueous acidic medium.[13] Here we report the synthesis and structural characterization of three novel organoantimony(III)-containing POMs, isolated as hydrated ammonium and alkali metals salts $(NH_4)_{12}[(PhSb^{III})_4(A\text{–}\alpha\text{–}Ge^{IV}W_9O_{34})_2]\cdot 20H_2O$ (**1a**), $Rb_9Na[(PhSb^{III})_4(A\text{–}\alpha\text{–}P^{V}W_9O_{34})_2]\cdot 20H_2O$ (**2a**) and $Rb_3[\{2\text{–}(Me_2NCH_2C_6H_4)Sb^{III}\}_3(B\text{–}\alpha\text{–}As^{III}W_9O_{33})]\cdot 7H_2O$ (**3a**). Preliminary studies on the biological activity of these compounds are also presented.

## RESULTS AND DISCUSSION

**Synthesis and Structure.** Polyanions **1 – 3** have been prepared in a facile self-assembly reaction of $PhSbCl_2$ or $[2\text{-}(Me_2NCH_2C_6H_4)]SbCl_2$ with the sodium salt of the respective polyoxometalate precursor ($Na_{10}[A\text{–}\alpha\text{–}Ge^{IV}W_9O_{34}]\cdot 18H_2O$, $Na_9[A\text{–}\alpha\text{–}P^{V}W_9O_{34}]\cdot 13H_2O$ or $Na_9[B\text{–}\alpha\text{–}As^{III}W_9O_{33}]\cdot 27H_2O$) in water, and isolated in crystalline form using appropriate aqueous solution of ammonium or rubidium chloride in yields of 73%, 68% and 46% for **1a**, **2a** and **3a**, respectively. These compounds are stable towards air and light in the solid state. They are also stable in solution, at least for a week, as it was shown by NMR spectroscopy

(see below). It is noted that the $Sb^{III}$ sources needed to be dissolved in a minimum amount of ethanol and were added dropwise as such.

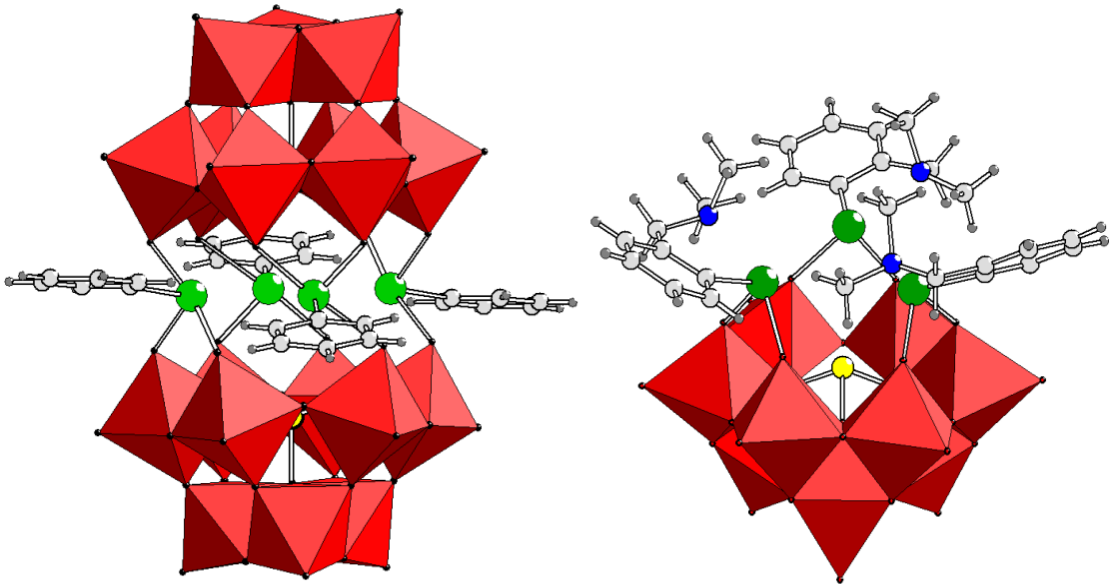


**Figure 1.** Combined polyhedral/ball-and-stick representation of: (a) $[(PhSb^{III})_4(A–\alpha–XW_9O_{34})_2]^{n-}$ (X = $Ge^{IV}$ (1), $P^V$ (2)) and (b) $[\{2–(Me_2NCH_2C_6H_4)Sb^{III}\}_3(B–\alpha–As^{III}W_9O_{33})]^{3-}$ (3). Color code: $WO_6$ red octahedra; X and As, yellow; Sb, green; C, light grey; N, blue; H, dark grey balls.

The single-crystal X-ray analysis shows that the compounds **1a** and **2a** crystallize in the triclinic crystal system, space group *P-1*. The two respective anions $[(PhSb^{III})_4(A–\alpha–XW_9O_{34})_2]^{n-}$ (X = $Ge^{IV}$ (**1**), $P^V$ (**2**)) are isostructural and consist of a dimeric, sandwich-type structure with two $\{A–\alpha–XW_9O_{34}\}$ units capping four $\{PhSb^{III}\}$ groups (see Figure 1a). Each antimony(III) center is tetra-coordinated and exhibits seesaw geometry, with the bulky phenyl group and the lone pairs of $Sb^{III}$ in the equatorial positions. The three remaining positions are occupied by oxo bridges at the lacunary sites of the $\{A–\alpha–XW_9O_{34}\}$ units, bridging to two edge shared $WO_6$ octahedra from one unit and one $WO_6$ octahedron from the other, having two of the three oxo ligands sitting in the axial position ($O–Sb^{III}–O$ ca. 169–172°) and the third oxo in the equatorial position alongside the phenyl group. This is in contrast with the reported polyanion containing three organoantimony(V) units $[\{PhSb^V(OH)\}_3(A–\alpha–P^VW_9O_{34})_2]^{9-}$, where each antimony(V) has octahedral coordination, being in oxidation state +5 with no lone pair of electrons, with four oxo ligands from the sandwiching $[A–\alpha–P^VW_9O_{34}]^{9-}$ units and a hydroxo ligand trans to the phenyl group.[13] The bond lengths in **1**, **2** and $[\{PhSb^V(OH)\}_3(A–\alpha–P^VW_9O_{34})_2]^{9-}$ are very similar (Table 1), except Sb–O bonds, which are longer for **1** and **2** and can be correlated to the lower oxidation state of the antimony centers. Moreover, in comparison to $[\{PhSb^V(OH)\}_3(A–\alpha–P^VW_9O_{34})_2]^{9-}$, the synthetic procedures of **1** and **2** are much 'softer'. This is not surprising, as the starting material for antimony(V) ($Ph_2SbCl_3$) contains two phenyl groups bonded to antimony, requiring therefore hydrothermal condition in order to release on of them, reduce steric

hindrance and allow the antimony(V) atom to coordinate to the lacunary site. Whereas for **1** and **2**, antimony(III) can readily coordinate to $\{A\text{–}\alpha\text{–}XW_9O_{34}\}$ units without such a step.

**Table 1. Selected Bond Lengths for 1, 2, and $[\{PhSb^{V}(OH)\}_3(A\text{-}\alpha\text{-}P^{V}W_9O_{34})_2]^{9-}$ (Data for the Latter Taken from ref 13)**

| | Bond Lengths [Å] | | |
|---|---|---|---|
| | **1** | **2** | $[\{PhSb^{V}(OH)\}_3(A\text{-}\alpha\text{-}P^{V}W_9O_{34})_2]^{9-}$ |
| W–$O_t$ | 1.708(18)–1.750(17) | 1.719(12)–1.746(12) | 1.698(13)–1.734(13) |
| W–O(X) | 2.196(15)–2.309(15) | 2.365(11)–2.427(10) | 2.350(11)–2.411(11) |
| W–O(W) | 1.813(17)–2.095(17) | 1.816(12)–2.061(12) | 1.849(12)–1.982(12) |
| W–O(Sb) | 1.792(17)–1.900(16) | 1.793(11)–1.883(12) | 1.831(13)–1.862(13) |
| Sb–O | 1.993(15)–2.380(18) | 2.000(12)–2.335(11) | 1.986(12)–2.036(13) |
| Sb–C | 2.134(12)–2.157(12) | 2.152(8)–2.174(8) | 2.096(16)–2.140(13) |
| X–O | 1.728(15)–1.793(16) | 1.527(11)–1.576(11) | 1.523(12)–1.584(12) |
| Sb–OH | | | 1.926(15)–1.935(18) |

The four $Sb^{III}$ atoms in **1** and **2** are coplanar with the coordinated phenyl rings arranged in an up-down fashion with reference to the plane. Interestingly, the up-up/down-down ring pairs are adjacent to each other instead of being opposite to each other. Such arrangements alongside the overall structures give polyanions **1** and **2** an idealized $C_{2v}$ point group symmetry.

In the solid state (Figure 2) polyanions **1** and **2** form 2D layers parallel to the *a* axis, with the phenyl rings from adjacent polyanion molecules exhibiting displaced $\pi - \pi$ stacking.

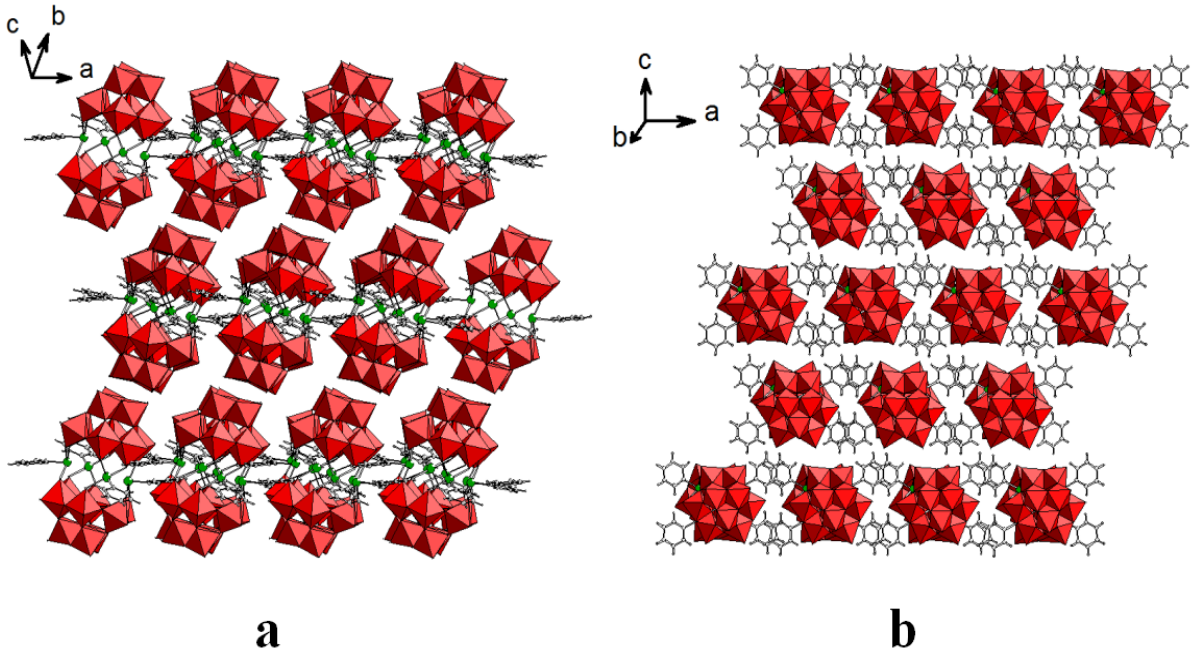


**Figure 2.** The crystal packing arrangement of **1a** and **2a**: (a) view of the layers; (b) top view of one layer. Counter cations and crystal waters have been omitted for clarity. Color code is the same as in Figure 1.

The polyanion $[\{2\text{–}(Me_2NCH_2C_6H_4)Sb^{III}\}_3(B\text{–}\alpha\text{–}As^{III}W_9O_{33})]^{3-}$ (**3**) comprises the $[B\text{–}\alpha\text{–}As^{III}W_9O_{33}]^{9-}$ lacunary fragment, which is composed of an inner $As^{III}$ heteroatom linked to three corner-shared $\{W_3O_{13}\}$ triads (consisting of three edge-shared $WO_6$ octahedra). This unit is further coordinated by three $\{2\text{–}(Me_2NCH_2C_6H_4)Sb^{III}\}^{2+}$ moieties resulting in an assembly with $C_3$ symmetry in the solid state (Fig. 1b). Each $Sb^{III}$ ion in **3** coordinates two oxygens of the vacant sites of the $[B\text{–}\alpha\text{–}AsW_9O_{33}]^{9-}$ ligand, associated with the $W^{VI}$ centers of the two adjacent triads, as well as the carbon atom of the organic moiety (see Table 2 for the bond lengths). The resulting $\{CSb^{III}O_2\}$ core possesses a trigonal pyramidal geometry with a lone pair on the $Sb^{III}$ center directed to the center of the polyanion. The nitrogen atom in each $\{2\text{–}(Me_2NCH_2C_6H_4)Sb^{III}\}^{2+}$ unit forms an additional weak bond (bond valence is about 0.5[14]) with the antimony atom in *trans* to one of the Sb–O bonds. The N–Sb distances (2.360(11) – 2.390(11) Å) lie between the sums of the corresponding covalent ($\Sigma r_{cov}$(Sb,N) 2.11 Å) and van der Waals radii ($\Sigma r_{vdW}$(Sb,N) 3.74 Å).[15] These N→Sb interactions are of the same strength as observed in the dichloride $[2\text{-}(Me_2NCH_2C_6H_4)]SbCl_2$ used as starting material (2.407(5) Å),[16] but considerably stronger than in *cyclo*-$[\{2\text{–}(Me_2NCH_2C_6H_4)\}SbO]_3$ in which the N→Sb interaction (2.613(4) – 2.660(4) Å) is also placed in *trans* to a Sb–O bond.[17] Taking into account the N–Sb bond the overall coordination geometry around antimony(III) ions can be described as distorted *pseudo*-trigonal bipyramidal ("*see-saw*"), with nitrogen and one of the oxygen atoms in axial positions (N–Sb–O 157.2(3) – 158.3(4) Å). In addition the N–Sb interactions play an important structural directing role as they determine the symmetrical relative orientation of the three organic ligands.

**Table 2. Selected Bond Lengths for Polyanion 3**

| bond | bond length [Å] |
|---|---|
| W–$O_t$ | 1.690(14)–1.735(13) |
| W–O(As) | 2.298(12)–2.380(12) |
| W–O(W) | 1.901(12)–1.926(12) |
| Sb–O(W) | 1.950(13)–2.144(12) |
| Sb–C | 2.100(19)–2.144(12) |
| Sb–N | 2.360(11)–2.390(11) |
| As–O | 1.770(12)–1.789(12) |

Overall, the structure of the polyanion **3** resembles that of the previously reported flower-pot-shaped organotin-containing POMs $[\{Me_2Sn^{IV}(H_2O)_2\}_3(\beta\text{–}X^{III}W_9O_{33})]^{3-}$ (X = As, Sb)[9a] and allows to make some analogies in the reactivity of organotin and organoantimony species towards POM ligands. Nevertheless the structure of the polyanion **3** is still unique considering the distorted *pseudo*-trigonal bipyramidal coordination geometry of the $Sb^{III}$ ions *vs* the octahedral coordination mode of the $Sn^{IV}$ centers in the latter flower-pot-shaped POMs.

In the crystal polyanions **3** are connected *via* intermolecular C–$H_{(aromatic\ ring)}$-$\pi$ bonds directed along diagonals between crystallographic axes *a* and *b* as well as –*a* and *b* to form *pseudo*-layers in the *ab* plane (Figure 3a). These *pseudo*-layers alternate in an ABAB sequence along the crystallographic axis *c* being connected by C–H-$\pi$ interactions between $CH_2$ group of one

POM with the $\pi$-system of the phenyl group of the polyanion in the adjacent pseudo-layer (**Figure 3b**).

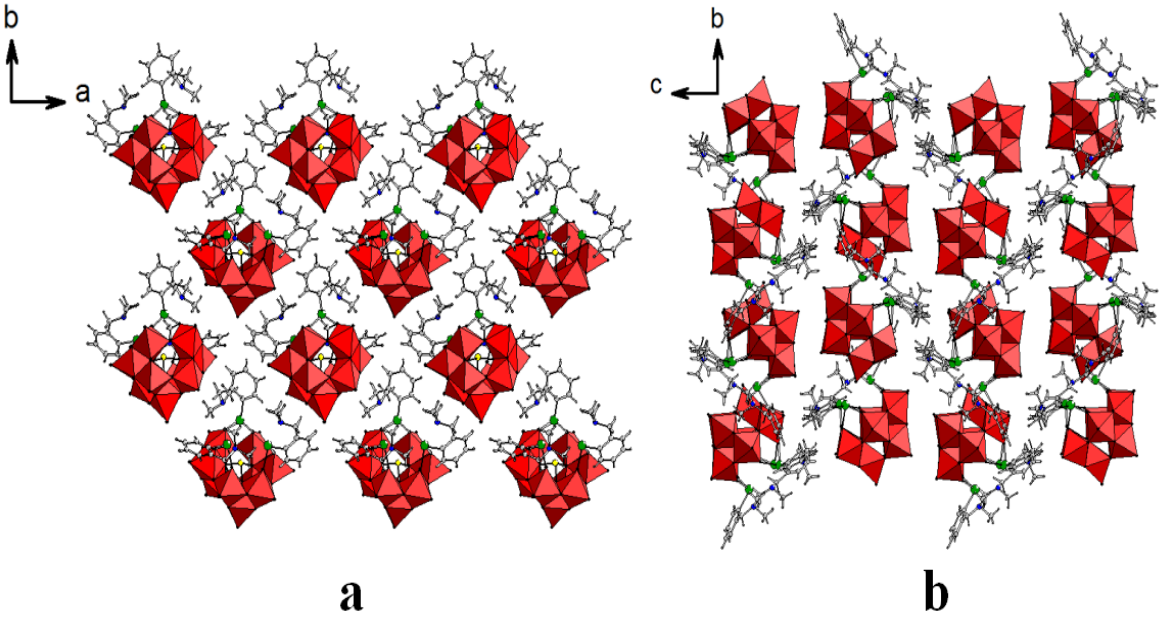


**Figure 3.** The crystal packing arrangement of **3a**: (a) a view along *c* axis; (b) a view along *a* axis. Counter cations and crystal waters have been omitted for clarity. Color code is the same as in Figure 1.

**FT-IR Spectra.** FT-IR spectra recorded on the sample of **1a**, **2a** and **3a** are shown in the Supporting Information (Fig. S1, S2 and S3 respectively). The stretching and bending vibrations of the C–H and C–C bonds of organic groups appear at 1184, 1065, 721 and 618 $cm^{-1}$ in case of **1a**, in the region between 1480 and 1060 $cm^{-1}$, and at 721 and 618 $cm^{-1}$ for **2a**, and between 3060 – 2790 $cm^{-1}$ and 1440 – 1030 $cm^{-1}$, and at 749 and 692 $cm^{-1}$ for **3a**.[18] The band at 780 $cm^{-1}$ corresponds to Ge–O vibrations in **1a**. For **2a** the band at 1013 $cm^{-1}$ corresponds to P–O antisymmetric stretching modes. The band at 854 $cm^{-1}$ corresponds to As–O antisymmetric stretching modes for **3a**. The other peaks below 1000 $cm^{-1}$ are assigned to terminal W=O as well as bridging W–O–W stretching modes for all of the compounds.[19] The bands at 3142, 3020, 2834 and 1401 $cm^{-1}$ correspond to $NH_4^+$ ions for **1a**. The broad bands at 1625 $cm^{-1}$ for **1**, at 1619 $cm^{-1}$ for **2a** and at 1618 $cm^{-1}$ for **3a** belong to asymmetric vibrations of the crystal water molecules.[20]

**Thermogravimetric analysis (TGA).** The thermogravimetric process of **1a** revealed several weight-loss steps (see Fig. S4). The first step occurs between 25 and 160 °C and corresponds to the loss of 20 water molecules per formula unit (6.2 % found *vs* 6.1 % calc). The several consecutive weight loss steps covering the temperature range 160 – 480 °C are attributed to the release of four phenyl groups and twelve $NH_3$ molecules per formula unit (8.0 % found *vs* 8.7 % calc). The experimental percentage weight loss for the organic groups is less than calculated due to incomplete decomposition. The total observed weight loss for **1a** at 1000°C is 17.9 %.

The thermogram of **2a** also showed several weight-loss steps (see Fig. S5). The first step occurs between 25 and 170 °C and corresponds to the loss of 16 water molecules per formula unit (4.5% found *vs* 4.6% calc). The number of water molecules determined by TGA is slightly lower than that obtained by crystallography (20 molecules). This fact can be easily explained by partial loss of crystal water molecules during sample drying. Single crystals for XRD measurements were taken directly from the mother liquid, put in oil and frozen under nitrogen flow on the diffractometer, whereas the samples for TGA were air-dried for at least one day. The combustion of four phenyl groups per formula unit proceeds in the temperature range of 380 – 600 °C (5.0 % found *vs* 4.9 % calc). The total observed weight loss for **2a** at 1000 °C is 10.8 %.

In case of **3a** the first step on the thermogram occurs between 25 and 200 °C and corresponds to the loss of 9 water molecules per formula unit of **3a** (4.5% found *vs* 4.7% calc; Fig. S6). In this case the number of water molecules determined by TGA is slightly higher than that obtained by crystallography (7 molecules) due to high disorder of the crystallization water molecules in the crystal structure of **3a**. Dehydration step is followed by the release of the organic moieties confirmed by the series of steps between 200 and 590 °C (11.5 % found *vs* 11.7 % calc). The total observed weight loss for **3a** at 1000 °C is 28.7 %.

**NMR Studies.** The solution stability of **1**, **2** and **3** was investigated by multinuclear NMR spectroscopy. The experiments were carried out on the solutions of the compounds in $H_2O/D_2O$. It should be noted that the final pH values of the studied solutions were around 7. The $^{183}W$ NMR spectra of isomorphous **1** and **2** showed the expected five peaks for each polyanion (at -78, -93, -102, -148, -195 ppm for **1** and at -105, -112, -115, -168, -178 ppm for **2**) with an intensity ratio of 2:1:2:2:2, respectively, which is fully consistent with the $C_{2v}$ symmetry in the crystal structure (see Figure 4).

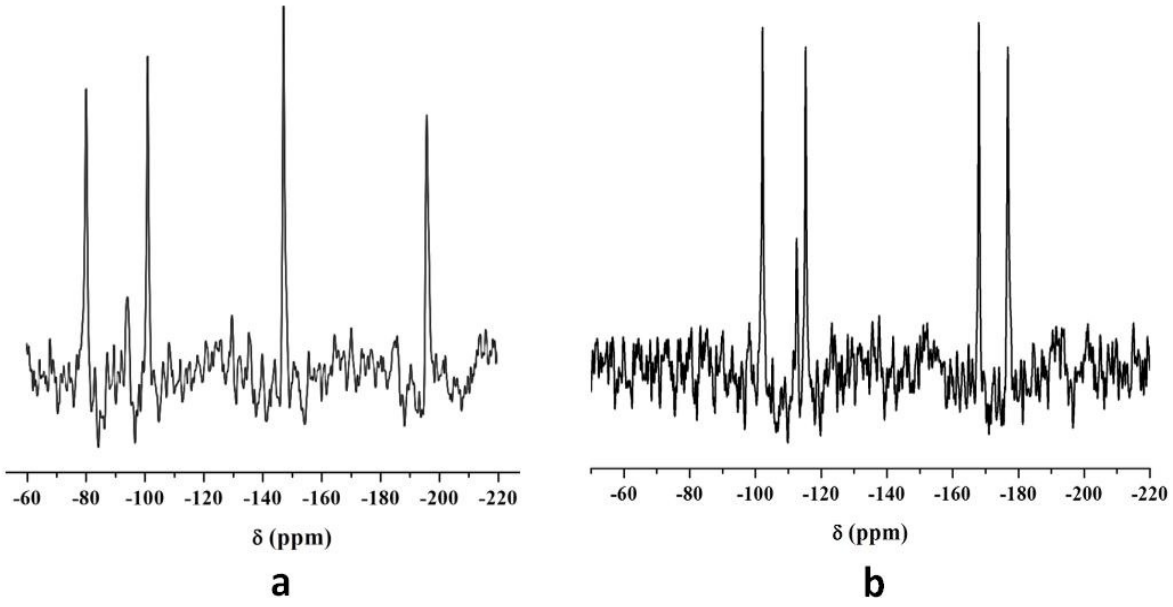


**Figure 4.** $^{183}W$ NMR spectra of **1a** (a) and **2a** (b) recorded at room temperature in $H_2O/D_2O$.

The $^{13}C$ NMR spectra of **1a** and **2a** are as expected for coordinated phenyl groups (Fig. S7). The $^{1}H$ NMR spectra of **1a** and **2a** also prove the presence of coordinated phenyl groups as

well as $NH_4^+$ ions in case of **1a** (Fig. S8). The $^{31}P$ NMR spectra of **2a** revealed one signal at -11.1 ppm (see Figure 5).

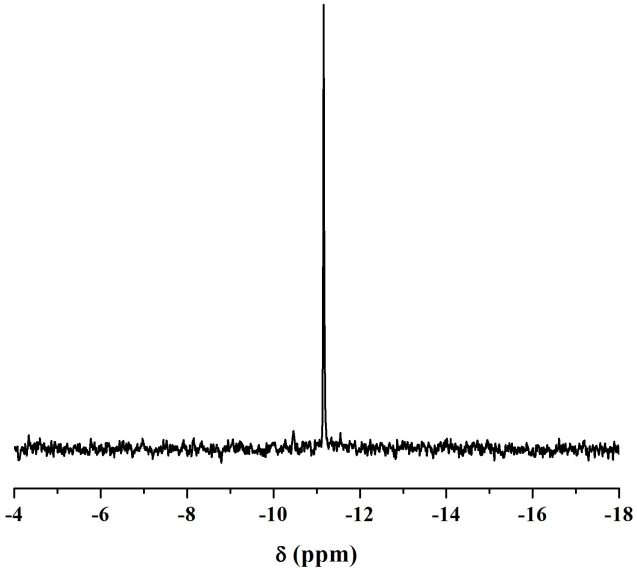


**Figure 5.** $^{31}P$ NMR spectrum of **2a** recorded at room temperature in $H_2O/D_2O$.

Due to the low solubility of **3a** we were not able to carry out a solution $^{183}W$ NMR study on the compound. The $^1H$ NMR spectrum of **3a** proves the presence of the $\{Me_2NCH_2C_6H_4\}$ groups (Fig. S9).

According to the results of the multinuclear NMR study we could conclude that the polyanions **1**, **2** and **3** are stable at physiological pH values and so could be used for the biologic studies.

**Table 3. MIC Determination of the Different Polyanions in *Escherichia coli* DH5α and *Bacillus subtilis*[a]**

| | MIC Determination (μg/mL) | | | | | |
|---|---|---|---|---|---|---|
| | 1 | | 2 | | 3 | |
| microorganism | MHB | LB | MHB | LB | MHB | LB |
| *E. coli* | 80 | 80 | 110 | 110 | 130 | 130 |
| *B. subtilis* | 80 | 40 | 50 | 50 | 60 | 60 |

[a]MHB = Mueller–Hinton–Bouillon medium; LB = Luria–Bertani medium.

**Biological Activity.** Since we have shown the stability of all three test compounds in aqueous media at physiological pH value (around 7.0) we decided to study their antimicrobial activity. Results of the MIC assays showed that all three test compounds very efficiently inhibited the

growth of the used indicator bacterial strains, which represented gram-negative and gram-positive bacteria. The MICs for each compound are summarized in Table 3. Use of the two different media did not reveal any significant differences. Interestingly, compounds **2a** and **3a** had a slightly stronger activity against the gram-positive *B. subtilis*, as compared to the gram-negative organism, *E. coli*. Compound **1a** showed this increased activity against gram-positive microbes only when *B. subtilis* was grown in LB medium. These results indicated that all three compounds have the potential to act as antibacterial agents despite of their structural differences.

## EXPERIMENTAL SECTION

**Materials and Physical Measurements:** All reagents were purchased from commercial sources and used without further purification. The IR spectra for solid samples were obtained in KBr pellets on a Nicolet Avatar 370 FTIR spectrophotometer. Thermogravimetric analyses were carried out on a TA Instruments SDT Q600 thermobalance with 10-30 mg samples in 100 µl alumina pans under a 100 ml/min flow of nitrogen; the temperature was ramped from 20 to 1000 °C at a rate of 5 °C/min. The NMR spectra of the obtained compounds were recorded on a 400 MHz JEOL ECX instrument at room temperature using 5 mm tubes for $^{1}H$, $^{13}C$ and $^{31}P$, and 10 mm tubes for $^{183}W$ NMR. The respective resonance frequencies were 399.78 MHz ($^{1}H$), 100.71 MHz ($^{13}C$), 162.14 MHz ($^{31}P$), and 16.69 MHz ($^{183}W$). The chemical shifts are reported with respect to the references $Si(CH_3)_4$ ($^{1}H$ and $^{13}C$), 85% $H_3PO_4$ ($^{31}P$) and $Na_2WO_4$ ($^{183}W$). Elemental analyses were performed by KANTI LABS, Tirupathi (India) for **1a**, by Analytische Laboratorien, Lindlar (Germany) for **2a** and by Service Central d'Analyse, Solaize (France) for **3a**.

**$(NH_4)_{12}[(PhSb^{III})_4(A\text{–}\alpha\text{–}Ge^{IV}W_9O_{34})_2]\cdot 20H_2O$ (1a):** Polyoxometalate precursor $Na_{10}[A\text{–}\alpha\text{–}Ge^{IV}W_9O_{34}]\cdot 18H_2O$ (0.417 g, 0.145 mmol), synthesized according previously published procedure,[21] was dissolved in 20 ml of distilled water, whereas 0.078 g (0.290 mmol) of $PhSbCl_2$[22] was dissolved in a separate beaker in a minimum amount of ethanol. The solution of the $PhSbCl_2$ was added dropwise to the precursor solution under vigorous stirring. The resulting solution was stirred for 30 min, and then it was filtered. Several drops of 1 M $NH_4Cl$ were added to the final solution, and then it was cooled to 4 – 5 °C. After 1 day yellow crystals suitable for XRD measurements were obtained. Yield: 0.315 g, (73 % based on {W}). Elemental analysis (%) calcd: N 2.84, H 1.84, C 4.87, Sb 8.23, Ge 2.46, W 56.0; found: N 2.91, H 1.92, C 4.77, Sb 8.12, Ge 2.48, W 55.9. IR (2% KBr pellet, ν/cm$^{-1}$): 3142(s), 3020(sh), 2834(sh), 1625(m), 1401(s), 1184(w), 1065(w), 926(s), 879(s), 780(s), 721(s), 618(sh), 533(m), 479(m).

**$Rb_9Na[(PhSb^{III})_4(A\text{–}\alpha\text{–}P^{V}W_9O_{34})_2]\cdot 20H_2O$ (2a):** $Na_9[A\text{–}\alpha\text{–}P^{V}W_9O_{34}]\cdot 13H_2O$ (0.417 g, 0.145 mmol), prepared as described previously,[23] was dissolved in 20 ml of distilled water, whereas 0.078 g (0.290 mmol) of $PhSbCl_2$[22] was dissolved in a separate beaker in a minimum amount of ethanol. The solution of the $PhSbCl_2$ was added dropwise to the precursor solution under vigorous stirring. The resulting solution was stirred for 30 min, filtered, and several drops of 0.5 M RbCl were added. The final solution was cooled to 4 – 5 °C. After 1 day yellow crystals were obtained. Yield: 0.345 g, (68 % based on {W}). Elemental analysis (%) calcd: Rb 12.01, Na 0.36, H 0.94, C 4.50, Sb 7.60, P 0.97, W 51.65; found: Rb 11.53, Na 0.30, H 1.05, C 4.73, Sb 9.34, P 1.10, W 51.25. IR (2% KBr pellet, ν/cm$^{-1}$): 1619 (m), 1478 (w), 1428 (w), 1185 (w), 1066 (s), 1013 (m), 942 (s), 913 (s), 892 (sh), 822(sh), 741 (s), 592 (w), 516 (m), 459 (m).

**$Rb_3[\{2\text{–}(Me_2NCH_2C_6H_4)Sb^{III}\}_3(B\text{–}\alpha\text{–}As^{III}W_9O_{33})]\cdot 7H_2O$ (3a):** $Na_9[B\text{–}\alpha\text{–}As^{III}W_9O_{33}]\cdot 27H_2O$ (0.134 g, 0.05 mmol), obtained according to the known procedure[24] was dissolved in 10 ml of water. 0.047 g (0.15 mmol) of $[2\text{–}(Me_2NCH_2C_6H_4)]SbCl_2$[16] was dissolved in ethanol with heating at 40 °C. The solution of the organoantimony dichloride was added dropwise to the precursor solution under vigorous stirring. The mixture was stirred for 30 minutes at room temperature and filtered off. 1 ml of 0.5 M RbCl was added to the resulting solution. Yellow crystals were obtained after several days, filtered off and air dried. Yield: 0.080 g (46% based on {W}). Elemental analysis (%) calcd: Rb 7.45, N 1.22, H 1.58, C 9.42, Sb 10.61, As 2.18, W 48.0; found: Rb 7.09, N 1.19, H 1.45, C 9.55, Sb 10.30, As 2.11, W 47.6. IR (2% KBr pellet, $\nu/cm^{-1}$): 3056(m), 2998(m), 2968(m), 2906(m), 2835(m), 2797(m), 1618(m), 1437(m), 1360(w), 1287(w), 1208(w), 1113(w), 1031(w), 997(s), 955(s), 854(s), 790(s), 749(s), 692(s), 655(s), 481(m), 447(m).

**X-ray Crystallography:** Data for the structures of **1a – 3a** were collected at 173 K on a Bruker Kappa X8 APEX CCD single-crystal diffractometer equipped with a sealed Mo tube and graphite monochromator (l = 0.71073 Å). Crystals were mounted in a Hampton cryoloop with light oil to prevent water loss. The SHELX software package (Bruker) was used to solve and refine the structures.[25] Absorption corrections were applied empirically using the SADABS program.[26] The structures were solved by direct methods and refined by the full-matrix least-squares method minimization of $(\Sigma w(Fo - Fc)^2)$ with anisotropic thermal parameters for all skeleton non-hydrogen atoms. The hydrogen atoms of the organic groups in **1 – 3** were introduced in geometrically calculated positions. Additional crystallographic data are summarized in Table S1 (see Supporting Information). Further details of the crystal structure investigation are available free of charge from The Cambridge Crystallographic Data Center via www.ccdc.cam.ac.uk/data_request/cif on quoting the depository numbers CCDC 891299 (**1a**), 891300 (**2a**), 891301 (**3a**).

**Biological Studies – Determination of Minimal Inhibitory Concentrations:** *Escherichia coli* DH5α and *Bacillus subtilis* were used to test the antimicrobial activity of solutions of the compounds **1a** – **3a** in deionized water (Table 4). The minimum inhibitory concentration (MIC) of the compounds against the microorganisms was assayed in micro-titer plates using a standardized method.[27] For the generation of the MIC assay plates two bacterial growth media, Mueller-Hinton Bouillon (MHB) and Luria Bertani medium (LB), were used. Aliquots of 180 µl of media were added into row A of the micro-titer plate, and 100 µl aliquots were added to rows B-H. 20 µl of the antimicrobial compounds at the concentrations indicated in Table 4 were added into row A. Dilution series (1/2) were made from row A-H by transferring 100 µl from well to well using a multi-channel pipetman. Next, 100 µl of the bacterial suspension (approximately $2x10^6$ bacteria/ml) were added into each well of the micro-titer plate. All MIC assay plates were incubated overnight for *E. coli* at 37 °C and for *B. subtilis* at 30°C. For each compound the MIC assay was performed in triplicate with deionized water used as negative control.

**Table 4. Polyanions and Their Concentrations Used in the MIC Assay**

| polyanion | molecular formula | POM concentration in deionized water (mM) |
|---|---|---|
| **1** | $[(PhSb^{III})_4(A\text{-}\alpha\text{-}Ge^{IV}W_9O_{34})_2]^{12-}$ | 4.2 |
| **2** | $[(PhSb^{III})_4(A\text{-}\alpha\text{-}P^{V}W_9O_{34})_2]^{10-}$ | 2.7 |
| **3** | $[\{2\text{-}(Me_2NCH_2C_6H_4)Sb^{III}\}_3(B\text{-}\alpha\text{-}As^{III}W_9O_{33})]^{3-}$ | 2.9 |

## CONCLUSIONS

In summary, we have synthesized three novel polyoxotungstates functionalized by organoantimony units, *i.e.* $[(PhSb^{III})_4(A\text{–}\alpha\text{–}Ge^{IV}W_9O_{34})_2]^{12-}$ (**1**), $[(PhSb^{III})_4(A\text{–}\alpha\text{–}P^{V}W_9O_{34})_2]^{10-}$ (**2**) and $[\{2\text{–}(Me_2NCH_2C_6H_4)Sb^{III}\}_3(B\text{–}\alpha\text{–}As^{III}W_9O_{33})]^{3-}$ (**3**). The obtained POMs were isolated as the hydrated ammonium and alkali metals salts, respectively, and characterized in the solid state by single-crystal XRD, TGA and FT-IR spectroscopy. The multinuclear NMR study of the resulting compounds redissolved in $H_2O/D_2O$ reveals their solution stability.

The gram-positive bacterium *B. subtilis*, showed a slightly higher sensitivity towards the tested compounds **1a**, **2a** and **3a** as compared to the gram-negative organism *E. coli.* This difference may be due to differences in the composition of the cell envelopes of gram-positive and -negative bacteria.[28] Since gram-negative bacteria are surrounded by a hydrophobic outer membrane, our results might indicate that the hydrophilic character or specific hydrophilic residues of the tested compounds could prevent an efficient entry into gram-negative bacterial cells. In contrast, structural features of the compounds could potentially facilitate a more efficient entry into gram-positive bacterial cells and thus make those organisms more susceptible. However, it should be noted that the differences in MIC values are rather small allowing the conclusion that all three compounds might act as potent antimicrobial agents.

## ASSOCIATED CONTENT

**Supporting Information.** Crystallographic data in CIF format, a table with the main crystallographic and refinement parameters (Table S1), IR spectra (Figures S1 – S3) and thermograms (Figures S4 – S6), $^{13}C$ and $^{1}H$ NMR spectra of **1a**, **2a** and **3a** (Figures S7 – S9), are available at http://pubs.acs.org.

## ACKNOWLEDGMENTS

U. K. and M. B.-S. thank Jacobs University for research support. Financial support from National Research Council (CNCS) of Romania through Research Project No. PN-II-ID-PCE-2011-3-0933 is highly acknowledged by C.S. S. Koppala is thanked for the help with reproducing of the compounds and biological studies. Figures 1-2 were generated by Diamond Version 3.2 (copyright Crystal Impact GbR).

## REFERENCES

(1) (a) Pope, M. T. *Heteropoly and Isopoly Oxometalates*; Springer-Verlag: Berlin, 1983. (b) Day, V. W.; Klemperer, W. G. *Science*. 1985, *228*, 533-541. (c) Pope, M. T.; Müller, A. *Angew. Chem. Int. Ed. Engl.* 1991, *30*, 34-48. (d) *Polyoxometalates: From Platonic Solids to Antiretroviral Activity* (Eds.: Pope, M. T.; Müller A.); Kluwer: Dordrecht, 1994. (e) Okuhara, T.; Mizuno, N.; Misono, M. *Adv. Catal*. 1996, *41*, 113-252. (f) *Chem. Rev.* 1998, *98* (Special Issue on Polyoxometalates; Ed.: Hill, C.L.). (g) Talismanov, S. S.; Eremenko, I. L. *Russ. Chem. Rev*. 2003, *72*, 555–569. (h) Müller, A.; Roy, S. *Coord. Chem. Rev.* 2003, *245*, 153-166. (i) Cronin, L. in *Comprehensive Coordination Chemistry* II, Vol. 7 (Eds.: McCleverty, J. A.; Meyer, T. J.); Elsevier: Amsterdam, 2004. (j) Coronado, E.; Day, P. *Chem. Rev.* 2004, *104*, 5419-5448. (k) Hill, C. L. *J. Mol. Catal. A. Chem.* 2007, *262*, 2-6. (l) Hasenknopf, B.; Micoine, K.; Lacote, E.; Thorimbert, S.; Malacria, M.; Thouvenot, R. *Eur. J. Inorg. Chem.* 2008, 5001-5013. (m) Kortz, U.; Müller, A.; van Slageren, J.; Schnack, J.; Dalal, N. S.; Dressel, M. *Coord. Chem. Rev*. 2009, *253*, 2315-2327. (n) *Eur. J. Inorg. Chem*. 2009, *34* (Issue dedicated to Polyoxometalates; Guest Ed.: Kortz, U.). (o) Long, D.-L.; Tsunashima, R.; Cronin, L. *Angew. Chem.* 2010, *122*, 1780-1803; *Angew. Chem. Int. Ed.* 2010, *49*, 1736-1758.

(2) (a) Proust, A.; Thouvenot, R.; Gouzerh, P. *Chem. Commun*. 2008, 1837–1852. (b) Hasenknopf, B.; Micoine, K.; Lacote, E.; Thorimbert, S.; Malacria, M.; Thouvenot, R. *Eur. J. Inorg. Chem.* 2008, 5001-5013. (c) Dolbecq, A.; Dumas, E.; Mayer, C. R.; Mialane, P. *Chem. Rev.* 2010, *110*, 6009-6048.

(3) Coronado, E.; Curreli, S.; Giménez-Saiz, C.; Gómez-García, C. J.; Roth, J. *Synth. Met.* 2005, *154*, 241-244.

(4) (a) Coronado, E.; Gómez-García, C. J. *Chem. Rev*. 1998, *98*, 273-296. (b) Coronado, E.; Galán-Mascarós, J. R. *J. Mater. Chem*. 2005, *15*, 66-74. (c) Coronado, E.; Giménez-Saiz, C.; Gómez-García, Coord. C. J. *Chem. Rev.* 2005, *249*, 1776-1796. (d) Coronado, E.; Day, P. *Chem. Rev.* 2004, *104*, 5419-5448.

(5) Carraro, M.; Sandei, L.; Sartorel, A.; Scorrano, G.; Bonchio, M. *Org. Lett*. 2006, *8*, 3671-3674.

(6) (a) Barnard, D. L.; Hill, C. L.; Gage, T.; Matheson, J. E.; Huffman, J. H.; Sidwell, R. W.; Otto, M. I.; Schinazi, R. F. *Antiviral Res.* 1997, *34*, 27-37. (b) Flütsch, A.; Schroeder, T.; Grütter, M. G.; Patzke, G. R. *Bioorg. Med. Chem. Lett*. 2011, *21*, 1162-1166. (c) Dong, Z.; Tan, R.; Cao, J.; Yang, Y.; Kong, C.; Du, J.; Zhu, S.; Zhang, Y.; Lu, J.; Huang, B.; Liu, S. *Eur. J. Med. Chem.* 2011, *46*, 2477-2484.

(7) (a) Knoth, W. H. *J. Am. Chem. Soc*. 1979, *101*, 759-760. (b) Knoth, W. H. *J. Am. Chem. Soc.* 1979, *101*, 2211-2213. (c) Zonnevijlle, F.; Pope, M. T. *J. Am. Chem. Soc*. 1979, *101*, 2731-2732. (d) Knoth, W. H.; Domaille, P. J.; Roe, D. C. *Inorg. Chem*. 1983, *22*, 818-822. (e) Knoth, W. H.; Domaille, P. J.; Farlee, R. D. *Organometallics* 1985, *4*, 62-68. (f) Xin, F.; Pope, M. T. *Organometallics* 1994, *13*, 4881-4886. (g) Xin, F.; Pope, M. T.; Long, G. J.; Russo, U. *Inorg. Chem*. 1996, *35*, 1207-1213. (h) Xin, F.; Pope, M.T. *Inorg. Chem*. 1996, *35*, 5693-5695. (i) Yang, Q. H.; Dai, H. C.; Liu, J. F. *Transition Met. Chem*. 1998, *23*, 93-95. (j) Wang, X. H.; Dai, H. C.; Liu, J. F. *Polyhedron* 1999, *18*, 2293-2300. (k) Wang, X. H.; Dai, H. C.; Liu, J. F. *Transition Met. Chem.* 1999, *24*, 600-604. (l) Wang, X. H.; Liu, J. F. *J. Coord. Chem*. 2000, *51*, 73-82. (m) Sazani, G.; Dickman, M. H.; Pope, M. T. *Inorg. Chem*. 2000, *39*, 939-943. (n) Wang, X. H.; Liu, J. T.; Zhang, R. C.; Li, B.; Liu, J. F. *Main Group Met. Chem*. 2002, *25*, 535-539. (o) Bareyt, S.; Piligkos, S.; Hasenknopf, B.; Gouzerh, P.; Lacôte, E.; Thorimbert, S.; Malacria, M. *Angew. Chem. Int. Ed*. 2003, *42*, 3404-3406. (p) Sazani, G.; Pope, M. T. *Dalton Trans.* 2004, 1989-1994. (q) Bareyt, S.; Piligkos, S.; Hasenknopf, B.; Gouzerh, P.; Lacôte, E.; Thorimbert, S.; Malacria, M. *J. Am. Chem. Soc*. 2005, *127*, 6788-6794. (r) Belai, N.; Pope, M. T. *Polyhedron* 2006, *25*, 2015-2020. (s) Micoine, K.; Thorimbert, S.; Lacote, E.; Malacria, M.; Hasenknopf, B. *Organic Letters* 2007, *9*, 3981-3984. (t) Bar-Nahum, I.; Ettedgui, J.; Konstantinovski, L.; Kogan, V.; Neumann R. *Inorg. Chem*. 2007, *46*, 5798-5804. (u) Boglio, C.; Micoine, K.; Derat, E.; Thouvenot, R.; Hasenknopf, B.; Thorimbert, S.; Lacôte, E.; Malacria, M. *J. Am. Chem. Soc*. 2008, *130*, 4553–4561. (v) Micoine, K.; Hasenknopf, B.; Thorimbert, S.; Lacôte, E.; Malacria, M. *Angew. Chem. Int. Ed.* 2009, *48*, 3466–3468. (w) Khoshnavazi, R.; Bahrami, L. *J. Coord. Chem.* 2009, *62*, 2067-2075. (x) Zhang, L.-C.; Zheng, S.-L.; Xue, H.; Zhu, Z.-M.; You, W.-S.; Li, Y.-G.; Wang, E. *Dalton Trans*. 2010, *39*, 3369-3371. (y) Zhang, L.-C.; Xue, H.; Zhu, Z.-M.; Wang, Q.-X.; You, W.-S.; Li, Y.-G.; Wang, E.-B. *Inorg. Chem. Comm*. 2010, *13*, 609-612. (z) Yokoyama, A.; Kojima, T.; Ohkubo, K.; Shiro, M.; Fukuzumi, S. *J. Phys. Chem. A.* 2011, *115*, 986-997.

(8) (a) Kandasamy, B.; Wills, C.; McFarlane, W.; Clegg, W.; Harrington, R. W.; Rodríguez-Fortea, A.; Poblet, J. M.; Bruce, P. G.; Errington R. J. *Chem. Eur. J.* 2012, *18*, 59-62. (b) Wang, Z.-J.; Zhang, L.-C.; Zhu, Z.-M.; Chen, W.-L.; You, W.-S.; Wang, E.-B. *Inorg. Chem. Comm*. 2012, *17*, 151-154.

(9) (a) Hussain, F.; Reicke, M.; Kortz, U. *Eur. J. Inorg. Chem*. 2004, 2733-2738. (b) Hussain, F.; Kortz, U.; Clark, R. J. *Inorg. Chem*. 2004, *43*, 3237-3241. (c) Hussain, F.; Kortz, U. *Chem. Commun*. 2005, 1191-1193. (d) Kortz, U.; Hussain, F.; Reicke, M. *Angew. Chem. Int. Ed*. 2005, *44*, 3773-3777. (e) Hussain, F.; Kortz, U.; Keita, B.; Nadjo, L.; Pope, M. T. *Inorg. Chem*. 2006, *45*, 761-766. (f) Reinoso, S.; Dickman, M. H.; Reicke, M.; Kortz, U. *Inorg. Chem*. 2006, *45*, 10422-10424. (g) Reinoso, S.; Dickman, M. H.; Reicke, M.; Kortz, U. *Inorg. Chem*. 2006, *45*, 9014-9019. (h) Hussain, F.; Dickman, M. H.; Kortz, U.; Keita, B.; Nadjo, L.; Khitrov, A.; Marshall, A. G. *J. Clust. Sci.* 2007, *18*, 173-191. (i) Reinoso, S.; Dickman, M. H.; Matei, M. F.; Kortz, U. *Inorg. Chem*. 2007, *46*, 4383–4385. (j) Reinoso, S.; Dickman, M. H.; Praetorius, A.; Piedra-Garza, L. F.; Kortz, U. *Inorg. Chem*. 2008, *47*, 8798–8806. (k) Reinoso, S.; Dickman, M. H.; Kortz, U. *Eur. J. Inorg. Chem*. 2009, 947–953. (l) Piedra-Garza, L. F.; Reinoso, S.; Dickman, M. H.; Sanguineti, M. M.; Kortz, U. *Dalton Trans*. 2009, 6231–6231. (m) Reinoso, S.; Bassil, B. S.; Barsukova, M.; Kortz, U. *Eur. J. Inorg. Chem.* 2010, 2537-2542. (n) Reinoso, S.; Piedra-Garza, L. F.; Dickman, M. H.; Praetorius, A.; Biesemans, M.; Willem, R.; Kortz, U. *Dalton Trans.* 2010, 248–255.

(10) Liu, B.-y.; Ku, Y.-t.; Wang, M.; Wang, B.-y.; Zheng, P.-j. *J. Chem. Soc., Chem. Commun*. 1989, 651-652.

(11) Baskar, V.; Shanmugam, M.; Helliwell, M.; Teat, J. S.; Winpenny, R. E. P. *J. Am. Chem. Soc.* 2007, *129*, 3042-3043.

(12) (a) Ali, S.; Baskar, V.; Muryn, C. A.; Winpenny, R. E. P. *Chem. Commun.* 2008, 6375-6377. (b) Prabhu, M. S. R.; Jami, A. K.; Baskar, V. *Organometallics* 2009, *28*, 3953-3956. (c) Jami, A. K.; Prabhu, M. S. R.; Baskar, V. *Organometallics* 2010, *29*, 1137-1143. (d) Nicholson, B. K.; Clark, C. J.; Wright, C. E.; Groutso, T. *Organometallics* 2010, *29*, 6518-6526. (e) Nicholson, B. K.; Clark, C. J.; Wright, C. E.; Telfer, S. G.; Groutso, T. *Organometallics* 2011, *30*, 6612-6616.

(13) Piedra-Garza, L. F.; Dickman, M. H.; Moldovan, O.; Breunig, H. J.; Kortz, U. *Inorg. Chem.* 2009, *48*, 411-413.

(14) Brown, I.D.; Altermatt, D. *Acta Crystallogr.* 1985, *B41*, 244-247.

(15) Emsley, J. *Die Elemente*; Walter de Gruyter: Berlin, 1994.

(16) Opris, L. M.; Silvestru, A.; Silvestru, C.; Breunig, H. J.; Lork, E. *Dalton Trans*. 2003, 4367-4374.

(17) Opris, L. M.; Silvestru, A.; Silvestru, C.; Breunig, H. J.; Lork, E. *Dalton Trans*. 2004, 3575-3585.

(18) Pretsch, E.; Buehlmann, P.; Affolter, C. *Structure Determination of Organic Compounds: Tables of Spectral Data*; Springer Verlag: Berlin, 2000.

(19) Rocchiccioli-Deltcheff, C.; Fournier, M.; Franck, R.; Thouvenot, R. *Inorg. Chem*. 1983, *22*, 207-216.

(20) Nakamoto, K. *Infrared and Raman Spectra of Inorganic and Coordination Compounds-Part A: Theory and Applications in Inorganic Chemistry, 5th ed.*; Wiley and Sons: New York, 1997.

(21) Hervé, G.; Tézé, A. *Inorg. Chem*. 1977, *16*, 2115-2117.

(22) (a) Nunn, M.; Sowerby, D. B.; Wesolek, D. M. *J. Organometal. Chem*. 1983, *251*, C45-C46; (b) Alonzo, G.; Breunig, H. J.; Denker, M.; Ebert, K. H.; Offermann, W. *J. Organometal. Chem*. 1996, *522*, 237-240.

(23) Domaille, P. J. *Inorg. Synth*. 1990, *27*, 100.

(24) Kim, K.-C.; Gaunt, A.; Pope, M. T. *J. Clust. Sci.* 2002, *13*, 423-436.

(25) Sheldrick, G. M. *Acta Crystallogr.* 2007, *A64*, 112-122.

(26) Sheldrick, G. M. *SADABS, Program for empirical X-ray absorption correction*; Bruker-Nonius, 1990.

(27) Al-Karablieh, N.; Weingart, H.; Ullrich, M. S. *Int. J. Mol. Sci.* 2009, *10*, 629-645.

(28) (a) Beveridge, T. *J. Bacteriol.* 1999, *181*, 4725–4733. (b) Desvaux, M.; Dumas, E.; Chafsey, I.; Hébraud, M. *FEMS Microbiol. Lett*. 2006, *256*, 1–15.

## 6.3 Reduction of cytotoxicity of benzalkonium chloride and octenidine by Brilliant Blue G

Melinda Bartok*, Rashmi Tandon, Gabriela Alfaro-Espinoza, Matthias S. Ullrich and Detlef Gabel

Molecular Life Science Research Center, Jacobs University Bremen, Campus Ring 1, 28759, Bremen, Germany

*Corresponding Author: m.bartok@jacobs-university.de. Tel: +49-421-2003253; Fax: +49 421 2003249.

Keywords: Brilliant Blue G; Brilliant Blue R; Benzalkonium chloride; Octenidine dihydrochloride; P2x7 receptor antagonist

---

**ABSTRACT**

The irritative effects of preservatives found in ophthalmologic solution, or of antiseptics used for skin disinfection is a consistent problem for the patients. The reduction of the toxic effects of these compounds is desired. Brilliant Blue G (BBG) has shown to meet the expected effect in presence of benzalkonium chloride (BAK), a well known preservative in ophthalmic solutions, and octenidine dihydrochloride (Oct), used as antiseptic in skin and wound disinfection. BBG shows a significant protective effect on human corneal epithelial (HCE) cells against BAK and Oct toxicity, increasing the cell survival up to 51% at the highest BAK or Oct concentration tested, which is 0.01%, both at 30 min incubation. Although BBG is described as a P2x7 receptor antagonist, other selective P2x7 receptor antagonists, OxATP (adenosine 5'-triphosphate-2',3'-dialdehyde) and DPPH (N'-(3,5-dichloropyridin-4-yl)-3-phenylpropanehydrazide), did not reduce the cytotoxicity of neither BAK nor Oct. Therefore we assume that the protective effect of BBG is not due to its action on the P2x7 receptor. Brilliant Blue R (BBR), a dye similar to BBG, was also tested for protective effect on BAK and Oct toxicity. In presence of BAK no significant protective effect was observed. Instead, with Oct a comparable protective effect was seen with that of BBG. To assure that the bacteriostatic effect is not affected by the combinations of BAK/BBG, Oct/BBG and Oct/BBR, bacterial growth inhibition was analyzed on different Gram-negative and Gram-positive bacteria. All combinations of BAK or Oct with BBG hinder growth of Gram-positive bacteria. The combinations of 0.001% Oct and BBR above 0.025% do not hinder the growth of *B. subtilis*. For Gram-negative bacteria, BBG and BBR reduce, but do not abolish, the antimicrobial effect of BAK nor of Oct. In conclusion, the addition of BBG at bacterial inhibitory concentrations is suggested in the ready-to-use ophthalmic preparations and antiseptic solutions.

---

## INTRODUCTION

Brilliant Blue G (BBG) is widely used as a dye for proteins in gel electrophoresis. Its power to stain proteins has led to its application in vitreoretinal surgery for the staining of the internal limiting membrane (ILM), as it showed no toxic effects at the clinically suggested concentration, 0.025%, while showing good staining ability (Enaida et al. 2006). Later, BBG was found to be a great asset also in the treatment of the spinal cord injury, because it reduced the local inflammatory responses, showed protective effects towards the spinal cord neurons and improved the motor recovery (Marcillo et al. 2012; Peng et al. 2009). The authors paired the physiological function of BBG with its activity as a P2x7 receptor antagonist as the spinal cord neurons express this receptor abundantly at their surface.

In previous studies, we showed that BBG protects ARPE retinal pigment epithelium cells against the toxicity of trypan blue (TB), which is another widely used dye for the staining of the ILM in eye surgery (Awad et al. 2013). This observation was unexpected, and no clear mechanism was proposed. Also, it was not known whether the protective effect of BBG was limited to TB, or whether it was more universal. Brilliant Blue R (BBR) is a dye very similar to BBG, which differs only by the absence of two methyl groups. BBR, in contrast to BBG, has never been used medically. In the literature, BBR is used only as a sensitive protein stain in polyacrylamide gel electrophoresis (Servaites et al. 2012). In this study we have tested the cytotoxicity of benzalkonium chloride (BAK) and octenidine (Oct) in combination with BBG or BBR in order to see whether there is any significant reduction in the toxicity of the compounds on human corneal epithelial cells (HCE). BAK is a widely used preservative in ophthalmic drops, even though it is known to have cytotoxic effects and causes easily inflammation in the eye surface (Ammar and Kahook 2011; Dutot et al. 2006; Liang et al. 2012; Paimela et al. 2012). Oct is an antiseptic agent for skin, mucous membranes and wounds, and is used in many preparations as a replacement for other antiseptics, because it shows a significantly higher efficiency already at very low concentrations (Hübner et al. 2010; Koburger et al. 2010). At the clinically and industrially used concentrations, both compounds show high cytotoxicity against mammalian cells. After only 5 minutes incubation with HCE cells, less than 20% of the cells were found to be metabolically active. Interestingly, we found a high protective effect of BBG against the cytotoxic action of BAK and Oct, without an excessive reduction of the bacteriostatic effect.

## MATERIALS AND METHODS

### Materials

Dulbecco's Modified Eagles Medium with Ham's F12 (DMEM + F12), BAK, BBG, BBR, OxATP (adenosine 5'-triphosphate-2',3'-dialdehyde) were purchased from Sigma-Aldrich (Schnelldorf, Germany). Oct was provided by Schülke & Mayr GmbH (Norderstedt, Germany). HCE cells were from Riken Bioresource Center (Tsukuba, Japan). WST-1 cell proliferation reagent was from Roche Diagnostics (Mannheim, Germany). Fetal bovine serum (FBS) and penicillin/streptomycin (Pen/Strep) were from Biochrom (Germany). Human epithelial growth factor (hEGF), insulin, amphotericin B, and L-glutamine were from Sigma-Aldrich (Steinheim, Germany), TrypLE Express was from Gibco (USA). DPPH (N'-(3,5-dichloropyridin-4-yl)-3-phenylpropanehydrazide) was synthesized as described by Lee

et al. (Lee et al. 2012). The medium MHB (Mueller-Hinton Bouillon) was from Carl Roth (Germany).

**Test solutions**

BBG was used between 0.0025 and 0.075%, in combination with either BAK between 0.001 and 0.01%, or Oct between 0.002 and 0.01%. BBR was tested between 0.0025 and 0.05% in the presence of BAK at 0.004% and Oct at 0.003%. As negative control PBS was used. Each of these concentrations were tested also alone on HCE cells as well as on the below mentioned bacterial strains.

**Cell culture and cell viability assay**

HCE cells were cultivated in DMEM + F12 media, supplemented with 15% FBS, 1% Pen/Strep, 25 µg/ml amphotericin B, 5 µg/ml insulin, 10 ng/ml hEGF and 2 mM L-glutamine, at 37°C and 5% $CO_2$. The cells were passaged by trypsinization with TrypLE Express and seeded at a density of 20,000 cells/well in a 96 well, flat bottom plate and grown for 48 h prior to experiment. After the cells reached confluence, they were incubated with 50 µl/well of different test solutions for 5, 30 and 60 min at 37°C and then washed 3 times with PBS (w/o $Ca^{2+}$ and $Mg^{2+}$). One hundred µl of diluted WST-1 cell proliferation reagent (diluted 1:4 in PBS, then 1:10 in cell culture medium) was added to each well and incubated with the cells at 37°C for 4 h. The WST-1 reagent, which is a tetrazolium salt, is reduced to a red formazan dye by the mitochondrial dehydrogenases of metabolically active cells. We had checked previously that the readings for this dye are not influenced by any remaining BBG (Awad et al. 2013). The amount of formazan dye formed was taken as a measure of cell survival. The absorbance of the plate was measured in an MR5000 plate reader (Dynatech) at 450 nm. All test solutions were tested in three independent experiments, with 6 to 12 measurements for each experiment.

**Determination of inhibitory concentrations for bacterial cells**

The Gram-positive bacteria *Bacillus subtilis, Clavibacter michiganensis* and *Paenibacillus sp.* as well as the Gram-negative bacteria *Escherichia coli* DH5α, *Pseudomonas putida* DSM 291 and *Vibrio sp.* Gal12 were used in the assay. The antimicrobial activities of the compound mixtures were assayed in micro-titer plates. For this, 100 µl of MHB were aliquoted into each well of the micro-titer plate, followed by 20 µl of a mixture of antimicrobial compounds and 100 µl of the bacterial suspension (approximately $2 \cdot 10^6$ cells/ml). Deionized water was used as negative control. All micro-titer plates were incubated overnight at 28 ºC, except for *E. coli* plates, which were incubated at 37 ºC. Following overnight incubation, the plates were examined for visible bacterial growth evidenced by the turbidity. Where no turbidity was seen, we assumed that there is no bacterial growth. For each compound, the assay was performed in triplicate in three independent experiments and in accordance with Jorgensen and Turnidge (2007).

**RESULTS**

To investigate the influence of the time and the concentrations of BBG, BAK and Oct on the HCE cell viability, as well as their impact on the bacterial growth inhibition, the cells were exposed to different concentrations of these compounds. Our results showed that BAK was highly toxic for HCE cells. Already in concentrations of 0.001% and 5 min incubation, 30% cell loss was observed. For longer exposure, as would be used in wound treatment, concentrations of 0.002% reduced the cell survival to 20% or less. The inclusion of BBG, in the concentration of 0.025% used clinically for staining procedures, reduced the toxicity of BAK considerably (**Fig. 1**). This protective effect of BBG led to an increase of cell survival, with 50% at 5 min, with 35% at 30 min and with 27% at 60 min incubation at a concentration of BAK 0.01%, the highest concentration tested in this study.

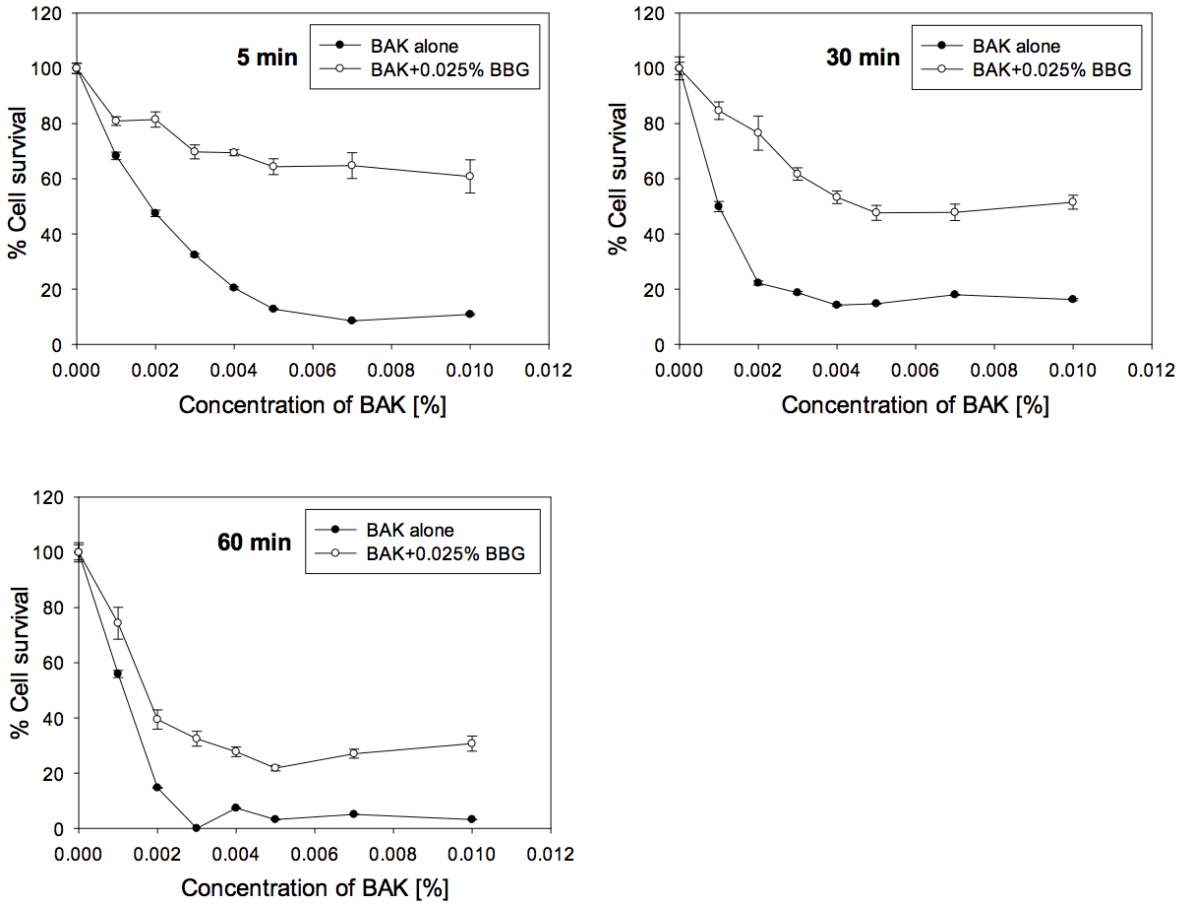


**Fig. 1.** Survival of HCE cells after exposure for 5, 30 and 60 minutes to different concentrations of BAK in PBS ("BAK alone") and in combination with 0.025% BBG. The error bars represent the standard deviations of 6 to 12 replicates performed within the same experiment.

The cell survival after exposure to BAK in the presence of different BBG concentrations is shown in **Fig. 2**. Even at low BBG concentrations, the compound showed significant increase of the cell survival: at 0.007% BBG, 67% of the cells survived exposure to 0.004% BAK, and

48% survived when exposed to 0.006% BAK. Without BBG, cell survival at these concentrations of BAK was around 15% (**Fig. 1**). At higher BAK concentrations, higher BBG concentrations have to be chosen; for example at 0.01% BAK with 0.015% BBG the cell survival increased to 37% and with 0.030% BBG to 46%, at 30 min incubation, whereas in the absence of BBG, cell survival of only a few percent was seen.

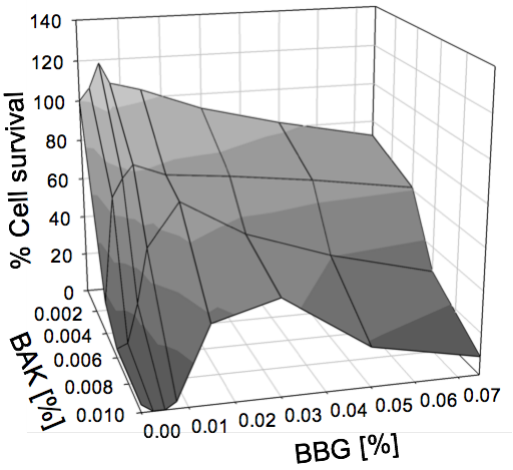


**Fig. 2.** Cell survival of HCE cells after exposure for 30 min to combinations of BAK and BBG in different concentrations.

Oct is an antiseptic agent which, in comparison with BAK, had a higher bacteriostatic effect, but at the same time was more toxic to the cells, as shown in Fig. 3a. BBG protected the cells against Oct toxicity even more than against BAK toxicity. After 5 min incubation with 0.009% Oct and 0.025% BBG, the cell survival increased to 95%, and after 30 min incubation, to 85%, while in the absence of BBG, Oct led to almost complete cell death. In order to find the best combination between Oct and BBG, different concentrations of BBG and Oct were tested in mixture for 30 min incubation (Fig. 3b). For 0.003% Oct, already 0.007% BBG abolished the toxicity of the antiseptic. For 0.007% Oct, a higher concentration of BBG, namely 0.025%, had to be taken, in order to achieve the same effect. At 0.01% Oct concentration, the minimal concentration of BBG needed is 0.025%, and the cell survival increased to 95%.

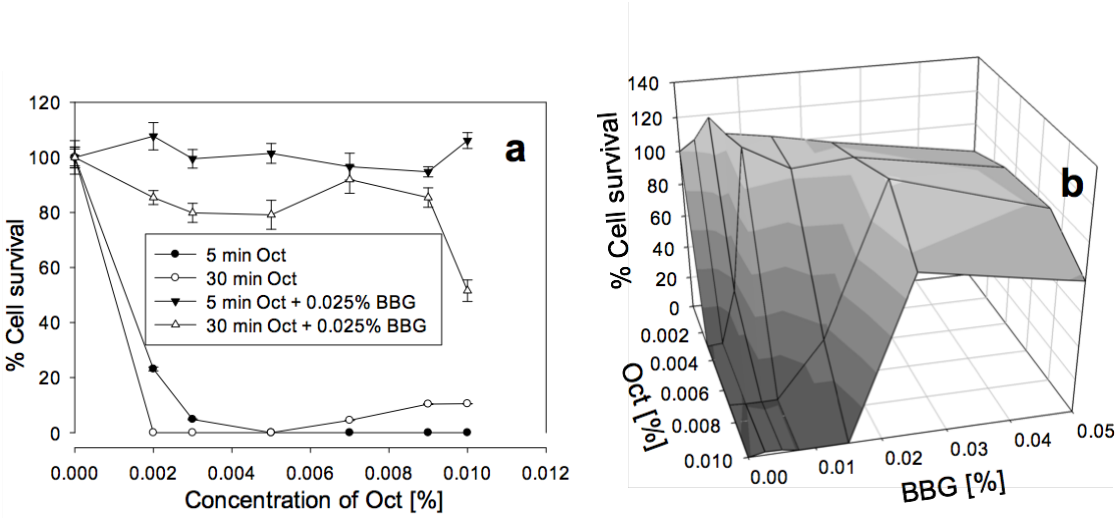


**Fig. 3.** Cell survival of HCE cells after exposure for 5 and 30 min to different concentrations of Oct with and without 0.025% BBG (**a**) and after exposure for 30 min to different combinations of BBG and Oct (**b**). The error bars represent the standard deviations of 6 to 12 replicates performed within the same experiment.

BBR is a dye which differs from BBG only by the absence of two methyl groups. This difference changed significantly the protective activity of BBR against BAK and only slightly against Oct. At 0.004% of BAK there was no considerable cell survival in presence of BBR at 0.025% or higher, while with BBG, the cell survival increased up to 74% (**Fig. 4 a**). The highest protective effect of BBR was obtained at 0.0075%, where the HCE cell survival increased to 52%. This was considerably less than the protective effect of BBG at the same concentration, which was 83%. At 0.003% of Oct BBR showed comparable protective effect with that of BBG (**Fig. 4 b**). The highest cell survivals at this Oct concentration was found at 0.015% and 0.025% BBR concentrations, which was 102% and 90%, respectively. While with BBG at the same concentrations the cell survival was 115% and 100%, respectively. Above 0.05% of BBR or BBG, in presence of Oct, the HCE cells showed a considerable decrease in cell survival.

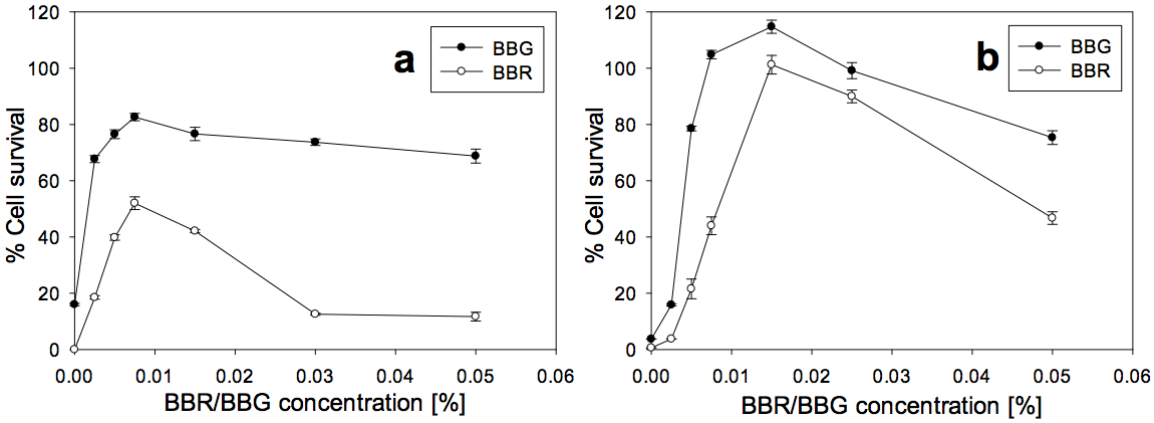


**Fig. 4.** Cell survival of HCE cells after exposure for 30 min to BBR or BBG, in the presence of 0.004% BAK (**a**) or 0.003% Oct (**b**). The error bars represent the standard deviations of 6 to 12 replicates performed within the same experiment.

To determine if the protective effect of BBG on antiseptics was due to its P2x7 receptor antagonist activity, other reported selective P2x7 receptor antagonist were tested in this study. One of them was OxATP. It is known as an irreversible P2x7 receptor antagonist, which blocks human P2x7 receptors at 10 µM concentration (Hibell et al. 2001; Wang et al. 2004). The other antagonist was DPPH, recently synthesized by Lee et al. (2012), which has an $IC_{50}$ of 0.65 µM with ethidium bromide uptake assay. Neither OxATP, used between 2 µM and 2mM (preincubated for 30 min with HCE cells prior to exposure to BAK), nor DPPH, used between 0.1 µM and 10 µM, showed any protective effect against BAK toxicity, when BAK is present between 0.001 and 0.01%. Oct was tested between 0.003% and 0.01% only in presence of DPPH and no protective effect of the P2x7 receptor antagonist was found (data not shown).

**Bacteriostatic effect of Oct and BAK in the presence of BBG and BBR**

Mixtures of BAK or Oct with BBG and BAK or Oct with BBR were used to determine the susceptibility of diverse bacterial strains towards the compound combinations. The BAK and Oct at concentrations between 0.002% and 0.01% inhibited the growth of all tested Gram-positive bacterial strains, even when mixed with the highest applied BBG concentration. In general, Gram-positive bacteria were more susceptible towards the compounds than Gram-negative bacteria. The inhibitory concentrations for Gram-negative bacterial growth were summarized **in Fig. 5** and **Fig. 6**. All tested Gram-negative bacteria showed similar responses towards Oct and BAK when the same concentration of BBG was used. These results suggested that the growth of different bacterial organisms were efficiently inhibited by the use of 0.015 % BBG with 0.009 % BAK or 0.007 % Oct, as well as by the use of 0.007 % BBG with 0.005 % BAK or 0.003% Oct.

BBR was assayed in combination with Oct on the Gram-negative and Gram-positive bacterial strains used before, to test whether BBR has the same bacterial inhibitory effect as BBG. The results showed that the bacterial growth of the Gram-positive bacterium, *B. subtilis* was not inhibited in presence of high BBR concentrations, i.e. 0.025% or 0.030% combined with 0.001% Oct there. For the Gram-negative bacteria, increasing Oct concentrations were required with increasing BBR concentrations, similar to BBG (see **Fig. 6**). The results showed that the growth of all tested bacterial strains were inhibited by the use of 0.007% BBR with 0.005% of Oct, 0.012% BBR with 0.007% Oct and 0.020% BBR with 0.009% Oct. Combinations between BBR and BAK have not been investigated, because no significant protective activity of BBR on human cell lines was seen in presence of BAK.

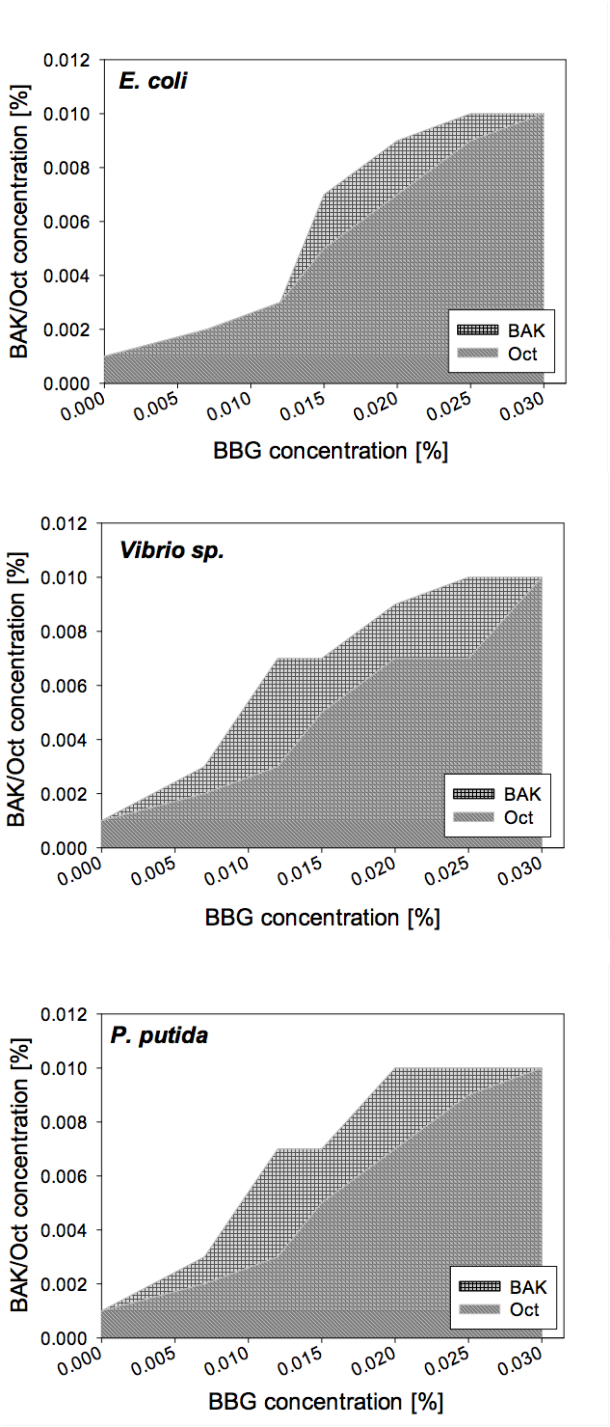


**Fig. 5.** Concentrations of BAK and Oct required to inhibit Gram-negative bacterial growth, when BBG is present. At combinations within the shaded area bacterial growth is observed; combinations above the shaded areas prevent bacterial growth.

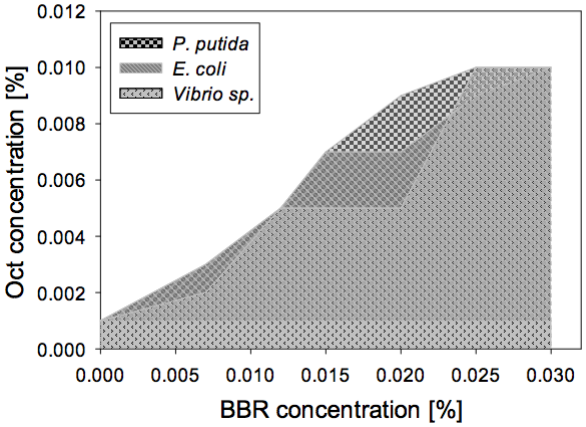


**Fig. 6.** Concentrations of BAK and Oct required to inhibit Gram-negative bacterial growth, when BBR is present. At combinations within the shaded area bacterial growth is observed; combinations above the shaded areas prevent bacterial growth.

The concentrations of BAK used in this study are in the range of concentrations used in the commercially available eye drops, 0.004-0.02% (Liang et al. 2012), where 0.025% BBG exerted a significant cell viability increase on HCE cells. To achieve bacterial growth inhibition, as well as a significant increase of the cell viability, higher concentrations of BBG required higher BAK concentrations. The best combinations between these two compounds were 0.015% BBG for BAK between 0.008% and 0.01%, and 0.007% BBG for BAK between 0.004% and 0.006%. The HCE cell viability increased between 40-60% in the first set of combinations between BBG and BAK, and with 50-80% in the second case.

Oct was used in this study between 0.002% and 0.01%, because according to Hübner et al. (2010) 22.5 mg/l of OPE (Oct with phenoxyethanol) was sufficient to reduce with $3\log_{10}$ the bacterial growth after 30 min incubation. At these concentrations of Oct, 0.025% BBG increased the HCE cell survival with up to 100% at 30 min incubation. Also BBR at the same concentration and incubation time increased the HCE cell survival up to 90%, when 0.003% Oct was present. To reduce the toxicity of the antiseptic agent, without affecting the bacterial inhibitory effect, we suggest the following combinations: 0.025% of BBG with 0.01% Oct; 0.015% BBG with 0.007% Oct; and 0.007% BBG with 0.003% Oct. With these combinations, the HCE cell survival increased with 35-115%.

## DISCUSSION

The inflammatory responses of the eyes or skin due to the repeated contact with preservatives and antiseptics used in different eye drops, wound disinfectants or cosmetical products, are unwanted side effects, and are present in many patients using these products on a daily basis. The reason for these inflammatory effects is the high toxicity of the compounds on the target cells. Therefore, reducing the toxicity of antiseptics and preservatives on human tissues, while maintaining their bacteriostatic effect, is desired. Ways to reduce these inflammatory effects, by combination of bacteriostatic agents with protective agents, were not yet investigated.

We found that the protective effect of BBG against BAK and Oct toxicity on human eye cells is remarkable. However, there are only limited numbers of possible combinations between different concentrations of BBG and BAK or Oct, at which the bacterial growth is inhibited. Very high concentrations of BBG, 0.03% or higher, in presence of either of the two antiseptics, at the tested concentrations, does no longer inhibit the bacterial growth of Gram-negative bacteria. BBR showed protective effect only against Oct toxicity, however this effect is little lower than the one caused by BBG.

The microbiology experiments showed that the mixtures between BAK with BBG, Oct with BBG and Oct with BBR had stronger inhibitory effects against Gram-positive than against Gram-negative bacterial cells. Since the cell wall composition in both groups of bacteria differs remarkably (Silhavy et al. 2010), the hydrophobic outer membrane of Gram-negative bacteria potentially might prevent the compounds to efficiently enter the cells. However, hydrophilic features of the compounds might aid the entrance of the antimicrobials into Gram-positive cells thus making them more susceptible. Previously McDonnell and Russell (1999) and Fazlara and Ekhtelat (2012) reported that BAK is more effective on Gram-positive bacterial organisms. They also mentioned that the mechanism of action of BAK, as a cationic quaternary ammonium compound, is based on the interaction of the negatively charged bacterial surface with the positively charged headgroup of BAK. After the binding on the bacterial surface, BAK will enter the cell wall and cause its disruption and leakage of the cytoplasmic material to the outside. The mechanism of action of Oct has not been described yet, but we assume that it is similar to BAK. Both of them have an amphiphilic structure, but Oct is a more complex molecule, with two cationic centers and long hydrophobic chains at both ends of the molecule. Oct and BAK had previously been successfully tested as antimicrobial compounds (Hübner et al. 2010; Sedlock and Bailey 1985). In comparison with BAK, Oct showed a higher efficiency against Gram-negative bacteria.

We have demonstrated here that BBG reduces the antibacterial effect of Oct and BAK for Gram-negative bacteria. Nevertheless, the use of certain concentration combinations of the compounds, presented in Fig. 5, will efficiently inhibit the growth of bacteria in eye drops, skin, mucous membranes and wounds disinfectants, while protecting the epithelial cells against the cytotoxic action of the disinfectants. BBR reduces the growth of gram-negative bacteria less efficiently than BBG at any of the tested concentrations, when mixed with Oct.

Recently, Müller and Kramer (2008) defined the biocompatibility index (BI) of antiseptic compounds. They measured the $IC_{50}$ value of the antiseptics on fibroblast cells and divided this value with the concentration at which 99.9% of the Gram-positive and Gram-negative bacteria are killed. A BI bigger than 1 would mean that an antiseptic compound is more toxic to the bacterial organisms in comparison with the mammalian cells. In order to quantify, in our case, the effectiveness of the different concentration combinations between BBG and Oct or BAK in antiseptic treatments, a similar BI of the two antiseptic compounds in the presence of BBG will be defined as the next step of this study.

Previously Dutot et al. (2006) reported that BAK induces apoptosis in corneal and conjunctival cell lines through the activation of the P2x7 receptor. The activation of this receptor leads to pore formation and influx of $Ca^{2+}$ and other extracellular molecules into the cell, but also to the escape of intracellular small metabolites (Chung et al. 2000; Dutot et al. 2006; Wang et al. 2004). The exact mechanism of the protective activity of BBG and BBR is not yet known. We assume, however, that it does not involve the P2x7 receptor, because

other selective P2x7 receptor antagonists, OxATP and DPPH, did not show any protection against the cytotoxic effect of these antiseptics. Recently Jo and Bean (2011) showed that BBG at micromolar concentrations also causes inhibition of neuronal voltage gated sodium channels in neuroblastoma cells. The binding constants to these channels are far higher than those of the classic sodium channel blockers used in medical treatments of traumatic brain injury (Pitkanen et al. 2014). Further investigations are needed to elucidate on which target BBG and BBR acts when inhibiting the toxicity of BAK or Oct on HCE cells. BBR, in contrast to BBG, was less studied in the past. This dye is often used in literature as a stain for detection of proteins in polyacrylamide gel electrophoresis. No protective effect of the dye on human cells has been described yet, nor any activity on any cellular receptors.

The chemical interaction between negatively charged dye molecules and antiseptics, which have one (BAK) or two (Oct) positive charges, could be one reason, why BBG and BBR reduces the toxicity of Oct or BAK on HCE cells. This idea is supported also by our data, where certain mixtures between the dyes and the antiseptics reduce the bacteriostatic effect of the antiseptics on Gram-negative bacteria. This interaction could result in a compound that is not anymore toxic to neither the mammalian cells nor to the Gram-negative bacteria. Interestingly, the bacteriostatic effect of the dye-preservative mixtures on Gram-positive bacteria is not affected by these interactions. In the literature it is mentioned that BBR, during the protein staining procedure, binds reversibly and especially to positively charged parts of the proteins (Tal et al. 1985), with a slightly different molecular mechanism than BBG (Lee et al. 2001). Casero et al. (1997) described studies of the interaction of the negatively charged BBG with several types of cationic surfactants and the formation of dye-detergent premicellar aggregates at surfactant concentrations far below their critical micelle concentration. Ma et al. (2014) showed that BAK is able to interact with other negatively charged dye molecules, eosin Y and eosin B and form stable dye-surfactant aggregates. Also Sütterlin et al. (2008) presented studies where other negatively charged molecules, such as linear alkylbenzene sulfonate, naphthalene sulfonic acid, benzene sulfonic acid or SDS, can considerably modify the bacteriostatic effect of BAK on two Gram-negative bacterial strains, *P. putida* and *V. fischeri*.

There are several preparations with BAK or Oct as an antiseptic already available on the market. The combinations between Oct and BBG or BBR, or BAK and BBG, proposed by us in this study, will help in marking the disinfected area and in protecting the skin from possible irritations or inflammations caused by the antiseptics. The protective effect of BBG and BBR will also allow to use higher concentrations of the antiseptics in the ready-to-use preparations. However, the daily use of BBG based solutions on skin or in eyes will have as a side effect the staining of the surface in blue, where the treatment is applied, but according to Peng et al. (2009) and our own experience, the staining disappears rapidly, and is gone about a week after the treatment. With BBR no such effect has been described yet in the literature, but we assume that it has a similar staining effect with BBG, because BBR is widely used as a high sensitivity protein stain.

## ACKNOWLEDGMENTS

The research was partially funded by the Dr. Helmut und Margarete Meyer-Schwarting Stiftung. We are also grateful for the octenidine dihydrochloride gift from Schülke and Mayr GmbH.

**REFERENCES**

Ammar DA, Kahook MY (2011) Effects of benzalkonium chloride- or polyquad-preserved fixed combination glaucoma medications on human trabecular meshwork cells. Mol Vis 17:1806-13

Awad D, Schrader I, Bartok M, Sudumbrekar N, Mohr A, Gabel D (2013) Brilliant Blue G as protective agent against trypan blue toxicity in human retinal pigment epithelial cells in vitro. Graefes Arch Clin Exp Ophthalmol 251(7):1735-40 doi:10.1007/s00417-013-2342-3

Casero I, Sicilia D, Rubio S, Perez-Bendito D (1997) Study of the formation of dye-induced premicellar aggregates and its application to the determination of quaternary ammonium surfactants. Talanta 45(1):167-80

Chung HS, Park KS, Cha SK, Kong ID, Lee JW (2000) ATP-induced [Ca(2+)](i) changes and depolarization in GH3 cells. Br J Pharmacol 130(8):1843-52 doi:10.1038/sj.bjp.0703253

Dutot M, Pouzaud F, Larosche I, Brignole-Baudouin F, Warnet JM, Rat P (2006) Fluoroquinolone eye drop-induced cytotoxicity: role of preservative in P2X7 cell death receptor activation and apoptosis. Invest Ophthalmol Vis Sci 47(7):2812-9 doi:10.1167/iovs.06-0224

Enaida H, Hisatomi T, Hata Y, et al. (2006) Brilliant blue G selectively stains the internal limiting membrane/brilliant blue G-assisted membrane peeling. Retina 26(6):631-6 doi:10.1097/01.iae.0000236469.71443.aa

Fazlara A, Ekhtelat M (2012) The disinfectant effects of benzalkonium chloride on some important foodborne pathogens. Am Eurasian J Agric Environ Sci 12(1):23-29

Hibell AD, Thompson KM, Xing M, Humphrey PP, Michel AD (2001) Complexities of measuring antagonist potency at P2X(7) receptor orthologs. J Pharmacol Exp Ther 296(3):947-57

Hübner N-O, Siebert J, Kramer A (2010) Octenidine dihydrochloride, a modern antiseptic for skin, mucous membranes and wounds. Skin Pharmacol Phys 23(5):244-258 doi:10.1159/000314699

Jiang L-H, Mackenzie AB, North RA, Surprenant A (2000) Brilliant blue G selectively blocks ATP-gated rat P2X7 receptors. Mol Pharmacol 58(1):82-88 doi:10.1124/mol.58.1.82

Jo S, Bean BP (2011) Inhibition of neuronal voltage-gated sodium channels by brilliant blue G. Mol Pharmacol 80(2):247-57 doi:10.1124/mol.110.070276

Jorgensen J, Turnidge J (2007) Manual of Clinical Microbiology. In: Murray P, Baron E, Jorgensen J, Landry M, Pfaller M (eds) Antibacterial susceptibility tests: dilution and disc diffusion methods. 9th edn. ACM Press, Washington DC, p 1152-1172

Koburger T, Hübner N-O, Braun M, Siebert J, Kramer A (2010) Standardized comparison of antiseptic efficacy of triclosan, PVP–iodine, octenidine dihydrochloride, polyhexanide and chlorhexidine digluconate. J Antimicrob Chemother 65(8):1712-1719 doi:10.1093/jac/dkq212

Lee D, Lee EK, Lee JH, Chang CS, Paik SR (2001) Self-oligomerization and protein aggregation of alpha-synuclein in the presence of Coomassie Brilliant Blue. Eur J Biochem 268(2):295-301 doi:10.1046/j.1432-1033.2001.01877.x

Lee WG, Lee SD, Cho JH, et al. (2012) Structure-activity relationships and optimization of 3,5-dichloropyridine derivatives as novel P2X(7) receptor antagonists. J Med Chem 55(8):3687-98 doi:10.1021/jm2012326

Liang H, Brignole-Baudouin F, Riancho L, Baudouin C (2012) Reduced in vivo ocular surface toxicity with polyquad-preserved travoprost versus benzalkonium-preserved travoprost or latanoprost ophthalmic solutions. Ophthalmic Res 48(2):89-101 doi:10.1159/000335984

Ma W, Ma X, Sha O, Liu Y (2014) Two Spectrophotometric Methods for the Assay of Benzalkonium Chloride in Bandage Samples. J Surfactants Deterg 17(1):177-181 doi:10.1007/s11743-013-1446-4

Marcillo A, Frydel B, Bramlett HM, Dietrich WD (2012) A reassessment of P2X7 receptor inhibition as a neuroprotective strategy in rat models of contusion injury. Exp Neurol 233(2):687-92 doi:10.1016/j.expneurol.2011.06.008

McDonnell G, Russell AD (1999) Antiseptics and disinfectants: activity, action, and resistance. Clin Microbiol Rev 12(1):147-179

Müller G, Kramer A (2008) Biocompatibility index of antiseptic agents by parallel assessment of antimicrobial activity and cellular cytotoxicity. J Antimicrob Chemother 61(6):1281-7 doi:10.1093/jac/dkn125

Paimela T, Ryhanen T, Kauppinen A, Marttila L, Salminen A, Kaarniranta K (2012) The preservative polyquaternium-1 increases cytoxicity and NF-kappaB linked inflammation in human corneal epithelial cells. Mol Vis 18:1189-96

Peng W, Cotrina ML, Han X, et al. (2009) Systemic administration of an antagonist of the ATP-sensitive receptor P2X7 improves recovery after spinal cord injury. Proc Natl Acad Sci 106(30):12489-12493 doi:10.1073/pnas.0902531106

Pitkanen A, Immonen R, Ndode-Ekane X, Grohn O, Stohr T, Nissinen J (2014) Effect of lacosamide on structural damage and functional recovery after traumatic brain injury in rats. Epilepsy Res 108(4):653-65 doi:10.1016/j.eplepsyres.2014.02.001

Sedlock DM, Bailey DM (1985) Microbicidal activity of octenidine hydrochloride, a new alkanediylbis [pyridine] germicidal agent. Antimicrob Agents and Chemother 28(6):786-790 doi: 10.1128/AAC.28.6.786

Servaites JC, Faeth JL, Sidhu SS (2012) A dye binding method for measurement of total protein in microalgae. Anal Biochem 421(1):75-80 doi:10.1016/j.ab.2011.10.047

Silhavy TJ, Kahne D, Walker S (2010) The bacterial cell envelope. Cold Spring Harb Perspect Biol 2(5):a000414 doi:10.1101/cshperspect.a000414

Sütterlin H, Alexy R, Kümmerer K (2008) The toxicity of the quaternary ammonium compound benzalkonium chloride alone and in mixtures with other anionic compounds to bacteria in test systems with Vibrio fischeri and Pseudomonas putida. Ecotoxicol Environ Saf 71(2):498-505 doi:10.1016/j.ecoenv.2007.12.015

Tal M, Silberstein A, Nusser E (1985) Why does Coomassie Brilliant Blue R interact differently with different proteins? A partial answer. J Biol Chem 260(18):9976-80

Wang X, Arcuino G, Takano T, et al. (2004) P2X7 receptor inhibition improves recovery after spinal cord injury. Nat Med 10(8):821-7 doi:10.1038/nm1082

# 7. References

# 7. References

Alongi, D. (2009). *The energetics of mangrove forest*. Dordrecht: Springer.

Alongi, D. M. (2008). Mangrove forests: Resilience, protection from tsunamis, and responses to global climate change. *Estuar. Coast. Shelf Sci.* 76, 1–13. doi:10.1016/j.ecss.2007.08.024.

Alongi, D. M. (2002). Present state and future of the world's mangrove forests. *Environ. Conserv.* 29, 331–349. doi:10.1017/S0376892902000231.

Alongi, D. M., Boto, K. G., and Robertson, A. I. (1992). "Nitrogen and phosphorus cycles," in *Tropical Mangrove Ecosystems (Coastal and Estuarine Studies) Vol. 41* (Washington, DC: American Geophysical Union), 251–292.

Ball, M. C. (1998). Mangrove species richness in relation to salinity and waterlogging: a case study along the Adelaide River floodplain, northern Australia. *Glob. Ecol. Biogeogr. Lett.* 7, 73–82.

Bashan, Y., and Holguin, G. (2002). Plant growth-promoting bacteria: a potential tool for arid mangrove reforestation. *Trees* 16, 159–166. doi:10.1007/s00468-001-0152-4.

Bashan, Y., Puente, M. E., Myrold, D. D., and Toledo, G. (1998). *In vitro* transfer of fixed nitrogen from diazotrophic filamentous cyanobacteria to black mangrove seedlings. *FEMS Microbiol. Ecol.* 26, 165–170.

Boto, K., and Robertson, I. (1990). The relationship between nitrogen fixation and tidal exports of nitrogen in a tropical mangrove system. *Estuar. Coast. Shelf Sci.* 31, 531–540.

Bouillon, S., Borges, A. V., Castañeda-Moya, E., Diele, K., Dittmar, T., Duke, N. C., Kristensen, E., Lee, S. Y., Marchand, C., Middelburg, J. J., et al. (2008). Mangrove production and carbon sinks: A revision of global budget estimates. *Global Biogeochem. Cycles* 22, 1–12. doi:10.1029/2007GB003052.

Dahdouh-Guebas, F., Jayatissa, L. P., Di Nitto, D., Bosire, J. O., Lo Seen, D., and Koedam, N. (2005). How effective were mangroves as a defence against the recent tsunami? *Curr. Biol.* 15, R443–R447. doi:10.1016/j.cub.2005.06.008.

Dixon, R., and Kahn, D. (2004). Genetic regulation of biological nitrogen fixation. *Nat. Rev. Microbiol.* 2, 621–631. doi:10.1038/nrmicro954.

Donato, D. C., Kauffman, J. B., Murdiyarso, D., Kurnianto, S., Stidham, M., and Kanninen, M. (2011). Mangroves among the most carbon-rich forests in the tropics. *Nat. Geosci.* 4, 293–297. doi:10.1038/ngeo1123.

Duke, C. (1992). "Mangrove floristics and biogeography," in *Tropical Mangrove Ecosystems (Coastal and Estuarine Studies) Vol. 41* (Washington, DC: American Geophysical Union), 63–100.

Duke, N. ., Meynecke, J. ., Dittmann, S., Ellison, A. ., Anger, K., Berger, U., Cannicci, S., Diele, K., Ewel, K. ., Field, C., et al. (2007). A World Without Mangroves? *Science.* 317, 41–43.

Duke, N. C., Ball, M. C., and Ellison, J. C. (1998). Factors influencing biodiversity and distributional gradients in mangroves. *Glob. Ecol. Biogeogr. Lett.* 7, 27–47.

Ewel, K. C., Twilley, R. R., and Jin Eong, O. (1998). Different kinds of mangrove forests provide different goods and services. *Glob. Ecol. Biogeogr. Lett.* 7, 83–94.

Feller, I. C., Lovelock, C. E., Berger, U., Mckee, K. L., Joye, S. B., and Ball, M. C. (2010). Biocomplexity in mangrove ecosystems. *Ann. Rev. Mar. Sci.* 2, 395–417. doi:10.1146/annurev.marine.010908.163809.

Feller, I. C., Mckee, K. L., Whigham, D. F., and Neill, J. P. O. (2002). Nitrogen vs. phosphorus limitation across an ecotonal gradient in a mangrove forest. *Biogeochemistry* 62, 145–175.

Flores-Mireles, A. L., Winans, S. C., and Holguin, G. (2007). Molecular characterization of diazotrophic and denitrifying bacteria associated with mangrove roots. *Appl. Environ. Microbiol.* 73, 7308–7321. doi:10.1128/AEM.01892-06.

Food and Agriculture Organization of the United Nations (FAO) (2007). The world's mangroves 1980–2005 (FAO Forestry Paper 153). Rome, Italy.

Foster, R. a, Kuypers, M. M. M., Vagner, T., Paerl, R. W., Musat, N., and Zehr, J. P. (2011). Nitrogen fixation and transfer in open ocean diatom-cyanobacterial symbioses. *ISME J.* 5, 1484–1493. doi:10.1038/ismej.2011.26.

Gallon, J. R. (1981). The oxygen sensitivity of nitrogenase: a problem for biochemists and micro-organisms. *Trends Biochem. Sci.* 6, 19–23.

Giri, C., Ochieng, E., Tieszen, L. L., Zhu, Z., Singh, A., Loveland, T., Masek, J., and Duke, N. (2011). Status and distribution of mangrove forest of the world using earth observation satellite data. *Global Ecol. Biogeogr.* 20, 154–159. doi:10.1111/j.1466-8238.2010.00584.x

Gonzalez-Acosta, B., Bashan, Y., Hernandez-Saavedra, N. Y., Ascencio, F., and Cruz-Agüero, G. (2006). Seasonal seawater temperature as the major determinant for populations of culturable bacteria in the sediments of an intact mangrove in an arid region. *FEMS Microbiol. Ecol.* 55, 311–321. doi:10.1111/j.1574-6941.2005.00019.x.

Gotto, J. W., and Taylor, B. F. (1976). $N_2$ fixation associated with decaying leaves of the red mangrove (*Rhizophora mangle*). *Appl. Environ. Microbiol.* 31, 781–783.

Hedges, S. B. (2002). The origin and evolution of model organisms. *Nat. Rev. Genet.* 3, 838–49. doi:10.1038/nrg929.

Hicks, B. J., and Silvester, W. B. (1985). Nitrogen fixation associated with the New Zealand mangrove (*Avicennia marina* (Forsk.) Vierh. var. *resinifera* (Forst. f.) Bakh.). *Appl. Environ. Microbiol.* 49, 955–959.

Holguin, G., Guzman, M. A., and Bashan, Y. (1992). Two new nitrogen-fixing bacteria from the rhizosphere of mangrove trees: Their isolation, identification and *in vitro* interaction with rhizosphere *Staphylococcus sp. FEMS Microbiol. Ecol.* 101, 207–216. doi:10.1016/0168-6496(92)90037-T.

Holguin, G., Vazquez, P., and Bashan, Y. (2001). The role of sediment microorganisms in the productivity, conservation, and rehabilitation of mangrove ecosystems: an overview. *Biol. Fertil. Soils* 33, 265–278. doi:10.1007/s003740000319.

Jennerjahn, T. C., and Ittekkot, V. (2002). Relevance of mangroves for the production and deposition of organic matter along tropical continental margins. *Naturwissenschaften* 89, 23–30. doi:10.1007/s00114-001-0283-x.

Karl, D., Michaels, A., Bergman, B., Capone, D., Carpenter, E., Letelier, R., Lipschultz, F., Paerl, H., Sigman, D., and Stal, L. (2002). Dinitrogen fixation in the world's oceans. *Biogeochemistry* 57, 47–98.

Kristensen, E., Bouillon, S., Dittmar, T., and Marchand, C. (2008). Organic carbon dynamics in mangrove ecosystems: A review. *Aquat. Bot.* 89, 201–219. doi:10.1016/j.aquabot.2007.12.005.

Lee, R., and Joye, S. (2006). Seasonal patterns of nitrogen fixation and denitrification in oceanic mangrove habitats. *Mar. Ecol. Prog. Ser.* 307, 127–141. doi:10.3354/meps307127.

Lovelock, C. E., and Ellison, J. (2007). "Vulnerability of mangroves and tidal wetlands of the Great Barrier Reef to climate change," in *Climate Change and the Great Barrier Reef: a vulnerability assessment.* (Townsville, Australia: The Great Barrier Reef Marine Park Authority), 238–269.

Lugomela, C., and Bergman, B. (2002). Biological $N_2$-fixation on mangrove pneumatophores: preliminary observations and perspectives. *Ambio* 31, 612–613.

Mcleod, E., and Salm, R. V (2006). Managing mangroves for resilience to climate change. Gland, Switzerland.

Oliveira Fernandes, S., Bonin, P. C., Michotey, V. D., Garcia, N., and LokaBharathi, P. A.(2012). Nitrogen-limited mangrove ecosystems conserve N through dissimilatory nitrate reduction to ammonium. *Sci. Rep.* 2, 1–5. doi:10.1038/srep00419.

Pelegrí, S., Rivera-monroy, V., and Twilley, R. (1997). A comparison of nitrogen fixation (acetylene reduction) among three species of mangrove litter, sediments, and pneumatophores in south Florida, USA. *Hidrobiología* 356, 73–79.

Postgate, J. R. (1982). Biological nitrogen fixation: fundamentals. *Philos. Trans. R. Soc. London B* 296, 375–385.

Ravikumar, S., Kathiresan, K., Ignatiammal, S. T. M., Babu Selvam, M., and Shanthy, S. (2004). Nitrogen-fixing azotobacters from mangrove habitat and their utility as marine biofertilizers. *J. Exp. Mar. Bio. Ecol.* 312, 5–17. doi:10.1016/j.jembe.2004.05.020.

Reef, R., Feller, I. C., and Lovelock, C. E. (2010). Nutrition of mangroves. *Tree Physiol.* 30, 1148–1160. doi:10.1093/treephys/tpq048.

Rojas, A., Holguin, G., Glick, B. R., and Bashan, Y. (2001). Synergism between *Phyllobacterium sp*. ($N_2$-fixer) and *Bacillus licheniformis* (P-solubilizer), both from a semiarid mangrove rhizosphere. *FEMS Microbiol. Ecol.* 35, 181–187. doi:10.1111/j.1574-6941.2001.tb00802.x.

Romero, I. C., Jacobson, M., Fuhrman, J. a., Fogel, M., and Capone, D. G. (2011). Long-term nitrogen and phosphorus fertilization effects on $N_2$ fixation rates and *nifH* gene community patterns in mangrove sediments. *Mar. Ecol.* 33, 1–11. doi:10.1111/j.1439-0485.2011.00465.x.

Sengupta, A., and Chaudhuri, S. (1991). Ecology of heterotrophic dinitrogen fixation in the rhizosphere of mangrove plant community at the Ganges river estuary in India. *Oecologia* 87, 560–564.

Smith, T. I. (1992). "Forest structure," in *Tropical Mangrove Ecosystems. (Coastal and Estuarine Studies) Vol. 41* (Washington, DC: American Geophysical Union), 101–136.

Spalding, M., Blasco, F., and Field, C. (1997). *World mangrove atlas*. Okinawa, Japan: The International Society For Mangrove Ecosystems.

Toledo, G., Bashan, Y., and Soeldner, A. (1995). *In vitro* colonization and increase in nitrogen fixation of seedling roots of black mangrove inoculated by a filamentous cyanobacteria. *Can. J. Microbiol.* 41, 1012–1020. doi:10.1139/m95-140.

Tomlinson, P. (1986). *The botany of mangroves*. Cambridge: Cambridge University Press.

Uchino, F., Hambali, G. G., and Yatazawa, M. (1984). Nitrogen-fixing bacteria from warty lenticellate bark of a mangrove tree, *Bruguiera gymnorrhiza* (L.) Lamk. *Appl. Environ. Microbiol.* 47, 44–48.

Valiela, I., Bowen, J. L., and York, J. K. (2001). Mangrove forests: one of the world's threatened major tropical environments. *Bioscience* 51, 807–815. doi:10.1641/0006-3568(2001)051[0807:MFOOTW]2.0.CO;2.

Ventosa, A., Nieto, J. J., and Oren, A. (1998). Biology of moderately halophilic aerobic bacteria. *Microbiol. Mol. Biol. Rev.* 62, 504–544.

Vovides, A. G., Bashan, Y., López-Portillo, J. a., and Guevara, R. (2011). Nitrogen fixation in preserved, reforested, naturally regenerated and impaired mangroves as an indicator of functional restoration in mangroves in an arid region of Mexico. *Restor. Ecol.* 19, 236–244. doi:10.1111/j.1526-100X.2010.00713.x.

Waycott, M., Mckenzie, L. J., Mellors, J. E., Ellison, J. C., Sheaves, M. T., Collier, C., Schwarz, A., Webb, A., Johnson, J. E., and Payri, C. E. (2011). "Vulnerability of mangroves, seagrasses and intertidal flats in the tropical Pacific to climate change," in *Vulnerability of tropical pacific fisheries and aquaculture to climate change.* (Noumea, New Caledonia: Secretariat of the Pacific Community), 297–368.

Woitchik, A. F., Ohowa, B., Kazungu, J. M., Rao, R. G., Goeyens, L., and Dehairs, F. (1997). Nitrogen enrichment during decomposition of mangrove leaf litter in an east African coastal lagoon (Kenya): Relative importance of biological nitrogen fixation. *Biogeochemistry* 39, 15–35.

Zehr, J. P., Jenkins, B. D., Short, S. M., and Steward, G. F. (2003). Nitrogenase gene diversity and microbial community structure: a cross-system comparison. *Environ. Microbiol.* 5, 539–554.

Zehr, J. P., and McReynolds, L. a (1989). Use of degenerate oligonucleotides for amplification of the *nifH* gene from the marine cyanobacterium *Trichodesmium thiebautii*. *Appl. Environ. Microbiol.* 55, 2522–2526.

Zhang, Y., Dong, J., Yang, Z., Zhang, S., and Wang, Y. (2008). Phylogenetic diversity of nitrogen-fixing bacteria in mangrove sediments assessed by PCR-denaturing gradient gel electrophoresis. *Arch. Microbiol.* 190, 19–28. doi:10.1007/s00203-008-0359-5.

Zuberer, D. A., and Silver, W. S. (1978). Biological dinitrogen fixation (acetylene reduction) associated with Florida mangroves. *Appl. Environ. Microbiol.* 35, 567–575.